

**Ecosystem carbon and nitrogen losses from temperate
agricultural peatland with mineral soil coverage**

Inauguraldissertation

zur

Erlangung der Würde eines Doktors der Philosophie

vorgelegt der

Philosophisch-Naturwissenschaftlichen Fakultät

der Universität Basel

von

Yuqiao Wang

Basel, 2022

Originaldokument gespeichert auf dem Dokumentenserver der Universität Basel

edoc.unibas.ch

Genehmigt von der Philosophisch-Naturwissenschaftlichen Fakultät
auf Antrag von

PD Dr. Jens Leifeld, Prof. Dr. Christine Alewell, Prof. Dr. Stephan Glatzel

Basel, 21. 06. 2022

Prof. Dr. Marcel Mayor
Dekan

Table of content

Table of content	I
Abbreviations.....	III
Summary	IV
Part A: Synopsis	1
1 Introduction.....	1
2 Objectives.....	6
3 Material and methods.....	7
4 Results and Discussion.....	12
5 Conclusions.....	15
6 Outlook.....	15
References.....	18
Part B: Publications	27
Paper I.....	28
Abstract.....	29
1 Introduction.....	30
2 Materials and methods	32
3 Results	38
4 Discussion.....	43
5 Conclusions.....	47
Acknowledgements.....	47
References.....	48
Supplemental Information	54
Paper II.....	58
Abstract.....	59
1 Introduction.....	60
2 Material and methods.....	61
3 Results	68

4 Discussion.....	76
5 Conclusions.....	80
Funding	80
Acknowledgement	80
References.....	81
Supplementary Material.....	88
Paper III	90
Abstract.....	91
1 Introduction.....	92
2 Materials and methods	93
3 Results	97
4 Discussion.....	104
5 Conclusion	107
Funding	108
Declarations	108
Acknowledgments	108
References.....	108
Supplementary Material.....	114
Acknowledgments.....	117
Curriculum vitae	119

Abbreviations

ATIC	Automatic time integrating chamber system
C	Carbon
CH ₄	Methane
CO ₂	Carbon dioxide
Cov	Drained peatland with mineral soil coverage
F ¹⁴ C	Radiocarbon signature
GHG	Greenhouse gas
N	Nitrogen
NH ₄ NO ₃	Ammonium nitrate
N ₂ O	Nitrous oxide
Ref	Drained peatland without mineral soil coverage
SOC	Soil organic carbon
Soil N _{r_min}	Soil nitrogen mineralization rate
Soil Rh	Heterotrophic soil respiration
SOM	Soil organic matter
Specific soil N _{sr_min}	Specific soil nitrogen mineralization rate

Summary

Draining peatlands for agricultural production induces massive amount of carbon (C) and nitrogen (N) losses, therefore contributing to climate change, environmental pollution and peat degradation. Full rewetting or restoration could decrease peat mineralization, by raising the water table and might save substantial parts of the soil organic matter (SOM) oxidation and halt peatland subsidence. However, with rewetting, intensive agricultural production is in many cases not possible anymore. Hence, there is a trade-off between environmental goals and agricultural production, creating challenges to implementing peatlands rewetting. Peatland management strategies, which could not only sustain the productive use of organic soil but also counterbalance soil subsidence and mitigate peat decomposition and climate change, are urgently needed for those regions where the peatlands surface contribute greatly to food and feed production and economics and thus where restoration of near-natural ecosystem is difficult to implement. Nowadays, in order to counteract the subsidence of drained peatland, mineral soil coverage is an increasingly used practice in Switzerland and other European countries e.g. Norway, Germany and the Netherlands.

The main objectives of this thesis were to investigate the effect of mineral soil coverage on peat decomposition, i.e. C loss and N balance, and on agricultural productivity. The objectives were achieved by in-situ quasi-continuous GHGs observation, an isotope labeling experiment and associated lab incubation. The experimental site was located in the Swiss Rhine Valley, a drained peatland with fen peat ~10 m thick. Drainage with ditches commenced before 1890. An intensive drainage system with drainage pipes and pump was built in 1973. The site was used as pasture until 2013, and since then as an intensively managed meadow. In 2006 to 2007, one part of the field (1.7 ha) was covered with mineral soil material, with a thickness ~ 40 cm, to improve the trafficability and agriculture usability and to counteract peat subsidence. The field experiments were established at this mineral soil coverage site (Cov), and the adjacent drained organic soil without mineral soil coverage was used as reference (Ref). Both sites have the identical farming practice, with 5 – 6 times cuts per year, receiving c. 230 kg N ha⁻¹ yr⁻¹ of nitrogen fertilizer, and similar vegetation. The C losses were determined by in-situ CO₂ and ¹⁴CO₂ fluxes measurement and soil profile-based C and ¹⁴C observation. The long-term drainage induced C loss was determined by comparing the hypothetical non-drainage C stock and the measured C stock. This hypothetical non-drainage C stock was estimated by the age gradient between the deeper ¹⁴C dated peat layer, the hypothetical non-drainage surface peat layer and its carbon accumulation rate. The source of C loss, i.e. its origin within the soil profile, was determined by Bayesian stable isotope mixing model with the measured soil respired F¹⁴CO₂ value, atmosphere F¹⁴C value, which here represents the radiocarbon signature of fresh plant residues, and the F¹⁴C value of topsoil C and middle layer soil C and the measurement uncertainty. The N losses were measured by in-situ quasi-continuous N₂O observation by using automatic time integrating chamber (ATIC) systems and an in-situ ¹⁵N tracer

experiment with labeled mineral fertilizer. The latter allowed to determine the N allocation in plant-soil system, and the N losses by an isotope and mass balances approach.

The results demonstrated that mineral soil coverage moved the source of decomposition of soil organic carbon (SOC) from a higher share of old peat towards a higher share of relatively younger material located in the topsoil. In this study, decadal drainage of organic soil for agriculture induced 41 – 75 kg C m⁻² loss, which is equivalent to annual C loss rates of 0.49 – 0.58 kg C m⁻² yr⁻¹ and 0.31 – 0.63 kg C m⁻² yr⁻¹ for drained peatland with (Cov) and without (Ref) mineral soil coverage, respectively. Correspondingly, the carbon sources of heterotrophic soil respiration (soil Rh) were a mixture of fresh plant residues and soil C. Carbon from peat decomposition contributed around half to the total heterotrophic CO₂ from the soil in site Ref, partially stemming also from carbon stored in the subsoil. Mineral soil coverage had no significant effect on the amount of heterotrophic respiration, however at Cov, the radiocarbon signature of heterotrophic CO₂ was significantly ($p < 0.01$) younger than at Ref.

The mass balances for ¹⁵N tracer in the system was used to account for the quantitatively recovery and loss, the ¹⁵N which is not retained in plant and soil system are defined as loss. ¹⁵N losses from site Cov was 10 % lower ($p < 0.05$) than Ref. The lower N losses from Cov might be driven by the higher soil ¹⁵N retention, with $20 \pm 2\%$ of the added ¹⁵N residing in the soil, however, it was only $9 \pm 3\%$ at Ref. The plant ¹⁵N uptake was not different between the two sites, despite the higher ($p < 0.05$) N uptake at site Cov. The lab incubation results showed that soil N_{r_min} and ¹⁵N_{r_min} release was ~ 3 times higher at Ref than Cov, however, the specific release per unit soil nitrogen (specific soil N_{sr_min}) release showed the opposite, indicating a faster SOM turnover rate at Cov. Importantly, mineral soil coverage induced a strong reduction of N₂O emissions. During the experimental period, site Ref released 20.5 ± 2.7 kg N ha⁻¹ yr⁻¹ N₂O-N, whereas the N₂O emissions from Cov was only 2.3 ± 0.4 kg N ha⁻¹ yr⁻¹. At both sites, N₂O peaks related to fertilization events contributed more than half of the overall N₂O emissions. However, not only the fertilization induced N₂O peaks, but also background N₂O emissions were lower with mineral soil coverage.

The agricultural productivity was determined over four harvest periods. Grass biomass and N uptake were used as indicators of agricultural productivity for the two sites. During the experimental period grass took up 274.34 ± 22.78 kg N ha⁻¹ from site Cov, more than at the Ref with 229.97 ± 10.56 kg N ha⁻¹ grass N uptake. However, the grass yield was not different for the two sites with 13817 ± 738 kg ha⁻¹ and 13011 ± 290 kg ha⁻¹ dry biomass harvested for site Cov and Ref, respectively. This indicates that mineral soil coverage could sustain the agricultural productivity of drained peatland

In conclusion, the field experiment results demonstrated that mineral soil coverage could maintain the agricultural productivity of drained peatland, while at the same time reducing the peat decomposition

rate as indicated by C and N losses. Mineral soil coverage, therefore, seems to be a promising environmental footprint reduction option for intensively used drained organic soils when a sustained use of the drained peatland for intensive agricultural production is foreseen and potential rewetting and restoration of the peatland is not possible.

Part A: Synopsis

1 Introduction

1.1 Climate change, peatlands and agricultural production

Since the 1800s, the anthropogenic release of greenhouse gases due to the burning of fossil fuels, food and feed production and land use change has been the main driver of climate change. It has already resulted in approximately 1.09 degree of global mean temperature increase and more frequent extreme weather events (IPCC, 2021). This human-induced climate change is threatening ecosystems and organisms (Pörtner and Farrell, 2008; Brierley and Kingsford, 2009). Many prevalent human diseases are also linked to climate change such as heatwaves related increases in cardiovascular mortality and respiratory illnesses, altered transmission of infectious diseases and exacerbated malnutrition from crop failures (Karl and Trenberth, 2003; Patz *et al.*, 2005). Moreover, climate change and more frequently extreme weather events stress agricultural production with implications for global food supply and a potential threat to food security (Adams *et al.*, 1998; Fischer *et al.*, 2005; Howden *et al.*, 2007; Piao *et al.*, 2010). It is therefore vitally important to take action to reduce anthropogenic greenhouse gas emissions.

Natural peatlands acted as a cooling mechanism for Earth's climate throughout the Holocene, due to their ability to sequester carbon (C) from atmospheric carbon dioxide (CO₂) (Turetsky, 2002; Belyea and Malmer, 2004; Frohking *et al.*, 2011). Peatlands are formed under waterlogged conditions, wherein the low oxygen availability under the water table results in very slow plant biomass decomposition, allowing organic matter to accumulate over thousands of years to form thick peat (Frohking *et al.*, 2001; Moore, 2002). Meanwhile, due to the high water level, peatlands are also a large source of atmosphere methane (CH₄), with an estimated annual release of 46 Mt CH₄-C (Gorham, 1991). In these ecosystems, the rate of net primary production is greater than that of litter and peat decomposition, resulting in a C sink for natural peatlands, despite being CH₄ emitters (Frohking *et al.*, 2011). Globally, intact peatlands contain ~25 % (600 Gt C) of the global soil C stock, despite occupying only 3 % of the terrestrial system (Yu *et al.*, 2010; Page *et al.*, 2011; Yu, 2012). In addition to the large and dense C stock, natural peatlands also contribute to important functions in the ecosystem including biological diversity, water retention and nutrient sequestration (De Groot *et al.*, 2002; Bonn *et al.*, 2014).

For centuries, large peatlands surfaces have been drained for crop cultivation, pasture, forestry and peat extraction. This initially occurred in Europe mostly and later in tropical regions. Originally peatlands were drained with ditches, and drainage became more intensive through the use of pipes in the nineteenth century and then electrical drainage pumps in the twentieth century (Holden *et al.*, 2016). This has

resulted in ~51 Mha of degraded peatlands worldwide, with a higher share in tropical and temperate regions, where around half of the initial peatlands surface is drained for agricultural production (Leifeld *et al.*, 2019). The drainage of peatlands reflects their potential usefulness for agricultural productions, especially because of their high fertility. With the growing population, the need for agricultural land and fuel has been a main driver of peatland drainage. The drainage of peatlands allows oxygen to enter the peat layer, increasing the surface litter and peat decomposition rates greatly, resulting in i) vast amount of C released to the atmosphere as CO₂ and ii) soil subsidence (IPCC, 2014). Subsidence of drained peat soil indicate the lowering of the soil surface through three components: 1) oxidation, 2) compaction and shrinkage, and 3) consolidation (Schothorst, 1977; Wösten *et al.*, 1997). This results in peatland subsidence rates of 0.5 – 7.5 cm yr⁻¹ worldwide (Leifeld *et al.*, 2011; Hoyt *et al.*, 2020). Moreover, when peatlands are drained for intensive agricultural production, e.g. cropland and grassland, the surface peat undergoes further disturbance through soil tillage, which induces more soil organic matter decomposition and the subsequent removal of the agricultural products reduces the plant residual input (Toet *et al.*, 2005). As a result, since ca. 1960, the global peatland biome is a net GHGs source owing to the higher GHGs release as compared to sequestration in natural ones (Leifeld *et al.*, 2019).

1.2 Overview of C and N losses from drained peatland

For grassland growing on drained peat, the ecosystem releases C and N mainly through two pathways: 1) Gaseous losses, e.g. CO₂ produced from microbial aerobic peat decomposition and gaseous N (N₂O, N₂, NH₃ and NO_x) from denitrification and nitrification, and. 2) Dissolved C and N leaching. Due to the high density of C and N in peat which accumulate over millennia, drainage can continuously release C and N for decades, or even centuries, until all of the peatland's deposits are exhausted (Frolking *et al.*, 2011; Page *et al.*, 2011). It is estimated that under current land use, managed peatlands globally will cumulatively release 80.8 Gt C and 2.3 Gt N to the environment in the future (Leifeld and Menichetti, 2018). The high C and N losses from drained peatland contribute greatly to peat degradation, environmental pollution, i.e. surface water contamination caused by nitrate and DOC leaching, air pollution due to gaseous emissions, and climate change (Murdiyarso *et al.*, 2010; Mishra *et al.*, 2021). It is therefore very important to implement peatland management strategies that could mitigate peat degradation and C and N losses.

1.2.1 C loss from drained peatland

The temporal and spatial variabilities of C loss in drained peatland are large. Environmental and ecological aspects (e.g. peatland type, climate zone, hydrology and land use history) explain part of the variability. It is widely recognized that although lowering the water table of peatlands reduces the CH₄ flux, the increases in the C flux as CO₂ is stronger than the climate benefits from CH₄ reduction (Limpens *et al.*, 2008; Tiemeyer *et al.*, 2016; Evans *et al.*, 2021; Huang *et al.*, 2021). Peatlands located in the warmer climate zone normally have the highest C fluxes (Chen *et al.*, 2021). Within a climate zone,

drained nutrient rich peatlands tend to have higher C fluxes than nutrient poor peatlands, and drained peatlands managed as cropland and grassland tend to have higher C fluxes than those managed as forest (IPCC, 2014). However, large uncertainties remain concerning the C fluxes, which are strongly related to the environmental conditions. Hence, continuous field observations of C fluxes in drained peatlands are still necessary under different spatial and temporal scales.

An established method to determine the C loss in drained peatlands is in-situ flux measurement. Continuous monitoring of the ecosystem–atmosphere C exchange provides important information about the C balance of drained peatlands. By using a flux based method, Paul *et al.* (2021) reported $\sim 4.5 \text{ t C ha}^{-1} \text{ yr}^{-1}$ C loss from a grassland on drained fen peat in Switzerland. Tiemeyer *et al.* (2016) reported $3.8 \pm 2.6 \text{ t C ha}^{-1} \text{ yr}^{-1}$ C loss from grassland on drained nutrient poor bog peat and $8.4 \pm 4.7 \text{ t C ha}^{-1} \text{ yr}^{-1}$ C loss from grassland on drained fen peat in Germany. For the UK, Evans *et al.* (2021) reported $1.2 - 2.5 \text{ t C ha}^{-1} \text{ yr}^{-1}$ C loss from grassland on drained peatlands. However, the in-situ C exchange depends on the climatic conditions during the measuring period (Hatala *et al.*, 2012; Paul *et al.*, 2021). Additionally, compared with the long history of peatland drainage, the duration of the ecosystem C exchange measurements from in-situ flux method is limited (often 2 – 5 years), making it difficult to determine the long-term effect of peatland drainage on C loss.

Aside from flux based methods, profile based methods are also used to determine the long-term C loss from drained peatlands. With profile based methods, C losses are estimated by comparing the C stock in natural and drained soil profiles above a layer with the same radiocarbon age. With the assumption that C accumulated constantly in the peatland overtime, long-term peat C accumulation rates and drainage induced C losses are estimated (Krüger *et al.*, 2016). By radiocarbon dating of soil cores from different peatlands in Europe, Leifeld *et al.* (2018) reported a carbon accumulation rate of $\sim 0.4 \text{ t C ha}^{-1} \text{ yr}^{-1}$ in natural peatlands. The same study concluded that managed peatlands had lost on average 560 t C ha^{-1} , which was approximately half of their former C stock. By comparing the C stock above the layers with the same age for both drained and adjacent undrained peatland in Finland, Krüger *et al.* (2016) reported a C accumulation rate of $0.2 \text{ t C ha}^{-1} \text{ yr}^{-1}$ in a natural peatland, and estimated that $0.6 \text{ t C ha}^{-1} \text{ yr}^{-1}$ had been lost due to drainage.

1.2.2 N loss from drained peatland

Drained peatlands managed for agricultural production also alter soil N dynamics. It is estimated that, ca. 21 – 50 Mha of peatlands are drained and managed as cropland or grassland (Frolking *et al.*, 2011; Tubiello *et al.*, 2016; Leifeld and Menichetti, 2018; Gunther *et al.*, 2020; Evans *et al.*, 2021). In order to maintain the productivity of drained peatland, synthetic N is added to the agricultural system, but a substantial part of this N addition is lost to the environment through emission of gaseous N or leaching to the deeper soil layers and eventually the aquatic ecosystems. Previous studies have shown that in

agricultural systems 40 – 70 % of the applied fertilizer is lost to the environment, resulting in environmental problems e.g. eutrophication of freshwaters and air pollution (Byrnes, 1990; Raun and Johnson, 1999; Ju *et al.*, 2009; Savci, 2012). However, there are only few studies that have quantified the N balance in drained peatlands. It is reported from a ^{15}N tracer study on grassland in Germany that with from the 120 kg N ha^{-1} applied labelled mineral fertilizer $\sim 40 \%$ was lost over one growing season (Augustin *et al.*, 1997). Additionally, in field experiments conducted in different soil types, van Beek *et al.* (2008) reported that in grasslands, more than 200 kg N ha^{-1} were lost to the environment and the N loss was higher in organic soil than in mineral soil. Peat decomposition generally results in an increased soil N release. This often leads to a supply of N that exceed crops uptake, which consequently results in greater N losses to the environment from grass production on drained peatland compared with grass production on mineral soil (Pijlman *et al.*, 2020).

The increased soil N supply of drained peatlands also enhances the potential of N loss as N_2O through nitrification and denitrification (Robertson and Vitousek, 2009; Bowles *et al.*, 2018). Nitrous oxide is an important greenhouse gas and contributes to $\sim 15 \%$ of the GHG emissions from drained peatlands (Williams and Wheatley, 1988; Bayley *et al.*, 2016; Tubiello *et al.*, 2016). N_2O emissions in drained peatlands depend on drainage status and soil fertility (IPCC, 2014), and the addition of fertilizer N further increases N_2O fluxes. However, compared to C fluxes from drained peatlands, field measurements of N_2O fluxes are limited. Generally, a clear increase in N_2O emissions is observed after drainage, especially in warm regions (Parn *et al.*, 2018). The IPCC default value and its 95% confidence interval is $8.2 (4.9 - 11) \text{ kg N ha}^{-1} \text{ yr}^{-1}$ for grassland on drained nutrient-rich peatland in temperate zone (IPCC, 2014). Tiemeyer *et al.* (2016) reported average emissions of $2.9 \pm 2.7 \text{ kg N}_2\text{O-N ha}^{-1} \text{ yr}^{-1}$ from 25 measured fens in Germany. Leppelt *et al.* (2014) reported an average N_2O emissions of $5.8 \pm 10.3 \text{ kg N ha}^{-1} \text{ yr}^{-1}$ from drained grassland on organic soils from 217 annual budgets across Europe. Danevčič *et al.* (2010) even reported N_2O emissions of $37.1 \pm 0.2 \text{ kg N ha}^{-1} \text{ yr}^{-1}$ from drained fen peat with high organic carbon in Slovenia. The large variability of N_2O fluxes from drained peatland underpins the need for continuous field observation to better understand the feedback of N_2O emissions to peatland drainage.

1.3 Peatland management

1.3.1 Peatland rewetting

In the 21st century, peatland rewetting has become widely recognized as the most efficient way to mitigate GHG emissions from drained peatlands. The higher water table associated with rewetting or even restoration decreases the peat decomposition rate and halt peatland subsidence (Knox *et al.*, 2015; Hemes *et al.*, 2019). It has been reported that rewetting degraded agricultural peatlands can help to reduce soil subsidence and GHG emissions (Waddington *et al.*, 2010; Strack and Zuback, 2013; Knox

et al., 2015; Wilson *et al.*, 2016; Lee *et al.*, 2017; Warren *et al.*, 2017). However, with rewetting, agricultural production is in many cases not possible anymore. With the global demand for food and feed production, the pressure to create more agricultural land is enhanced. In many regions, especially those where agricultural products and economics from cultivation on organic soil contribute significantly to human well-being or the economy, rewetting of those agricultural lands is difficult to achieve (Collier, 2011; Dohong *et al.*, 2018). The conflict between food or feed production, GHG mitigation and peat production sets barriers for the rewetting of drained organic soils, in spite of the need for the reduction in GHG emissions. Therefore, research on management options that allow to sustain the agricultural production on drained peatlands, counteract soil subsidence, mitigate GHG emissions, and reduces environmental pollutions is urgently needed in addition to strategies of peatland rewetting.

1.3.2 Mineral soil coverage of drained peatland

Drainage induces the subsidence of surface peat and reduces the distance to the water level. Over time, the water table going back to the soil surface, and agricultural production is in many cases not possible anymore. In order to sustain the agricultural productivity of drained peatlands, either renewal of the drainage system or other peatland managements strategies are needed to compensate for the continuous peatland subsidence, and to improve the trafficability of agriculturally managed drained peatlands. Peatland management, i.e. mixing sand with peat and mineral soil coverage has been used for ~ 200 years to increase the crop yield in the Netherlands and Germany (Göttlich, 1990).

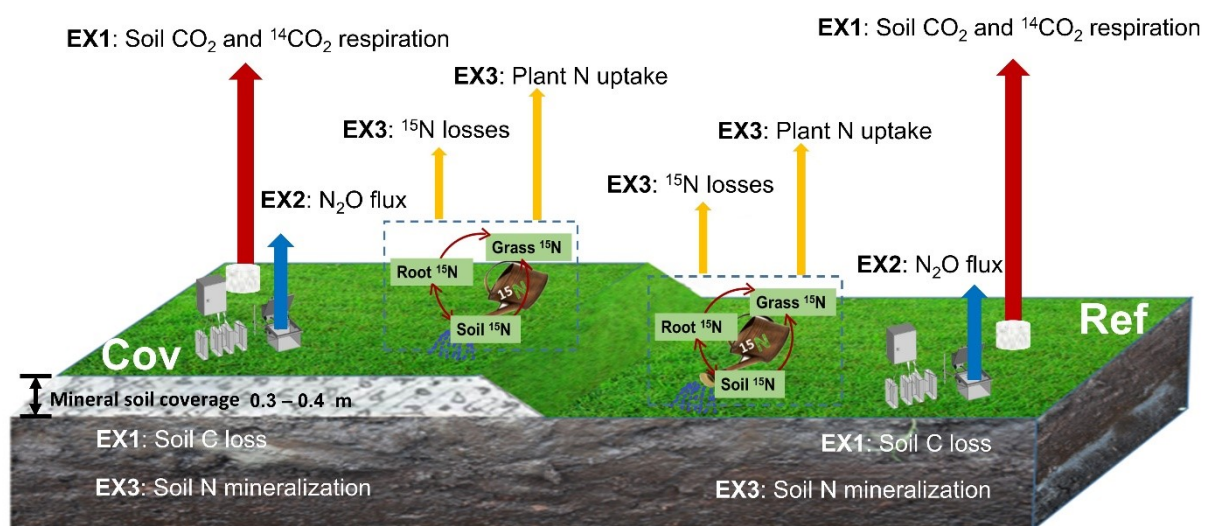
Nowadays, mineral soil coverage is an increasingly used practice in Switzerland and other European countries e.g. Germany, Denmark and the Netherlands (Schindler and Müller, 1999; Ferré *et al.*, 2019). Mineral soil cover may affect peat decomposition and the overall loss of C and N in drained peatlands as follows. Firstly, the addition of mineral soil material changes the topsoil properties of drained organic soil and influences substrate availability for GHGs production. After mineral soil coverage, the topsoil contains much less organic matter than the degrading peat. With this, C and N availability for oxidization, nitrification, and denitrification may become limited, and thereby eventually reducing soil CO₂ and N₂O production (Stehfest and Bouwman, 2006; Flechard *et al.*, 2007). This might be a relevant mechanism given that CO₂ production from the surface (< 30 cm) makes a great contribution to the total CO₂ emissions from organic soil and the soil depth from which emitted N₂O originates is only 0.7 – 2.8 cm (Neftel *et al.*, 2000; Wright *et al.*, 2011). Secondly, mineral soil coverage alters soil hydraulic properties and soil aeration due to the changing pore sizes distribution of the surface soil. Soil moisture and oxygen availability are important regulators of microbial activity, and therefore affect soil microbial activities, and subsequently C and N losses (Davidson *et al.*, 2000). Third, the mineral soil coverage might retain newly assimilated organic matter from the vegetation at a higher rate than the drained organic soil without coverage, owing to the stabilizing and absorbing nature of soil minerals and the formation of

aggregates (Kalbitz *et al.*, 2005; von Lützow *et al.*, 2006). Additionally, mineral soil coverage might compact the organic soil underneath and probably push it deeper into zones of lower oxygen availability or even below the water table, thereby reducing the aerobic decomposition of the older peat. As a result, mineral soil coverage may affect the contribution of decomposing old peat to CO₂ emissions and the amount of C and N losses, with potentially great importance for the sustained use of these soils and future needs for drainage.

Taken together, a fundamental understanding of the effect of mineral soil coverage on C and N losses from agricultural peatland is still missing despite the wide use of this practice. Yet, this is necessary to implement peatland management strategies, which sustain agricultural productivity and prevent peatland degradation and environmental pollution.

2 Objectives

The main aims of the thesis were to quantify the C and N losses from an agriculturally managed drained fen peatland and to evaluate the impact of mineral soil coverage on these losses, using field measurements and lab incubation. To the best of my knowledge, this is the first time that the impact of mineral soil coverage on C and N losses is studied on managed organic soil in the temperate zone. With this, this thesis aims to provide information to assess whether the sustained use of drained peatland for agriculture can co-occur with reduced GHG emissions and peat decomposition. The work is divided into three main research themes with three spatial synchronous experiments as presented in paper I to III (Figure 1).



Cov: Drained peatland with mineral soil coverage
 Ref: Drained peatland without mineral soil coverage

EX1: The first experiment
 EX2: The second experiment
 EX3: The third experiment

Figure 1. Overview of the setup of experiments 1 – 3 on the study site in the Swiss Rhine valley.

In the first experiment (**paper I**), the amount and origin of the soil-born CO₂ was determined by measuring CO₂ fluxes in the field in combination with ¹⁴CO₂ and soil ¹⁴C dating on the (long-term) drained peatland with and without mineral soil coverage to **i**) quantify the C loss from a drained, nutrient-rich managed peat meadow; **ii**) determine the contribution of decomposing old peat and recent organic carbon to heterotrophic soil respiration; **iii**) evaluate the effect of mineral soil coverage on the amount and source of CO₂ efflux.

N₂O fluxes from drained, natural and rewetted peatland have been determined widely in Europe to understand and manage the N₂O fluxes in drained peatland (Kasimir Klemetsson *et al.*, 2009; van Beek *et al.*, 2009; van Beek *et al.*, 2010; Petersen *et al.*, 2012; Leppelt *et al.*, 2014; Tiemeyer *et al.*, 2016). However, N₂O fluxes from drained peatland have not yet been quantified in Switzerland. More importantly, the impact of mineral soil coverage on N₂O fluxes from drained peatland was never evaluated, as far as I know. Therefore, in the second experiment (**paper II**), two years' continuous N₂O measurements from the drained peatland with and without mineral soil coverage were compared to **i**) quantify the N₂O fluxes from a drained, nutrient-rich managed peat meadow in the Swiss Rheine valley; and **ii**) quantify the effect of mineral soil coverage on N₂O fluxes from this soil.

In the third experiment (**paper III**), the fertilizer N recovery and loss from drained peatland with and without mineral soil coverage was compared by using a field ¹⁵N tracer experiment in conjunction with a lab incubation to **i**) determine the extent of fertilizer N recovery and the fertilizer allocation in the plant-soil system in drained peatland with and without mineral soil coverage; **ii**) quantify the net N_{r_min} release from drained peatland with and without mineral soil coverage; and **iii**) analyze the impact of mineral soil coverage on the amount and origin of N losses from drained peatland.

3 Material and methods

3.1 Studies sites

The measurements were carried out on the farm 'Moorhof' in the Swiss Rhine Valley, in the municipality Rüthi (canton St.Gallen, 47°17' N, 9°32' E, see Figure 2A&B), a drained peatland with fen peat ~10 m thick. The site has a cool temperate-moist climate with a mean annual precipitation of 1297 mm and a mean annual temperature of 10.1 °C (1981 – 2010, <https://www.meteoswiss.admin.ch>). Drainage with ditches commenced before 1890 (<https://map.geo.admin.ch>). An intensive drainage system with drainage pipes (depth 1 m, distance between pipes 14 m) and pump was built in 1973. The site was used as pasture until 2013, and since then as an intensively managed meadow. In 2006 to 2007, one part of the field (1.7 ha) was covered with mineral soil material, with a thickness ~ 40 cm, to improve the trafficability and agriculture usability and to counteract peat subsidence by raising the distance

between the soil surface and the water level (Figure 2E). The field experiments were established at this mineral soil coverage site (Cov, see Figure 2C) and the adjacent drained organic soil without mineral soil coverage was used as the reference (Ref, see Figure 2D). Both sites have the identical farming practice, with 5 – 6 times cuts per year, receiving c. 230 kg N ha⁻¹ yr⁻¹ of nitrogen fertilizer, and similar vegetation. Dominant species are *Lolium perenne*, *Alopecurus pratensis*, *Festuca arundinacea*, *Trifolium spec.* and *Festuca pratensis*. The atmospheric N deposition at the study site as estimated for 2015 is 20 – 30 kg N ha⁻¹ yr⁻¹ (Rihm and Künzle, 2019).

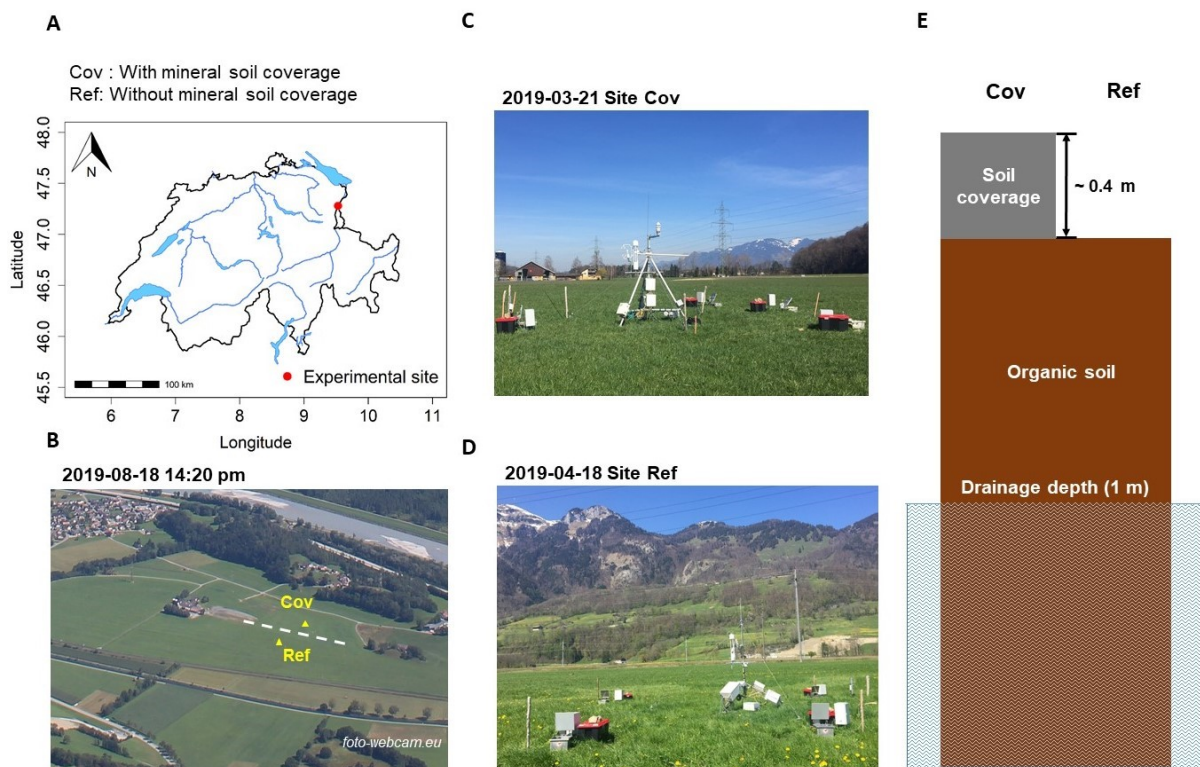


Figure 2. The location (A) of the experimental site and a photograph (B) showing the adjacent drained peatland with (Cov, C) and without (Ref, D) mineral soil coverage and the basic principle of mineral soil coverage (E).

3.2 Field installation, lab incubation and sampling

For the first experiment (**paper I**), soil-born CO₂ was collected with static chambers. Gas samples for each site were taken on July 16, August 18 and September 16 of 2019 in triplicate on Ref and Cov, respectively. Circular PVC frames for the chambers were installed in the soil. For sample collection, an opaque cylindrical PVC chamber was placed on the top of the frame. After allowing the CO₂ to accumulate in the chamber for 4 to 5 hours, gas from the headspace of the chamber was circulated through a battery-powered diaphragm pump (Thomas, Germany) to partially fill two 10 L Supel-Inert Foil Gas Sampling Bags (Supelco, Germany). Soil samples were collected at the center of each PVC frame. Soil cores were extracted by a motorized Humax with a 5 cm-diameter corer with internal plastic liner (Martin Burch AG, Switzerland) for the first 1 m depth, and a 5.2 cm-inner-diameter peat corer

(Eijkelkamp, The Netherlands) for the depth from 1 m to 2 m. Soil biochemical properties (pH, SOC, N content and bulk density) were determined throughout the whole soil profile. Samples representative of various depths and degradation status were investigated for ^{14}C content.

For the second experiment (**paper II**), N_2O fluxes were measured quasi-continuously for two entire years from 28 February 2019 to 02 March 2021. Gas samples were collected by an automatic time integrating chamber system (ATIC, Figure 3). The ATIC system was developed based on the automatic chamber system design introduced by Fiedler *et al.* (2005), and the air sampling follows the system introduced by Ambus *et al.* (2010). The ATIC is operated as a non-steady-state flow-through chamber with a main loop that recirculates the headspace chamber air. The lid of the chamber closes automatically for 15 min with a frequency of 3 – 9 hours per individual chamber (differing between growing season and non-growing season). During this period, four headspace gas samples are collected (at 3.50 min, 7.25 min, 11.50 min and 14.25 min after chamber closure) for 15 s and flushed into four different foil gas bags through a valve manifold. The use of the ATIC system allows flux measurements at relatively high frequency (like for online automatic chamber systems) but reduces the frequency of gas analysis and avoids the use of online trace gas analysis, which lowers the cost and energy consumption in the field.

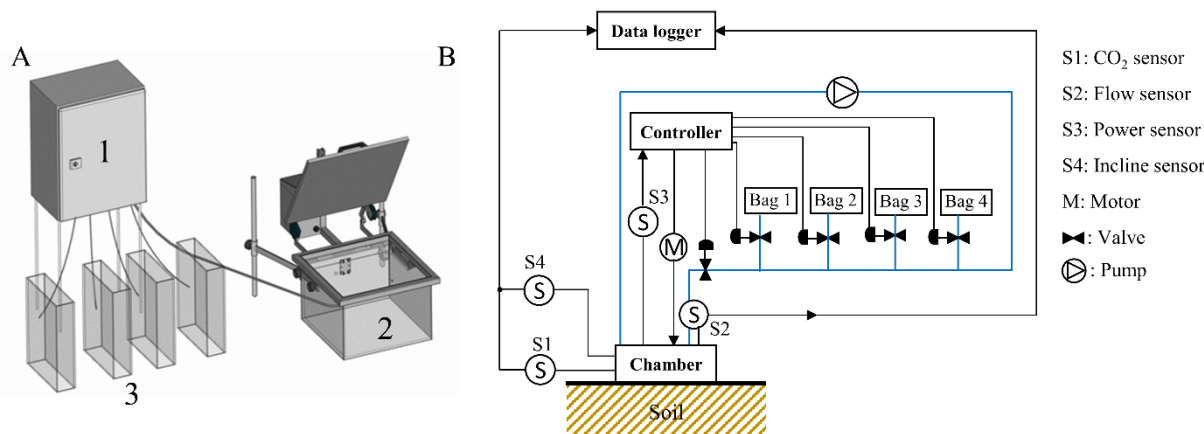


Figure 3. Brief overview of the automatic time integrating chamber system ATIC (A) and basic outline of ATIC gas sampling (B), black line indicate the control signal pathway, blue line indicates the sample gas pathway. From Wang *et al.* (2022)

The third experiment (**paper III**) was conducted from July 2020 to July 2021. In July 2020, eight plots (four for Cov, four for Ref; size, 3.5 m × 1.5m) were randomly selected in the experimental site. Each plot was divided into two subplots (1.5 m × 1.5m), one subplot received ^{15}N double-labelled ammonium nitrate ($^{15}\text{NH}_4^{15}\text{NO}_3$) as a treatment plot and the other one received the same amount but non-labelled ammonium nitrate (NH_4NO_3) as a control plot (see details in Figure 4A). ^{15}N fertilizer was applied at the same time as the regular fertilization events by the farmers. In order to spread the ^{15}N fertilizer salt solution homogeneously and to minimize the effect of soil disturbance during each soil sampling, each

subplot was divided into 15 units ($0.3 \text{ m} \times 0.5 \text{ m}$, see details in Figure 4B), the same amount of the salt solutions were applied to each unit. During the experimental period, each unit was sampled only once. Soil and plant samples were collected in combination with field harvest event on October 2020, May 2021, June 2021 and July 2021. Compositated soil samples were taken from three units at four different depths, 0 – 5 cm, 5 – 15 cm, 15 – 30 cm and 30 – 60 cm for each subplot. At the Cov site, samples from 30 – 60 cm were additionally divided at the boundary of the mineral soil cover and the underlying peat. In each plot from three unit, aboveground plant samples were cut by grass clippers to a height of 3 cm and root samples were collected by taking soil cores by 6.5 cm-inner-diameter corer down to 20 cm depth.

To determine the potential net soil mineralization rate for two sites, lab incubation was carried out in the third experiment (**paper III**). For this, 0 – 5 cm and 5 – 15 cm soil samples, which were collected in October 2020 were incubated for 28 days (4 weeks). Five duplicated ($n = 160$) soil samples, which equivalent to 10 g dry soils were weight into 50 ml PET containers, soil moisture were adjust to 60 % of the field water holding capacity every two days during incubation. The PET containers were incubated at 25 °C. Soil extractable N and ^{15}N were determined after 0, 7, 14, 21, 28 days of the incubation.

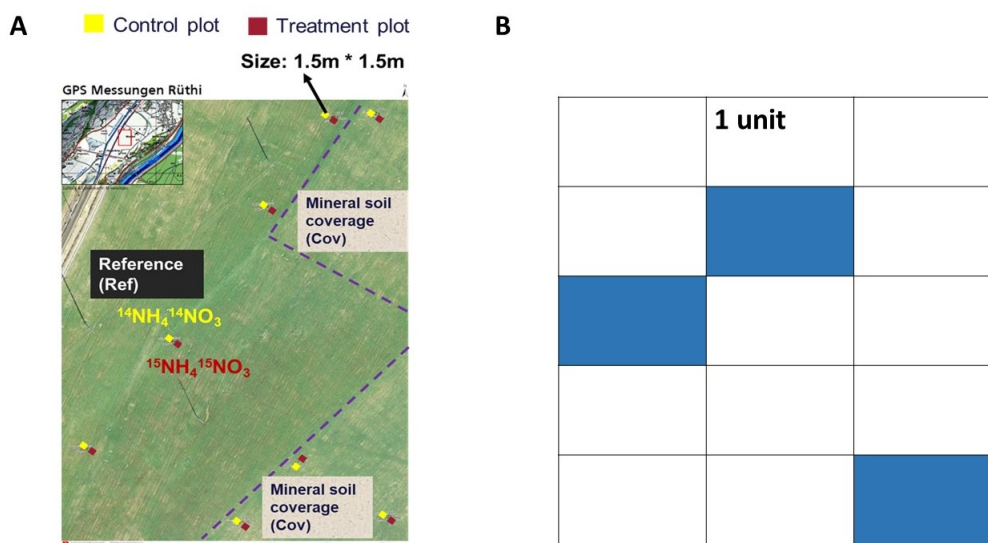


Figure 4. Brief overview of the field ^{15}N tracer experimental set up (A) and the 15 units of each subplot (B).

3.3 Sample pre-processing and analysis

3.3.1 Sample pre-processing

Soil samples from experiment one and three (**paper I** and **paper III**) were dried at 105 °C for 72 h, ground with mortar and pestle, and then milled in a ball mill (Retsch, MM 400, Germany) at 25-rotation

s⁻¹ for 3 min. Plant samples from experiment three (**paper III**) were dried at 60 °C in the oven for 72 h, cut into small pieces, milled in a ball mill (Retsch, MM 400, Germany) at 25-rotation s⁻¹ for 3 min and then loaded in a tin capsule to determine the elemental compositions. Soil extractable N and ¹⁵N from experiment three (**paper III**) were determined by mixing incubated soil samples with 80 ml 0.01M CaCl₂ solution, shaking at 160-cycles min⁻¹ for 30 min and subsequent filtration. Gas samples from experiment one and two (**paper I and II**) were pumped into the Supel-Inert Foil Gas Sampling Bags (Supelco, Germany) in the field and transferred to the lab for analysis.

3.3.2 Analytical instruments

The radiocarbon signature of soil and gas samples in experiment one (**paper I**) was performed with an accelerator mass spectrometer (AMS) at the Laboratory for the Analysis of Radiocarbon (LARA) of the University of Bern (Szidat *et al.*, 2014). For this, CO₂ was extracted from the collected samples and isolated from other air components using a cryogenic trap cooled with liquid nitrogen. The gas flow into and out of the trap was stabilized by a mass flow controller at the inlet and a scroll pump at the outlet, respectively, such that the pressure inside of the cryogenic trap remained at ~200 mbar in order to prevent condensation of liquid oxygen (Espic *et al.*, 2019). The isolated CO₂ was then transformed into solid graphite targets, which were employed in the AMS analysis (Szidat *et al.*, 2014). For soil samples, the pretreated samples were combusted in an elemental analyzer and the evolving CO₂ was transformed into graphite targets for AMS measurement. The gas (CO₂ and N₂O) concentration in experiment one and two (**paper I and II**) were performed with a cavity ring down spectroscopy gas concentration analyzer (Picarro, G2308, USA). The C and N contents in experiment one and three (**paper I and III**) was determined by elemental analysis (Hekatech, Germany). The ¹⁵N signature of soil, plant and soil extracts in experiment three (**paper III**) were determined by elemental analysis isotope ratio mass spectrometry (EA-IRMS). The pretreated soil and plant samples were combusted in an elemental analyzer (vario PYRO cube, Elementar, Germany for soil and plant samples; vario TOC cube, Elementar, Germany for soil extracts) and the gas transferred for isotope measurement to the isotope ratio mass spectrometer (isoprime precisION, Elementar, Germany).

3.4 Statistics

All the statistical analyses were performed in R (version 3.6.0 & version 4.1.3). The error probability was chosen as $p < 0.05$ for all the studies. Statistical procedures such as t-Test (**paper I, II and III**), linear regression (**paper II**) and ANOVA (**paper I and III**) were used to describe the data in this study. For **paper I**, a stable isotope mixing models was used to analyze the data. For **paper II**, a multiple linear regression (MLR) model with unstandardized explanatory variables was used to analyze the data. For **paper I and III**, a Tukey HSD test was performed for multiple pairwise-comparison of the data. Results are always reported as mean \pm 1 standard error (se).

4 Results and Discussion

4.1 Effect of mineral soil coverage on C loss from drained peatland

The first experiment (**paper I**) sought to explore the effect of mineral soil coverage on soil C loss and the source of CO₂ by combining a profile-based and a flux-based method. The profile based results showed that drainage induced 41 – 75 kg C m⁻² loss, which is equivalent to annual C loss rates of 0.49 – 0.58 kg C m⁻² a⁻¹ and 0.31 – 0.63 kg C m⁻² a⁻¹ for Cov and Ref, respectively. This finding is in agreement with other C loss studies in peatlands managed for grassland in Europe, where drainage induced 0.25 – 0.91 kg C m⁻² yr⁻¹ carbon loss (Rogiers *et al.*, 2008; Leifeld *et al.*, 2011; Krüger *et al.*, 2015; Fell *et al.*, 2016).

The flux-based method showed that mineral soil coverage had no significant effect on the amount of heterotrophic respiration. However, at Cov, the radiocarbon signature of heterotrophic CO₂ was significantly ($p < 0.01$) younger than at Ref, indicating that mineral soil coverage shifted the source of decomposition of soil organic carbon (SOC) from a higher share of old peat towards a higher share of relatively younger material. More specifically, the F¹⁴CO₂ values of heterotrophic soil respiration were lower than those of fresh plant residues, but higher than the topsoil's signature, implying that the CO₂ originated from a mixture of old SOC and recently accumulated plant residues. The more detailed analysis revealed that old carbon from the middle soil layer (peat layer) at a depth of 50 cm also contributed to the overall heterotrophic soil respiration with shares of 7.6–14.0 % and 11.1–22.4 % from the Cov and the Ref, respectively. These results suggest that the decomposition of old peat at the deeper layer contributes substantially to the evolved CO₂ in both treatments, and leads to the above described C loss from the soil in the long term. These results align with former research where it has been shown that not only the younger plant residues contributed to the emitted CO₂ in drained peatlands, but also older peat (Wright *et al.*, 2011; Bader *et al.*, 2017). A possible reduction in the decomposition rate of old peat at the Cov site must not be in contradiction to the observed long-term loss rates which were not different between Cov and Ref, considering that a gradual change in the loss rate of old peat will not be immediately visible in the profile record.

Overall, the results indicate coverage of the drained organic soil with mineral material seems not to decrease the C loss, but to shift the source of soil Rh from the surface peat to recent assimilates in the covered mineral soil material. This may move the system towards a reduced peat loss in the future, but further long-term and multiply field ¹⁴CO₂ observations are needed to support this interpretation.

4.2 Effect of mineral soil coverage on N₂O emissions from drained peatland

The second experiment (**paper II**) aimed to quantify the N₂O emissions from an agriculturally managed peatland in Switzerland and to evaluate the effect of mineral soil coverage on these emissions. N₂O emissions were continuously monitored over two years using an automatic time integrating chamber (ATIC) system. The result showed that mineral soil cover induced a strong and significant reduction of N₂O emissions by almost 90 %. During the experimental period, site Ref released $20.5 \pm 2.7 \text{ kg N ha}^{-1} \text{ yr}^{-1}$ N₂O-N, which was at the upper end of previously measured fluxes from drained peatland (Danevčič *et al.*, 2010; IPCC, 2014; Leppelt *et al.*, 2014; Tiemeyer *et al.*, 2016). In contrast the N₂O emissions from Cov were on average only $2.3 \pm 0.4 \text{ kg N ha}^{-1} \text{ yr}^{-1}$, which are in the range of N₂O emissions from grasslands on mineral soils in Switzerland (Flechard *et al.*, 2005; Fuchs *et al.*, 2020). At both sites, N₂O emission peaks were primarily triggered by fertilization events and lasted for 2 – 3 weeks before returning to background N₂O emissions. N₂O peaks related to fertilization events contributed more than half of the overall N₂O emissions. At the Cov site, not only the fertilization induced N₂O peaks, but also background N₂O emissions were lower than at the Ref site.

The data suggest a strong and continued reduction of N₂O emissions with mineral soil cover from the investigated peatland. Mineral soil coverage, therefore, seems to be a promising N₂O mitigation option for intensively used drained organic soils when a sustained use of the drained peatland for intensive agricultural production is foreseen.

4.3 Effect of mineral soil coverage on plant N uptake

Mineral soil cover induced a strong reduction of N₂O emissions from drained peatland (**paper II**). Based on this evidence, the third experiment (**paper III**) sought to further explore the effect of mineral soil coverage on the plant-soil system N loss. Grass biomass (above- and belowground) were sampled at four consecutive harvest events. During the experimental period (from August 2020 to July 2021), site Cov had slightly higher yield than the drained peatland site, which also resulted in higher ($p < 0.05$) grass N uptake from the Cov site ($274.34 \pm 22.78 \text{ kg N ha}^{-1}$) compared with the Ref site ($229.97 \pm 10.56 \text{ kg N ha}^{-1}$). This indicates that application of a mineral soil coverage does sustain the productivity of drained peatland. Moreover, the field ¹⁵N experiment showed that mineral soil coverage had no significant effect on the plant and root ¹⁵N uptake. The cumulative tracer exports through grass harvest accounted for $32.2 \pm 2.2 \%$ and $30.0 \pm 0.3 \%$ of the applied ¹⁵N for site Cov and Ref, respectively, and root took up $2.5 \pm 0.3 \%$ and $3.9 \pm 0.5 \%$ of the applied ¹⁵N from Cov and Ref respectively. For both sites, the share of applied ¹⁵N fertilizer taken up by plants was similar with the results reported in a meta-analysis of ¹⁵N tracer studies on grassland worldwide. That analysis indicated that plant took up ~30 % of the applied ¹⁵N tracer (Templer *et al.*, 2012).

4.4 Effect of mineral soil coverage on N losses from the plant-soil system

In the third experiment (**paper III**), the mass balance of ^{15}N in the plant-soil system was used to account for the quantitative recovery of ^{15}N . It is based on the premise that any ^{15}N which was not retained in plants or soil can be defined as an N loss from the system, whereby the contribution of the loss pathways i.e. leaching, gaseous losses, remains unknown. During the experimental period, the Ref site had higher ^{15}N losses ($p < 0.05$) than the Cov. At Ref, 56.2 ± 3.1 % of the applied tracer was lost whereas at site Ref, 45.4 ± 3.0 % of the applied tracer was lost. The lower ^{15}N loss at the Cov site might be related to the greater ^{15}N retention in the soil organic pool from the covered mineral soil material. Mineral soil coverage induced a higher ^{15}N retention in the soil organic pool, with more ^{15}N tracer remaining at Cov (19.8 ± 2.0 %) than Ref (9.8 ± 3.2 %) over the experimental period. The latter number is at the lower end of the ^{15}N retention from drained fen peatland as reported by Augustin *et al.*, (1997), who found that 10 – 20 % of the applied ^{15}N tracer was recovered in the soil organic pool over one growing season. The soil ^{15}N recovery (~ 20 % of the applied ^{15}N tracer) from site Cov was generally within the range of the data reported from other ^{15}N tracer study on mineral soil grassland in Europe, which is 15 – 40 % (Jenkinson *et al.*, 2004; De Vries *et al.*, 2011; Zistl-Schlingmann *et al.*, 2020). In short, mineral soil coverage significantly reduced the overall ^{15}N loss, indicating that mineral soil coverage has the potential to reduce the fertilization-induced N loss from drained peatland.

As well as a lower N loss from the Cov site, the soil $\text{N}_{\text{r_min}}$ release was also slower with mineral soil coverage. The lab incubation over four weeks showed that average soil $\text{N}_{\text{r_min}}$ release was significantly higher ($p < 0.05$) at site Ref (6.07 ± 0.84 mg N kg $^{-1}$ soil day $^{-1}$) compared with Cov (2.1 ± 0.15 mg N kg $^{-1}$ soil day $^{-1}$) at the 0 – 5 cm's soil depth. It was also significantly higher ($p < 0.01$) at site Ref (5.45 ± 0.26 mg N kg $^{-1}$ soil day $^{-1}$) compared with Cov (1.71 ± 0.13 mg N kg $^{-1}$ soil day $^{-1}$) at 5 – 15 cm's soil depth. A similar trend was also found for the soil $^{15}\text{N}_{\text{r_min}}$ release, where site Ref had higher soil $^{15}\text{N}_{\text{r_min}}$ than Cov at both 0 – 5 cm and 5 – 15 cm depth. However, the specific release per unit soil nitrogen (specific soil $\text{N}_{\text{sr_min}}$ release) was lower ($p < 0.05$) at site Ref (0.35 ± 0.03 mg N g $^{-1}$ N day $^{-1}$) than Cov (0.60 ± 0.07 mg N g $^{-1}$ N day $^{-1}$). This finding indicates that, SOM in the surface soil at site Cov is more labile compared with Ref, and that the higher soil $\text{N}_{\text{r_min}}$ release from Ref is mainly caused by the larger quantity of SOM.

Altogether, the higher soil ^{15}N retention and lower soil $\text{N}_{\text{r_min}}$ release indicate that the surface soil at the Cov site stabilize more fertilizer N than the Ref, those part of the stabilized N may stay in the labile soil N pool and become the source for microbial mineralization instead of the “native” soil N. However, at the Ref site, the lower soil ^{15}N retention and higher soil $\text{N}_{\text{r_min}}$ indicates that the original peat N must contribute to the microbial mineralization with a higher share than at Cov. This may lead to more peat decomposition at the Ref site than at Cov in the long run.

5 Conclusions

This thesis quantifies the change of GHG emissions, soil C and N balances associated with a peatland management measure that is being more and more applied by farmers. Findings outlined here provide evidence that mineral soil coverage, which itself is a technique used by farmers to counterbalance soil subsidence, could have the potential to mitigate C and N losses from drained peatland. However, the findings also indicate that the potential of GHG mitigation is smaller as the one typically found for rewetting. Yet, the findings from this thesis encourage further research on this measure, particularly for those regions where rewetting is in principle possible but limited by social-economic and political reasons.

This work demonstrates that drainage of organic soil for agriculture caused large C and N losses due to the decomposition of the peat. Correspondingly, C from peat decomposition contributed to around half of the total heterotrophic CO₂ from soil in the Ref site, partially stemming also from carbon stored in the subsoil. N loss from drained peatland was not only caused by peat mineralization, but was also stemming from fertilizer N application, 56% of the applied fertilizer was lost to the environment in the drained peatland without mineral soil coverage. Among those N losses, ~ 20 kg N ha⁻¹ yr⁻¹ was emitted to the atmosphere as N₂O.

Coverage of this drained organic soil with mineral material does not decrease the SOC loss, but shifts the source of soil Rh from peat to recent assimilates. The CO₂ emissions remain high, but the peat decomposition rate is reduced. Moreover, mineral soil coverage of drained peat reduces the system N losses significantly, as the N₂O emission were reduced 9-fold with mineral soil coverage. The N loss reduction was not only caused by the lower N losses from fertilization with ~ 46 % of the applied fertilizer lost, but also related to the slower soil N_{r_min}, with only 2.1 ± 0.15 mg N kg⁻¹ day⁻¹ at 0 – 5 cm depth. Lastly, the measurements showed that mineral soil coverage can sustain the agricultural productivity of a drained peatland.

Overall, our results imply that mineral soil coverage provides an opportunity for not only sustaining the agricultural productivity of drained peatlands but also for reducing the peat decomposition rate and environmental pollution as induced by N₂O emissions and N losses via leaching. Hence, mineral soil coverage provides a less environmentally harmful management compared to agriculturally use drained peatland without any actions.

6 Outlook

The comparison of the fate of C and N between a drained peatland with and without mineral soil coverage allowed us to better understand the effect of mineral soil coverage on peat decomposition and

environmental pollutions from agricultural management. This thesis provides data that support a management strategy for agriculturally-used peatlands that not only sustains agricultural productivity but also reduces some of the environmental costs of farming these lands. It therefore provides opportunities for reducing the environmental cost of using agricultural peatlands in the future.

This thesis provides a unique data set from long-term field observation of C loss and plant – soil system N balance, which are two important indicators for environmental pollution and peatland degradation. However, many other aspects e.g. nutrient (NO_3^- , dissolved organic matter) leaching and cycling, biodiversity, and the GHGs emission during the transportation of the mineral soil material, which are crucial indicators for the environmental impact of drained peatland with and without mineral soil coverage, were not included in this thesis. Evaluating those missing parameters should be a vital part for further studies for a more comprehensive assessment of the impact of mineral soil coverage on the environmental cost of agricultural production on drained peatlands. In addition, for grassland on organic soil, the influence of mineral soil coverage on the nutrient (other than N) supply to the crop also need to be evaluated.

The findings presented in this thesis were obtained from only one drained fen peat located in the temperate zone; it is therefore not representative of all types of peat and climate zones e.g. peatlands with bog peat (nutrient-poor) in the temperate zone, or peatlands in other climate regions, where the peat properties and environmental conditions are different. Therefore, testing the universality of this peatland management in different climate zones with different mineral soil coverage depths and types is highly recommended. To further dig into those questions, the following three research topics could be done:

I. Multiple field observations. Field experiment from peatlands with different types of peat and different types of mineral soil material as well as thickness of the mineral soil cover, and in different climatic zone, are needed to evaluate the effectiveness of this measure in more general terms, in particularly with respect to the ecosystems GHG balance.

II. Ecosystem manipulation experiments. Controlled experiments, for example using microcosms, with soil taken from different sites and depths, are needed for determining the influence of mineral soil coverage on microbial activities, soil biochemical properties and soil structure. Such experiments would help to gain deeper mechanistic insight into impact of mineral soil coverage on soil degradation and environmental pollution from drained peatland.

III. Model studies. To better explore the large- scale effect of mineral soil cover on peat degradation and environmental pollution from drained organic soils, it is necessary to set up mechanistic models with the existing data for simulating the effect of mineral soil cover on organic matter decomposition, environmental pollution and GHG emissions, and agricultural productivity on drained peatlands. Models that comprehensively describe the C and N dynamics of drained peatlands are only about to develop. There is a range of models that have been used to simulate GHG emissions from drained peatland

(Farmer *et al.*, 2011). However, there is currently no suitable model for application to drained peatland with mineral soil coverage. Further developing these models with the now available and future data from mineral soil cover sites would be an important next step that would also allow to better constrain the modelling of feedbacks mechanisms occurring between mineral soil coverage, peatland degradation and climate change.

References

- Adams, R.M., Hurd, B.H., Lenhart, S., Leary, N., 1998. Effects of global climate change on agriculture: an interpretative review. *Climate Research*. 11, 19-30. <https://doi.org/10.3354/cr011019>.
- Ambus, P., Skiba, U., Drewer, J., Jones, S.K., Carter, M.S., Albert, K.R., Sutton, M.A., 2010. Development of an accumulation-based system for cost-effective chamber measurements of inert trace gas fluxes. *European Journal of Soil Science*. 61, 785-792. <https://doi.org/10.1111/j.1365-2389.2010.01272.x>.
- Augustin, J., Merbach, W., Käding, H., Schmidt, W., Schalitz, G., Russow, R., Ende, H.P., 1997. N Balance experiments on fen grassland with ¹⁵N labelled fertilizer. *Isotopes in Environmental and Health Studies*. 33, 31-37. <https://doi.org/10.1080/10256019808036356>.
- Bader, C., Müller, M., Schulin, R., Leifeld, J., 2017. Amount and stability of recent and aged plant residues in degrading peatland soils. *Soil Biology and Biochemistry*. 109, 167-175. <https://doi.org/10.1016/j.soilbio.2017.01.029>.
- Bayley, S.E., Thormann, M.N., Szumigalski, A.R., 2016. Nitrogen mineralization and decomposition in western boreal bog and fen peat. *Écoscience*. 12, 455-465. <https://doi.org/10.2980/i1195-6860-12-4-455.1>.
- Belyea, L.R., Malmer, N., 2004. Carbon sequestration in peatland: patterns and mechanisms of response to climate change. *Global Change Biology*. 10, 1043-1052. <https://doi.org/10.1111/j.1365-2486.2004.00783.x>.
- Bonn, A., Reed, M.S., Evans, C.D., Joosten, H., Bain, C., Farmer, J., Emmer, I., Couwenberg, J., Moxey, A., Artz, R., Tanneberger, F., von Unger, M., Smyth, M.-a., Birnie, D., 2014. Investing in nature: Developing ecosystem service markets for peatland restoration. *Ecosystem Services*. 9, 54-65. <https://doi.org/10.1016/j.ecoser.2014.06.011>.
- Bowles, T.M., Atallah, S.S., Campbell, E.E., Gaudin, A.C.M., Wieder, W.R., Grandy, A.S., 2018. Addressing agricultural nitrogen losses in a changing climate. *Nature Sustainability*. 1, 399-408. <https://doi.org/10.1038/s41893-018-0106-0>.
- Brierley, A.S., Kingsford, M.J., 2009. Impacts of climate change on marine organisms and ecosystems. *Current Biology*. 19, R602-614. <https://doi.org/10.1016/j.cub.2009.05.046>.
- Byrnes, B., 1990. Environmental effects of N fertilizer use—An overview. *Fertilizer Research*. 26, 209-215. <https://doi.org/10.1007/BF01048758>.
- Chen, H., Xu, X., Fang, C., Li, B., Nie, M., 2021. Differences in the temperature dependence of wetland CO₂ and CH₄ emissions vary with water table depth. *Nature Climate Change*. 11, 766-771. <https://doi.org/10.1038/s41558-021-01108-4>.

- Collier, M.J., 2011. Incorporating socio-economic factors into restoration: Implications from industrially harvested peatlands. *Restoration Ecology*. 19, 559-563. <https://doi.org/10.1111/j.1526-100X.2011.00794.x>.
- Danevčič, T., Mandić-Mulec, I., Stres, B., Stopar, D., Hacin, J., 2010. Emissions of CO₂, CH₄ and N₂O from Southern European peatlands. *Soil Biology and Biochemistry*. 42, 1437-1446. <https://doi.org/10.1016/j.soilbio.2010.05.004>.
- Davidson, E.A., Keller, M., Erickson, H.E., Verchot, L.V., Veldkamp, E., 2000. Testing a conceptual model of soil emissions of nitrous and nitric oxides: using two functions based on soil nitrogen availability and soil water content, the hole-in-the-pipe model characterizes a large fraction of the observed variation of nitric oxide and nitrous oxide emissions from soils. *Bioscience*. 50, 667-680. [https://doi.org/10.1641/0006-3568\(2000\)050\[0667:TACMOS\]2.0.CO;2](https://doi.org/10.1641/0006-3568(2000)050[0667:TACMOS]2.0.CO;2).
- De Groot, R.S., Wilson, M.A., Boumans, R.M., 2002. A typology for the classification, description and valuation of ecosystem functions, goods and services. *Ecological Economics*. 41, 393-408. [https://doi.org/10.1016/S0921-8009\(02\)00089-7](https://doi.org/10.1016/S0921-8009(02)00089-7).
- De Vries, F.T., van Groenigen, J.W., Hoffland, E., Bloem, J., 2011. Nitrogen losses from two grassland soils with different fungal biomass. *Soil Biology and Biochemistry*. 43, 997-1005. <https://doi.org/10.1016/j.soilbio.2011.01.016>.
- Dohong, A., Abdul Aziz, A., Dargusch, P., 2018. A review of techniques for effective tropical peatland restoration. *Wetlands*. 38, 275-292. <https://doi.org/10.1007/s13157-018-1017-6>.
- Espic, C., Liechti, M., Battaglia, M., Paul, D., Röckmann, T., Szidat, S., 2019. Compound-Specific Radiocarbon Analysis of Atmospheric Methane: A New Preconcentration and Purification Setup. *Radiocarbon*. 61, 1461-1476. <https://doi.org/10.1017/rdc.2019.76>.
- Evans, C.D., Peacock, M., Baird, A.J., Artz, R.R.E., Burden, A., Callaghan, N., Chapman, P.J., Cooper, H.M., Coyle, M., Craig, E., Cumming, A., Dixon, S., Gauci, V., Grayson, R.P., Helfter, C., Heppell, C.M., Holden, J., Jones, D.L., Kaduk, J., Levy, P., Matthews, R., McNamara, N.P., Misselbrook, T., Oakley, S., Page, S.E., Rayment, M., Ridley, L.M., Stanley, K.M., Williamson, J.L., Worrall, F., Morrison, R., 2021. Overriding water table control on managed peatland greenhouse gas emissions. *Nature*. 593, 548-552. <https://doi.org/10.1038/s41586-021-03523-1>.
- Farmer, J., Matthews, R., Smith, J.U., Smith, P., Singh, B.K., 2011. Assessing existing peatland models for their applicability for modelling greenhouse gas emissions from tropical peat soils. *Current Opinion in Environmental Sustainability*. 3, 339-349. <https://doi.org/10.1016/j.cosust.2011.08.010>.
- Fell, H., Roßkopf, N., Bauriegel, A., Zeitz, J., 2016. Estimating vulnerability of agriculturally used peatlands in north-east Germany to carbon loss based on multi-temporal subsidence data analysis. *Catena*. 137, 61-69. <https://doi.org/10.1016/j.catena.2015.08.010>.

- Ferré, M., Muller, A., Leifeld, J., Bader, C., Müller, M., Engel, S., Wichmann, S., 2019. Sustainable management of cultivated peatlands in Switzerland: Insights, challenges, and opportunities. *Land Use Policy*. 87, 104019. <https://doi.org/10.1016/j.landusepol.2019.05.038>.
- Fiedler, S., Holl, B.S., Jungkunst, H.F., 2005. Methane budget of a Black Forest spruce ecosystem considering soil pattern. *Biogeochemistry*. 76, 1-20. <https://doi.org/10.1007/s10533-005-5551-y>.
- Fischer, G., Shah, M., Tubiello, F.N., van Velhuizen, H., 2005. Socio-economic and climate change impacts on agriculture: an integrated assessment, 1990-2080. *Philosophical Transactions of the Royal Society B: Biological Sciences*. 360, 2067-2083. <https://doi.org/10.1098/rstb.2005.1744>.
- Flechar, C.R., Ambus, P., Skiba, U., Rees, R.M., Hensen, A., van Amstel, A., Dasselaar, A.v.d.P.-v., Soussana, J.F., Jones, M., Clifton-Brown, J., Raschi, A., Horvath, L., Neftel, A., Jocher, M., Ammann, C., Leifeld, J., Fuhrer, J., Calanca, P., Thalman, E., Pilegaard, K., Di Marco, C., Campbell, C., Nemitz, E., Hargreaves, K.J., Levy, P.E., Ball, B.C., Jones, S.K., van de Bulk, W.C.M., Groot, T., Blom, M., Domingues, R., Kasper, G., Allard, V., Ceschia, E., Cellier, P., Laville, P., Henault, C., Bizouard, F., Abdalla, M., Williams, M., Baronti, S., Berretti, F., Grosz, B., 2007. Effects of climate and management intensity on nitrous oxide emissions in grassland systems across Europe. *Agriculture, Ecosystems & Environment*. 121, 135-152. <https://doi.org/10.1016/j.agee.2006.12.024>.
- Flechar, C.R., Neftel, A., Jocher, M., Ammann, C., Fuhrer, J., 2005. Bi-directional soil/atmosphere N₂O exchange over two mown grassland systems with contrasting management practices. *Global Change Biology*. 11, 2114-2127. <https://doi.org/10.1111/j.1365-2486.2005.01056.x>.
- Frolking, S., Roulet, N.T., Moore, T.R., Richard, P.J.H., Lavoie, M., Muller, S.D., 2001. Modeling northern peatland decomposition and peat accumulation. *Ecosystems*. 4, 479-498. <https://doi.org/10.1007/s10021-001-0105-1>.
- Frolking, S., Talbot, J., Jones, M.C., Treat, C.C., Kauffman, J.B., Tuittila, E.-S., Roulet, N., 2011. Peatlands in the Earth's 21st century climate system. *Environmental Reviews*. 19, 371-396. <https://doi.org/10.1139/a11-014>.
- Fuchs, K., Merbold, L., Buchmann, N., Bretscher, D., Brill, L., Fitton, N., Topp, C.F.E., Klumpp, K., Lieffering, M., Martin, R., Newton, P.C.D., Rees, R.M., Rolinski, S., Smith, P., Snow, V., 2020. Multimodel evaluation of nitrous oxide emissions from an intensively managed grassland. *Journal of Geophysical Research: Biogeosciences*. 125, e2019JG005261. <https://doi.org/10.1029/2019jg005261>.
- Gorham, E., 1991. Northern peatlands: role in the carbon cycle and probable responses to climatic warming. *Ecological Applications*. 1, 182-195. <https://doi.org/10.2307/1941811>.
- Göttlich, K., 1990. *Moor-und Torfkunde*. Schweizerbart'sche Verlagsbuchhandlung, Stuttgart.
- Gunther, A., Barthelmes, A., Huth, V., Joosten, H., Jurasinski, G., Koebisch, F., Couwenberg, J., 2020. Prompt rewetting of drained peatlands reduces climate warming despite methane emissions. *Nature Communications*. 11, 1644. <https://doi.org/10.1038/s41467-020-15499-z>.

- Hatala, J.A., Detto, M., Sonnentag, O., Deverel, S.J., Verfaillie, J., Baldocchi, D.D., 2012. Greenhouse gas (CO₂, CH₄, H₂O) fluxes from drained and flooded agricultural peatlands in the Sacramento-San Joaquin Delta. *Agriculture Ecosystems & Environment*. 150, 1-18.
<https://doi.org/10.1016/j.agee.2012.01.009>.
- Hemes, K.S., Chamberlain, S.D., Eichelmann, E., Anthony, T., Valach, A., Kasak, K., Szutu, D., Verfaillie, J., Silver, W.L., Baldocchi, D.D., 2019. Assessing the carbon and climate benefit of restoring degraded agricultural peat soils to managed wetlands. *Agricultural and Forest Meteorology*. 268, 202-214. <https://doi.org/10.1016/j.agrformet.2019.01.017>.
- Holden, J., Chapman, P.J., Labadz, J.C., 2016. Artificial drainage of peatlands: hydrological and hydrochemical process and wetland restoration. *Progress in Physical Geography: Earth and Environment*. 28, 95-123. <https://doi.org/10.1191/0309133304pp403ra>.
- Howden, S.M., Soussana, J.F., Tubiello, F.N., Chhetri, N., Dunlop, M., Meinke, H., 2007. Adapting agriculture to climate change. *Proceedings of the national academy of sciences*. 104, 19691-19696. <https://doi.org/10.1073/pnas.0701890104>.
- Hoyt, A.M., Chaussard, E., Seppalainen, S.S., Harvey, C.F., 2020. Widespread subsidence and carbon emissions across Southeast Asian peatlands. *Nature Geoscience*. 13, 435-440.
<https://doi.org/10.1038/s41561-020-0575-4>.
- Huang, Y., Ciais, P., Luo, Y., Zhu, D., Wang, Y., Qiu, C., Goll, D.S., Guenet, B., Makowski, D., De Graaf, I., 2021. Tradeoff of CO₂ and CH₄ emissions from global peatlands under water-table drawdown. *Nature Climate Change*. 11, 618-622. <https://doi.org/10.1038/s41558-021-01059-w>.
- IPCC, 2014. 2013 Supplement to the 2006 IPCC Guidelines for National Greenhouse Gas Inventories (IPCC, Wetlands, 2014).
- IPCC, 2021. Climate Change 2021: The Physical Science Basis. Contribution of Working Group I to the Sixth Assessment Report of the Intergovernmental Panel on Climate Change.
- Jenkinson, D.S., Poulton, P.R., Johnston, A.E., Powlson, D.S., 2004. Turnover of nitrogen - 15 - labeled fertilizer in old grassland. *Soil Science Society of America Journal*. 68, 865-875.
<https://doi.org/10.2136/sssaj2004.8650>.
- Ju, X., Xing, G., Chen, X., Zhang, S., Zhang, L., Liu, X., Cui, Z., Yin, B., Christie, P., Zhu, Z., Zhang, F., 2009. Reducing environmental risk by improving N management in intensive Chinese agricultural systems. *Proceedings of the National Academy of Sciences*. 106, 3041-3046.
<https://doi.org/10.1073/pnas.0813417106>.
- Kalbitz, K., Schwesig, D., Rethemeyer, J., Matzner, E., 2005. Stabilization of dissolved organic matter by sorption to the mineral soil. *Soil Biology and Biochemistry*. 37, 1319-1331.
<https://doi.org/10.1016/j.soilbio.2004.11.028>.
- Karl, T.R., Trenberth, K.E., 2003. Modern global climate change. *Science*. 302, 1719-1723.
<https://doi.org/10.1126/science.1090228>.

- Kasimir Klemedtsson, Å., Weslien, P., Klemedtsson, L., 2009. Methane and nitrous oxide fluxes from a farmed Swedish Histosol. *European Journal of Soil Science*. 60, 321-331.
<https://doi.org/10.1111/j.1365-2389.2009.01124.x>.
- Knox, S.H., Sturtevant, C., Matthes, J.H., Koteen, L., Verfaillie, J., Baldocchi, D., 2015. Agricultural peatland restoration: effects of land-use change on greenhouse gas (CO₂ and CH₄) fluxes in the Sacramento-San Joaquin Delta. *Global Change Biology*. 21, 750-765.
<https://doi.org/10.1111/gcb.12745>.
- Krüger, J.P., Alewell, C., Minkinen, K., Szidat, S., Leifeld, J., 2016. Calculating carbon changes in peat soils drained for forestry with four different profile-based methods. *Forest Ecology and Management*. 381, 29-36. <https://doi.org/10.1016/j.foreco.2016.09.006>.
- Krüger, J.P., Leifeld, J., Glatzel, S., Alewell, C., 2015. Soil carbon loss from managed peatlands along a land use gradient—a comparison of three different methods. *BGS Bulletin*. 36, 45-50.
<https://doi.org/10.5451/unibas-ep40217>.
- Lee, S.C., Christen, A., Black, A.T., Johnson, M.S., Jassal, R.S., Ketler, R., Nesic, Z., Merkens, M., 2017. Annual greenhouse gas budget for a bog ecosystem undergoing restoration by rewetting. *Biogeosciences*. 14, 2799-2814. <https://doi.org/10.5194/bg-14-2799-2017>.
- Leifeld, J., Alewell, C., Bader, C., Krüger, J.P., Mueller, C.W., Sommer, M., Steffens, M., Szidat, S., 2018. Pyrogenic Carbon Contributes Substantially to Carbon Storage in Intact and Degraded Northern Peatlands. *Land Degradation & Development*. 29, 2082-2091.
<https://doi.org/10.1002/ldr.2812>.
- Leifeld, J., Menichetti, L., 2018. The underappreciated potential of peatlands in global climate change mitigation strategies. *Nature Communications*. 9, 1071. <https://doi.org/10.1038/s41467-018-03406-6>.
- Leifeld, J., Müller, M., Fuhrer, J., 2011. Peatland subsidence and carbon loss from drained temperate fens. *Soil Use and Management*. 27, 170-176. <https://doi.org/10.1111/j.1475-2743.2011.00327.x>.
- Leifeld, J., Wüst-Galley, C., Page, S., 2019. Intact and managed peatland soils as a source and sink of GHGs from 1850 to 2100. *Nature Climate Change*. 9, 945-947. <https://doi.org/10.1038/s41558-019-0615-5>.
- Leppelt, T., Dechow, R., Gebbert, S., Freibauer, A., Lohila, A., Augustin, J., Drösler, M., Fiedler, S., Glatzel, S., Höper, H., Järveoja, J., Lærke, P.E., Maljanen, M., Mander, Ü., Mäkiranta, P., Minkinen, K., Ojanen, P., Regina, K., Strömberg, M., 2014. Nitrous oxide emission budgets and land-use-driven hotspots for organic soils in Europe. *Biogeosciences*. 11, 6595-6612.
<https://doi.org/10.5194/bg-11-6595-2014>.
- Limpens, J., Berendse, F., Blodau, C., Canadell, J., Freeman, C., Holden, J., Roulet, N., Rydin, H., Schaepman-Strub, G., 2008. Peatlands and the carbon cycle: from local processes to global implications—a synthesis. *Biogeosciences*. 5, 1475-1491. <https://doi.org/10.5194/bg-5-1475-2008>, 2008.

- Mishra, S., Page, S.E., Cobb, A.R., Lee, J.S.H., Jovani - Sancho, A.J., Sjögersten, S., Jaya, A., Aswandi, Wardle, D.A., 2021. Degradation of Southeast Asian tropical peatlands and integrated strategies for their better management and restoration. *Journal of Applied Ecology*. 58, 1370-1387. <https://doi.org/10.1111/1365-2664.13905>.
- Moore, P.D., 2002. The future of cool temperate bogs. *Environmental Conservation*. 29, 3-20. <https://doi.org/10.1017/s0376892902000024>.
- Murdiyarmo, D., Hergoualc'h, K., Verchot, L.V., 2010. Opportunities for reducing greenhouse gas emissions in tropical peatlands. *Proceedings of the National Academy of Sciences* 107, 19655-19660. <https://doi.org/10.1073/pnas.0911966107>.
- Neftel, A., Blatter, A., Schmid, M., Lehmann, B., Tarakanov, S.V., 2000. An experimental determination of the scale length of N₂O in the soil of a grassland. *Journal of Geophysical Research: Atmospheres*. 105, 12095-12103. <https://doi.org/10.1029/2000JD900088>.
- Page, S.E., Rieley, J.O., Banks, C.J., 2011. Global and regional importance of the tropical peatland carbon pool. *Global Change Biology*. 17, 798-818. <https://doi.org/10.1111/j.1365-2486.2010.02279.x>.
- Parn, J., Verhoeven, J.T.A., Butterbach-Bahl, K., Dise, N.B., Ullah, S., Aasa, A., Egorov, S., Espenberg, M., Jarveoja, J., Jauhiainen, J., Kasak, K., Klemetsson, L., Kull, A., Laggoun-Defarge, F., Lapshina, E.D., Lohila, A., Lohmus, K., Maddison, M., Mitsch, W.J., Muller, C., Niinemets, U., Osborne, B., Pae, T., Salm, J.O., Sgouridis, F., Sohar, K., Soosaar, K., Storey, K., Teemusk, A., Tenywa, M.M., Tournebize, J., Truu, J., Veber, G., Villa, J.A., Zaw, S.S., Mander, U., 2018. Nitrogen-rich organic soils under warm well-drained conditions are global nitrous oxide emission hotspots. *Nature Communications*. 9, 1135. <https://doi.org/10.1038/s41467-018-03540-1>.
- Patz, J.A., Campbell-Lendrum, D., Holloway, T., Foley, J.A., 2005. Impact of regional climate change on human health. *Nature*. 438, 310-317. <https://doi.org/10.1038/nature04188>.
- Paul, S., Ammann, C., Alewell, C., Leifeld, J., 2021. Carbon budget response of an agriculturally used fen to different soil moisture conditions. *Agricultural and Forest Meteorology*. 300, 108319. <https://doi.org/10.1016/j.agrformet.2021.108319>.
- Petersen, S.O., Hoffmann, C.C., Schäfer, C.M., Blicher-Mathiesen, G., Elsgaard, L., Kristensen, K., Larsen, S.E., Torp, S.B., Greve, M.H., 2012. Annual emissions of CH₄ and N₂O, and ecosystem respiration, from eight organic soils in Western Denmark managed by agriculture. *Biogeosciences*. 9, 403-422. <https://doi.org/10.5194/bg-9-403-2012>.
- Piao, S., Ciais, P., Huang, Y., Shen, Z., Peng, S., Li, J., Zhou, L., Liu, H., Ma, Y., Ding, Y., Friedlingstein, P., Liu, C., Tan, K., Yu, Y., Zhang, T., Fang, J., 2010. The impacts of climate change on water resources and agriculture in China. *Nature*. 467, 43-51. <https://doi.org/10.1038/nature09364>.

- Pijlman, J., Holshof, G., van den Berg, W., Ros, G.H., Erisman, J.W., van Eekeren, N., 2020. Soil nitrogen supply of peat grasslands estimated by degree days and soil organic matter content. *Nutrient Cycling in Agroecosystems*. 117, 351-365. <https://doi.org/10.1007/s10705-020-10071-z>.
- Pörtner, H.O., Farrell, A.P., 2008. Physiology and climate change. *Science*. 322, 690-692. <https://doi.org/10.1126/science.1163156>.
- Raun, W.R., Johnson, G.V., 1999. Improving nitrogen use efficiency for cereal production. *Agronomy journal*. 91, 357-363. <https://doi.org/10.2134/agronj1999.00021962009100030001x>.
- Rihm, B., Künzle, T., 2019. Mapping nitrogen deposition 2015 for Switzerland. Technical Report on the Update of Critical Loads and Exceedance, including the years 1990, 2000, 2005 and 2010, Bern, Switzerland. <https://www.bafu.admin.ch>.
- Robertson, G.P., Vitousek, P.M., 2009. Nitrogen in Agriculture: Balancing the Cost of an Essential Resource. *Annual Review of Environment and Resources*. 34, 97-125. <https://doi.org/10.1146/annurev.enviro.032108.105046>.
- Rogiers, N., Conen, F., Furger, M., Stöckli, R., Eugster, W., 2008. Impact of past and present land-management on the C-balance of a grassland in the Swiss Alps. *Global Change Biology*. 2613-2625. <https://doi.org/10.1111/j.1365-2486.2008.01680.x>.
- Savci, S., 2012. An agricultural pollutant: chemical fertilizer. *International Journal of Environmental Science and Development*. 3, 73-80. <https://doi.org/10.7763/IJESD.2012.V3.191>.
- Schindler, U., Müller, L., 1999. Rehabilitation of the soil quality of a degraded peat site. In: Stott, D.E., Mohtar, R.H., Steinhardt, G.C. (Eds.), 10th International Soil Conservation Organization Meeting Purdue University, pp. 648-654.
- Schothorst, C., 1977. Subsidence of low moor peat soils in the western Netherlands. *Geoderma*. 17, 265-291. [https://doi.org/10.1016/0016-7061\(77\)90089-1](https://doi.org/10.1016/0016-7061(77)90089-1).
- Stehfest, E., Bouwman, L., 2006. N₂O and NO emission from agricultural fields and soils under natural vegetation: summarizing available measurement data and modeling of global annual emissions. *Nutrient Cycling in Agroecosystems*. 74, 207-228. <https://doi.org/10.1007/s10705-006-9000-7>.
- Strack, M., Zuback, Y.C.A., 2013. Annual carbon balance of a peatland 10 yr following restoration. *Biogeosciences*. 10, 2885-2896. <https://doi.org/10.5194/bg-10-2885-2013>.
- Szidat, S., Salazar Quintero, G.A., Vogel, E., Battaglia, M., Wacker, L., Synal, H.A., Türler, A., 2014. ¹⁴C analysis and sample preparation at the new Bern Laboratory for the Analysis of Radiocarbon with AMS (LARA). *Radiocarbon*. 56, 561-566. <https://doi.org/10.7892/boris.59263>.
- Templer, P., Mack, M., III, F.C., Christenson, L., Compton, J., Crook, H., Currie, W., Curtis, C., Dail, D., D'Antonio, C., 2012. Sinks for nitrogen inputs in terrestrial ecosystems: a meta - analysis of ¹⁵N tracer field studies. *Ecology*. 93, 1816-1829. <https://doi.org/10.1890/11-1146.1>.
- Tiemeyer, B., Albiac Borraz, E., Augustin, J., Bechtold, M., Beetz, S., Beyer, C., Drosler, M., Ebli, M., Eickenscheidt, T., Fiedler, S., Forster, C., Freibauer, A., Giebels, M., Glatzel, S., Heinichen,

- J., Hoffmann, M., Hoper, H., Jurasinski, G., Leiber-Sauheitl, K., Peichl-Brak, M., Rosskopf, N., Sommer, M., Zeitz, J., 2016. High emissions of greenhouse gases from grasslands on peat and other organic soils. *Global Change Biology*. 22, 4134-4149. <https://doi.org/10.1111/gcb.13303>.
- Toet, S., Bouwman, M., Cevaal, A., Verhoeven, J.T., 2005. Nutrient removal through autumn harvest of *Phragmites australis* and *Thypha latifolia* shoots in relation to nutrient loading in a wetland system used for polishing sewage treatment plant effluent. *Journal of Environmental Science and Health*. 40, 1133-1156. <https://doi.org/10.1081/ese-200055616>.
- Tubiello, F., Biancalani, R., Salvatore, M., Rossi, S., Conchedda, G., 2016. A worldwide assessment of greenhouse gas emissions from drained organic soils. *Sustainability*. 8, 371. <https://doi.org/10.3390/su8040371>.
- Turetsky, M., 2002. Current disturbance and the diminishing peatland carbon sink. *Geophysical Research Letters*. 29, 21-21-21-24. <https://doi.org/10.1029/2001gl014000>.
- van Beek, C.L., Pleijter, M., Jacobs, C.M.J., Velthof, G.L., van Groenigen, J.W., Kuikman, P.J., 2009. Emissions of N₂O from fertilized and grazed grassland on organic soil in relation to groundwater level. *Nutrient Cycling in Agroecosystems*. 86, 331-340. <https://doi.org/10.1007/s10705-009-9295-2>.
- van Beek, C.L., Pleijter, M., Kuikman, P.J., 2010. Nitrous oxide emissions from fertilized and unfertilized grasslands on peat soil. *Nutrient Cycling in Agroecosystems*. 89, 453-461. <https://doi.org/10.1007/s10705-010-9408-y>.
- van Beek, C.L., van der Salm, C., Plette, A.C.C., van de Weerd, H., 2008. Nutrient loss pathways from grazed grasslands and the effects of decreasing inputs: experimental results for three soil types. *Nutrient Cycling in Agroecosystems*. 83, 99-110. <https://doi.org/10.1007/s10705-008-9205-z>.
- von Lütow, M., Kogel-Knabner, I., Ekschmitt, K., Matzner, E., Guggenberger, G., Marschner, B., Flessa, H., 2006. Stabilization of organic matter in temperate soils: mechanisms and their relevance under different soil conditions - a review. *European Journal of Soil Science*. 57, 426-445. <https://doi.org/10.1111/j.1365-2389.2006.00809.x>.
- Waddington, J.M., Strack, M., Greenwood, M.J., 2010. Toward restoring the net carbon sink function of degraded peatlands: Short-term response in CO₂ exchange to ecosystem-scale restoration. *Journal of Geophysical Research-Biogeosciences*. 115, G01008. <https://doi.org/10.1029/2009jg001090>.
- Wang, Y., Paul, S.M., Jocher, M., Alewell, C., Leifeld, J., 2022. Reduced nitrous oxide emissions from drained temperate agricultural peatland after coverage with mineral soil. *Frontiers in Environmental Science*. 10, 856599. <https://doi.org/10.3389/fenvs.2022.856599>.
- Warren, M., Frohling, S., Dai, Z.H., Kurnianto, S., 2017. Impacts of land use, restoration, and climate change on tropical peat carbon stocks in the twenty-first century: implications for climate mitigation. *Mitigation and Adaptation Strategies for Global Change*. 22, 1041-1061. <https://doi.org/10.1007/s11027-016-9712-1>.

- Williams, B.L., Wheatley, R.E., 1988. Nitrogen mineralization and water-table height in oligotrophic deep peat. *Biology and Fertility of Soils*. 6, 141-147. <https://doi.org/10.1007/BF00257664>.
- Wilson, D., Blain, D., Couwenberg, J., Evans, C., Murdiyarso, D., Page, S., Renou-Wilson, F., Rieley, J., Sirin, A., Strack, M., 2016. Greenhouse gas emission factors associated with rewetting of organic soils. *Mires and Peat*. 17, 1-28. <https://doi.org/10.19189/MaP.2016.OMB.222>.
- Wösten, J., Ismail, A., Van Wijk, A., 1997. Peat subsidence and its practical implications: a case study in Malaysia. *Geoderma*. 78, 25-36. [https://doi.org/10.1016/S0016-7061\(97\)00013-X](https://doi.org/10.1016/S0016-7061(97)00013-X).
- Wright, E.L., Black, C.R., Cheesman, A.W., Drage, T., Large, D., Turner, B.L., Sjoersten, S., 2011. Contribution of subsurface peat to CO₂ and CH₄ fluxes in a neotropical peatland. *Global Change Biology*. 17, 2867-2881. <https://doi.org/10.1111/j.1365-2486.2011.02448.x>.
- Yu, Z., Loisel, J., Brosseau, D.P., Beilman, D.W., Hunt, S.J., 2010. Global peatland dynamics since the Last Glacial Maximum. *Geophysical Research Letters*. 37, L13402. <https://doi.org/10.1029/2010gl043584>.
- Yu, Z.C., 2012. Northern peatland carbon stocks and dynamics: a review. *Biogeosciences*. 9, 4071-4085. <https://doi.org/10.5194/bg-9-4071-2012>.
- Zistl-Schlingmann, M., Kwatcho Kengdo, S., Kiese, R., Dannenmann, M., 2020. Management intensity controls Nitrogen-Use-Efficiency and flows in grasslands—A ¹⁵N tracing experiment. *Agronomy*. 10, 606. <https://doi.org/10.3390/agronomy10040606>.

Part B: Publications

Paper I

Soil carbon loss from drained agricultural peatland after coverage with mineral soil

Yuqiao Wang^{1,2}, Sonja M. Paul¹, Markus Jocher¹, Christophe Espic^{3,4}, Christine Alewell², Sönke Szidat^{3,4}, Jens Leifeld¹

1. Climate and Agriculture Group, Agroscope, Reckenholzstrasse 191, 8046 Zürich, Switzerland

2. Environmental Geosciences, University of Basel, Bernoullistrasse 30, 4056 Basel, Switzerland

3. Department of Chemistry and Biochemistry, University of Bern, Freiestrasse 3, 3012 Bern, Switzerland

4. Oeschger Centre for Climate Change Research, University of Bern, Hochschulstrasse 4, 3012 Bern, Switzerland

Published as: Wang, Y., Paul, S. M., Jocher, M., Espic, C., Alewell, C., Szidat, S., Leifeld, J. (2021). Soil carbon loss from drained agricultural peatland after coverage with mineral soil. *Science of the Total Environment*, 800, 149498. <https://doi.org/10.1016/j.scitotenv.2021.149498>

Abstract

Drainage for agriculture has turned peatlands from a net sink to a net source of carbon (C). In order to reduce the environmental footprint of agricultural peatland drainage, and to counteract soil subsidence, mineral soil coverage is becoming an increasingly used practice in Switzerland. To explore the effect of mineral soil coverage on soil C loss and the source of CO₂ from peatland drained for agriculture, we utilized the radiocarbon signature (F¹⁴C) of soil C and emitted CO₂ in the field. The experiment, located in the Swiss Rhine Valley, was carried out on two adjacent drained organic soils, either without mineral soil cover (reference ‘Ref’), or covered with mineral soil (thickness ~ 40 cm) (coverage ‘Cov’) 13 years ago. Drainage already commenced 130 years ago and the site was managed as meadow since the 1970ies. Drainage induced 41 – 75 kg C m⁻² loss, which is equivalent to annual C loss rates of 0.49 – 0.58 kg C m⁻² a⁻¹ and 0.31 – 0.63 kg C m⁻² a⁻¹ for Cov and Ref, respectively. Mineral soil coverage had no significant effect on the amount of heterotrophic respiration, however, at Cov, the radiocarbon signature of heterotrophic CO₂ was significantly ($p < 0.01$) younger than at Ref, indicating that mineral soil coverage moved the source of decomposition of soil organic carbon (SOC) from a higher share of old peat towards a higher share of relatively younger material. In summary, our study lends support to the hypothesis that mineral soil coverage might reduce the decomposition of old peat underneath, and may therefore be a promising peatland management technique for the future use of drained peatland for agriculture.

Keywords: ¹⁴CO₂, peatland management, ¹⁴C, carbon loss, subsidence

1 Introduction

Natural peatlands are a sink of atmospheric CO₂ (Smith *et al.*, 2004; Lahteenoja *et al.*, 2012; Gallego-Sala *et al.*, 2018) and contain high amounts of soil organic carbon as peat, which accumulated over millennia (Yu *et al.*, 2010; Loisel *et al.*, 2014). Due to the high water level, the rate of net primary production is greater than that of litter and peat decomposition, resulting in a total soil organic carbon stock of ~600 Gt C, equivalent to ~20 % of the global soil organic carbon stock (Yu *et al.*, 2010). Human interventions such as land use change and drainage have a major impact on a peatland's C balance through the transformation of landscape hydrology and changes of the water level. These changes have turned global peatlands from a net carbon sink to a net carbon source (Leifeld *et al.*, 2019). It has been estimated that ~10 % of global peatlands are drained, with a higher share in some European countries, where most of the peatlands are considered to be artificially drained for agriculture (Bragg *et al.*, 2013). In the temperate region, resulting net CO₂ emissions amount, on average, for ~7.9 t C ha⁻¹ a⁻¹ in peatland drained for cropland, and between ~3.6 t C ha⁻¹ a⁻¹ and ~6.1 t C ha⁻¹ a⁻¹ for grasslands (IPCC, 2014), calling for enhanced mitigation efforts. Substantial parts of this net release might be saved by full peatland restoration or other measures that include rewetting (Worrall *et al.*, 2009; Kareksela *et al.*, 2015; Knox *et al.*, 2015; Hemes *et al.*, 2019). In agriculture, however, there is a trade-off between environmental goals and the need for agricultural production, setting barriers to implementing peatland restoration (Ferre *et al.*, 2019). Hence, measures allowing for a continued agricultural production, which at the same time reduce or even halt the continued decline of peatland carbon stocks, are sought for. Such measures should also counterbalance soil subsidence, another unwanted but equally unavoidable consequence of peatland drainage (Schothorst, 1977; Ewing and Vepraskas, 2006).

In Switzerland, organic soils cover an area of ~280 km², corresponding to ca. 0.68% of the country area (Tanneberger *et al.*, 2017). This area represents the remainder of a preindustrial peatland cover of ca. 1000 – 1500 km² and is mostly drained for agriculture (Wust-Galley *et al.*, 2020). In order to compensate for continued soil subsidence of the remaining organic soils, to maintain agricultural productivity, and to possibly reduce the environmental footprint of agricultural peatland management, mineral soil coverage with thicknesses of 0.2 – 0.5 m is becoming an increasingly used farmer's practice (Ferre *et al.*, 2019).

In drained peatland, heterotrophic soil respiration (soil Rh) has been shown to derive from a mixture of old peat and younger organic carbon (Schoor and Trumbore, 2006; Bader *et al.*, 2017; Kwon *et al.*, 2019), leading to an overall decline of the peat C stock over time. After mineral soil coverage, the carbon system might therefore change due to various factors: First, organic C contained in the mineral soil coverage becomes an extra C source of heterotrophic soil respiration. Second, the mineral soil coverage might retain newly assimilated organic matter from the vegetation at a higher rate than the drained

organic soil without coverage, owing to the stabilizing and absorbing nature of soil minerals (Kalbitz *et al.*, 2005; von Lützow *et al.*, 2006b). Third, mineral soil coverage might compact the organic soil underneath and probably pushes it deeper into zones of lower oxygen availability, thereby reducing the anaerobic decomposition of the older peat. This might be a relevant mechanism given that CO₂ production from the subsurface (> 30 cm) makes a great contribution to the total CO₂ emission from organic soil (Wright *et al.*, 2011). In consequence, mineral soil coverage may affect the contribution of old peat carbon to CO₂ emission, with potentially great importance for the sustained use of these soils and future needs for drainage. However, effects of mineral soil coverage on peat decomposition have not been studied yet.

Natural radiocarbon (¹⁴C) is a tracer, which can provide an information about the age of the soil C and respired C source (Trumbore, 2000). The organic carbon exposed from the drained peatland is typically old, owing to the ongoing loss of younger peat from the aerated surface, whereas fresh plant residues introduce carbon with a contemporary, modern radiocarbon signature to soil (Torn *et al.*, 2009). The resulting radiocarbon signature of the emitted CO₂ is a mixture of these sources (Clymo and Bryant, 2008), which make it possible to distinguish the carbon source of soil Rh by using a radiocarbon approach. Many researchers have studied radiocarbon signatures in both field experiments and laboratory incubations in different terrestrial ecosystems to understand the carbon source of soil respiration. Hicks Pries *et al.* (2013) combined laboratory incubations and field experiments to partition ecosystem respiration from thawing permafrost on organic soil and found that soil Rh from old carbon sources contributed 8% to 22% to the ecosystem respiration. Dioumaeva *et al.* (2002) reported, using laboratory incubations of boreal forest peat soil, that the decomposition of fine root and humified material contributed significantly to soil Rh, and peat decomposition contributed 0 ~ 40%. When incubating agriculturally used drained peat from the temperate zone, Bader *et al.* (2018) quantified the share of old soil organic carbon to total soil Rh as around 40% ~ 45%.

In addition to its application in CO₂ studies, radiocarbon dating of the peat also provided insights into C accumulation and loss. The radiocarbon age gradient between two or more ¹⁴C dated soil layer has been used to estimate the carbon accumulation rate and further evaluate the amount of carbon loss in peatlands. By using ¹⁴C dating of soil cores from northern peatlands, Vardy *et al.* (2000) reported a carbon accumulation rate of 0.012 – 0.016 kg C m⁻² yr⁻¹ over the past 6700 – 10000 years. By radiocarbon dating of soil cores from different peatlands in Europe Leifeld *et al.* (2018) reported a carbon accumulation rate of ~0.04 kg C m⁻² yr⁻¹ in natural peatlands. The same study concluded that managed peatlands had lost on average 56 kg C m⁻², which was approximately half of their former C stock. By comparing the carbon stock above the same age layer for both drained and adjacent undrained peatland in Finland, Krüger *et al.* (2016) reported a carbon accumulation rate of 0.02 kg C m⁻² yr⁻¹ in a natural peatland, and estimated that 0.06 kg C m⁻² yr⁻¹ were lost due to drainage.

To the best of our knowledge, no study to date has evaluated the effect of mineral soil coverage on carbon cycling in peatland drained for agriculture by using radiocarbon. In this study, we utilized the radiocarbon signature ($F^{14}C$) of soil C to quantify the C loss due to long-term drainage of an intensively managed temperate peatland. We also evaluated the effect of mineral soil coverage on soil carbon dynamics by studying the radiocarbon signature ($F^{14}C$) of CO_2 emitted from soil in situ. Our specific objectives were:

1. How much C has been lost during long-term drainage of the peatland?
2. What is the contribution of decomposing old peat and recent organic carbon to heterotrophic soil respiration from intensively managed organic soils?
3. Does mineral soil coverage affect the amount and source of CO_2 efflux from drained peatland?

2 Materials and methods

2.1 Field site description

The experimental site, a drained peatland with a peat thickness of around 10 m, is located in the Swiss Rhine Valley, Rütli SG (47°17' N, 9°32' E) (Fig. 1A). The site has a cool temperate - moist climate with 1174 mm annual precipitation and a mean annual temperature of 10.5 °C (<https://meteo.search.ch/sax>). According to historical maps, the drainage commenced before 1890 with drainage ditches (<https://map.geo.admin.ch>). In 1973, an integral drainage system with drainage pipes (depth 1 m, distance between pipes 14 m) and pump was built. At the same time, the site was used as grazing meadow until 2013, thereafter an intensively managed meadow was established, with mineral and slurry fertilization and 5 to 6 grass cuts per year. In 2006 to 2007, one part of the field (1.7 ha) was covered with mineral soil material (thickness around 40 cm) to improve the trafficability and agriculture usability by counterbalancing subsidence (Figs. 1B and 1C). We established our field experiment at this mineral soil coverage site (Cov) and used the adjacent drained organic soil without mineral soil coverage as the reference (Ref, see Fig. 1B). Surface (-3 to -8 cm) soil texture was sand 31.8%, silt 52.3% and clay 15.9% for Cov and sand 0.6%, silt 67.3% and clay 32.1% for Ref. Both sites have the identical farming practice and similar vegetation. Dominant grass species are *Lolium perenne*, *Alopecurus pratensis*, *Festuca arundinacea*, *Trifolium spec.* and *Festuca pratensis*.

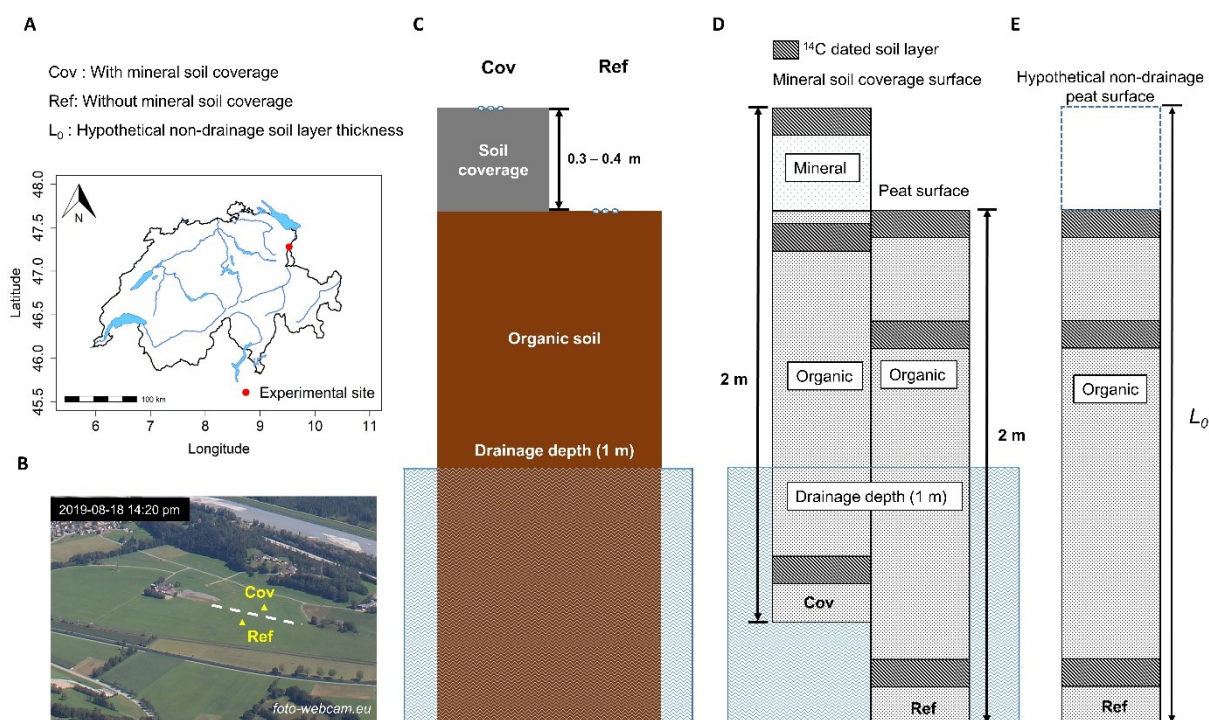


Fig. 1. The location (A) and image (B) of the experimental site, basic principle of mineral soil coverage (C), soil sample collection (D) and calculated hypothetical non-drainage peat thickness (E) description.

2.2 Gas sample collection

Soil surface CO_2 emissions were collected with static chambers. Gas samples for each site were taken on July 16, August 18 and September 16 of 2019 in triplicate on Ref and Cov, respectively. At May 18 of 2019, vegetation and the upper 5 cm of soil were removed from the six $1 \times 1 \text{ m}^2$ plots to minimize the contribution from above- and belowground plant respiration. Circular PVC frames for the chambers were installed in the soil (frame down to a depth of 10 cm) two weeks before the first gas sample collection. For sample collection, an opaque cylindrical PVC chamber (volume 27 L) was placed on the top of the frame. The space between the frame and the chamber was tightened with foam seal and tape. After allowing the CO_2 to accumulate in the chamber for 4 to 5 hours, gas from the headspace of the chamber was circulated through a battery-powered diaphragm pump (Thomas, Germany) to partially fill two 10 L Supel-Inert Foil Gas Sampling Bags (Supelco, Germany) during 1 min for sampling each. To avoid a pressure difference between the chamber and the atmosphere during gas removal and to reduce the ambient gas influx to the chamber, a pump with a low flow rate of 1 L min^{-1} was used for gas collection. One bag was thereafter used for radiocarbon measurements, and the other for CO_2 concentration measurement (G2308, Picarro, USA). The latter allowed calculating the CO_2 flux rate during chamber closure. The gas flux was calculated from the difference of the chamber headspace gas concentration before and after chamber closure vs. chamber closure time. To determine the ambient atmospheric CO_2 concentration and the ambient $^{14}\text{CO}_2$ value, air samples were collected at a height of 10 cm above the soil surface, and pumped to the 10 L gasbag for around 6 min at all (CO_2 concentration

measurement) or two of the three sampling dates ($^{14}\text{CO}_2$ value measurement). The radiocarbon measurement was performed with an accelerator mass spectrometer (AMS) at the Laboratory for the Analysis of Radiocarbon with AMS (LARA) of the University of Bern (Szidat *et al.*, 2014). For this, CO_2 was extracted from the collected samples and isolated from other air components using a cryogenic trap cooled with liquid nitrogen. The gas flow into and out of the trap was stabilized by a mass flow controller at the inlet and a scroll pump at the outlet, respectively, such that the pressure inside of the cryogenic trap remained at ~ 200 mbar in order to prevent condensation of liquid oxygen (Espic *et al.*, 2019). The isolated CO_2 was then transformed into solid graphite targets, which were employed in the AMS analysis (Szidat *et al.*, 2014)

2.3 Soil sample collection and analysis

Soil samples were sampled at the center of each PVC frame ($n = 3$ for each site) on December 4 of 2019, i.e. after the last gas sampling campaign. Soil cores were extracted by a motorized Humax with a 5 cm-diameter corer with internal plastic liner (Martin Burch AG, Switzerland) for the first 1 m depth, and a 5.2 cm-inner-diameter peat corer (Eijkelkamp, The Netherlands) for the depth from 1 m to 2 m. After sampling, all soil samples were stored in the 4°C cooling room overnight. The next day all soil samples were divided into 8 layers of 12.5 cm thickness each. Samples from the Cov were additionally divided at the boundary of mineral soil cover and underlying peat. Soil samples were dried at 105°C for 72 h, ground with mortar and pestle, and then milled in a ball mill (Retsch, MM 400, Germany) at 25-rotation s^{-1} for 3 min. For soil pH, (unground) soil was suspended 10 g in 0.01 M CaCl_2 , shaken at 160 cycles min^{-1} for 15 min, and left overnight before measuring the soil pH with a flat surface electrode (pH3310, WTW, Germany). Soil carbon (C) and total nitrogen (N) content was determined by elemental analysis (Hekatech, Germany). At both sites and from all plots, three layers of soil samples were used for radiocarbon measurement (Fig. 1D): the surface 0 – -12.5 cm, which is the main source of heterotrophic soil respiration, the soil layer underneath the mineral soil coverage at -37.5 – -50 cm, and the deeper peat soil at -175.0 – -187.5 cm. To determine the total and the ^{14}C fraction from the organic carbon only, acid fumigation was applied following (Agarwal and Bucheli, 2011), because presence of carbonates could not be excluded for some samples. The radiocarbon measurements were performed at the LARA in Bern (Szidat *et al.*, 2014). For this, the pretreated soil samples were combusted in an elemental analyzer and the evolving CO_2 was transformed into graphite targets for AMS measurement. In addition to these cores, undisturbed surface soil cylinders (depth 3-8 cm; volume 100 cm^3) were taken in close vicinity to the chamber collars for determining soil texture and soil pore volume.

2.4 $^{14}\text{CO}_2$ isotope analysis

For the determination of the radiocarbon signature of the respired CO_2 , we followed the approach of (Berhanu *et al.*, 2017). The measured CO_2 concentration from the chamber ($\text{CO}_{2\text{mea}}$) [ppm] consists of

two components: the original background CO₂ concentration (CO_{2atm}) [ppm] at onset of chamber closure, and the CO₂ from soil respiration accumulating in the chamber after closure (CO_{2resp}) [ppm].

$$CO_{2mea} = CO_{2atm} + CO_{2resp} \quad (1)$$

Eq. (1) is used to determine the accumulation of CO₂ during chamber closure. To assign a ¹⁴C signature to the CO₂ produced during closure, the signature of components in Eq. (1) must be known. Due to the different sources of the C in CO₂, each component has a specific F¹⁴C (Fraction Modern) value. For Eq. (1) a mass balance equation formulated for F¹⁴C as below.

$$CO_{2mea} \times F^{14}C_{mea} = CO_{2atm} \times F^{14}C_{atm} + CO_{2resp} \times F^{14}C_{resp} \quad (2)$$

The measured isotope values has to be corrected for atmospheric CO₂, which has already been in the chamber before seating it on the frame, and the $F^{14}C_{resp}$ was calculated following Eq. (3):

$$F^{14}C_{resp} = \frac{(CO_{2mea} \times F^{14}C_{mea} - CO_{2atm} \times F^{14}C_{atm})}{(CO_{2mea} - CO_{2atm})} \quad (3)$$

The $F^{14}C_{atm}$ was measured twice on 16 July and 16 September 2019 and its mean value was used for solving Eq. (3).

The fraction of the relative contribution of different carbon sources to the total CO₂ respired from soil were calculated with a two carbon-pool model approach (for a detailed information see supplementary material). However, the result showed that the contribution of relative old SOC from deeper layer cannot be excluded for some sampling dates (Fig. S1), thus Bayesian stable isotope mixing model (Parnell *et al.*, 2013) was applied to estimate the relative contribution of three different C sources, C from fresh plant residue, C from topsoil and middle soil layer. The measured atmosphere F¹⁴C value, which here represents the radiocarbon signature of fresh plant residues, and F¹⁴C value of topsoil C and middle layer soil C and the measurement uncertainty of each parameter were used in the model.

2.5 Soil organic carbon stock

The soil organic carbon stock was calculated as:

$$C_t = \sum_{i=1}^n C_i \times B_i \times D_i \times 0.1 \quad (4)$$

where C_i is the carbon stock (kg C m⁻²), n is the number of segments, C_i is the C concentration (%) of soil in segments i , B_i is the soil bulk density (g cm⁻³), D_i is the thickness (cm) and 0.1 is the transfer factor to the unit kg C m⁻². Carbon stocks were calculated down to 200 cm for both site, and for the Cov site carbon stocks were calculated separately for the mineral soil layer and the peat layer.

2.6 Determination of the amount of carbon loss from drainage in the long-term

Drainage-derived C loss was determined by comparing the hypothetical non-drainage C stock and the measured C stock. The integrated calculation of hypothetical non-drainage C stock of peatland was

based on the simplified assumption of constant peat and C accumulation of the peatland (Krüger *et al.*, 2016), who estimated peat accumulation rates based on age gradients between two or more dated samples in undisturbed peat layers. Here in our study, only deeper layer (-175.0 cm – -187.5 cm) of ^{14}C dated samples were underneath the drainage depth, and represent undisturbed peat, whereas middle (-37.5 cm – -50 cm) and surface (0 – -12.5 cm) layers of ^{14}C dated samples were generally above the drainage depth (Fig. 1D). For the latter two, the radiocarbon age of peat organic carbon and the peat structure were already affected by drainage, i.e. loss of organic matter by oxidation. Hence, the remaining carbon is older than it has been in the same depth before drainage. Including these data would thus overestimate the C accumulation rate and, in turn, increase the estimated carbon loss due to drainage. To lower the uncertainty of the calculation of the non-drainage C stock, we used the age gradient between deeper ^{14}C dated peat layer and the hypothetical non-drainage surface peat layer to calculate the peat accumulation rate (Fig. 1E). For the calculation of the hypothetical non-drainage peat thickness we followed the approach of (Leifeld *et al.*, 2011) with the assumption that the current deep-layer peat (underneath the drainage depth) is representative for the soil bulk density and C concentration of the peat layer before drainage. Hypothetical non-drainage soil layer thickness (L_0) for the sampled soil core is calculated as:

$$L_0 = \sum_{i=1}^{i=n} \frac{BD_a}{BD_0} \times L_{ia} \quad (5)$$

Where, L_0 is the peat layer thickness (cm) before drainage; L_{ia} is the thickness (cm) of peat layer i after drainage; BD_0 and BD_a is the soil bulk density (g cm^{-3}) of soil before and after drainage. For each soil profile the mean value of soil bulk density from the undisturbed soil layer (-150 – -200 cm) is used to represent the soil bulk density before drainage (BD_0).

With assuming the hypothetical non-drainage surface peat to be modern (Pontevedra-Pombal *et al.*, 2019; Bunsen and Loisel, 2020), we can define the age of hypothetical non-drainage surface peat at the time of sampling (2019 CE) and calculate the accumulation rate as:

$$P_a = \frac{L_0}{yr_d + yr_t} \times 10 \quad (6)$$

P_a is the peat accumulation rate (mm/yr); yr_d is the calibrated radiocarbon age (cal yr BP) from the deep soil layer (-175 – -187.5 cm), the radiocarbon age is reckoned as “before present (BP)” (present is defined as 1950 CE), determined by the F^{14}C value and calibrated using the IntCal 20 dataset (Reimer *et al.*, 2020) by OxCal 4.4 (Ramsey, 2009); yr_t is the time span in years between non-drainage surface peat age (2019 CE) and 1950 CE, which is 69; L_0 is the hypothetical non-drainage peat thickness above this layer (cm), and 10 is the conversion factor from cm to mm.

To match the C stock of all the three replicates for each site by age, the deeper layer of each soil core was normalized to a depth of the same calibrated radiocarbon age. In order to set the reference depth for each soil core within the soil sample collection depth (200 cm), the soil core with the youngest calibrated

radiocarbon age in the deepest layer was used to determine the depth of the soil layer of the same age for all other sampled cores. By doing so, we got six individual depths with the same radiocarbon age. The depth of the layer of the same age was determined as:

$$D_s = D_d - (yr_d - yr_s) \times P_a \times 0.1 \quad (7)$$

where D_s represents the depth of the soil with the same calibrated radiocarbon age as the reference layer (cm); D_d is the depth of the deeper soil layer (-181.25 cm, the middle depth of the deep ^{14}C dated soil layer), yr_d and yr_s (cal yr BP) are the calibrated radiocarbon age of the deep soil layer and the standard soil layer, respectively.

Moreover, the real - C stock (kg C m^{-2}) above the reference layer of same age was estimated as:

$$C_s = \sum_{i=1}^a C_i \times B_i \times D_i \times 0.1 + C_{a+1} \times B_{a+1} \times (12.5 - b) \times 0.1 - C_m \quad (8)$$

where, C_s is the C stock (kg C m^{-2}) above the reference layer of same age; C_m is the C stock of the mineral soil layer (kg C m^{-2}); for Ref, C_m is zero. a is the number of 12.5 cm segments and b is the depth of the reference layer of same age and the end layer of last segments (cm), a and b are determined by $D_s/12.5$, where a is the integer division result and b is the rest of $D_s/12.5$.

By following the approach from (Tolonen and Turunen, 1996; Page *et al.*, 2004), C accumulation rates (C_{ac} , $\text{g C m}^{-2} \text{ yr}^{-1}$) and hypothetical non-drainage C stocks (C_{nd} , kg C m^{-2}) can be calculated as:

$$C_{ac} = P_a \times BD_0 \times C_0 \times 0.1 \quad (9)$$

$$C_{nd} = C_{ac} \times yr_s \times 0.001 \quad (10)$$

The amount of C loss (C_{loss} , kg C m^{-2}) due to long-term drainage was determined as:

$$C_{loss} = C_{nd} - C_s \quad (11)$$

2.7 Auxiliary measurements

During the three gas sampling dates on July 16, August 18 and September 16 of 2019, soil temperature and soil moisture ($n=3$ at each site) was recorded by 5TE decagon devices (NE Hopkins Court, USA) at a soil depth of -5 cm. The groundwater level ($n=1$ at each site) was measured with a pressure probe (CTD/CTD-GPRS, UIT, Germany). Measurements were taken in close vicinity to the gas sampling plots.

2.8 Statistical analysis

Statistical analyses were performed in R (version 3.6.0). The relative contribution of different carbon source to heterotrophic soil respiration was determined by “SIMMR” package in R. The variability of the replicates in hypothetical C stocks, hypothetical peat accumulation rate, hypothetical C accumulation rate, the contribution of fresh C, topsoil C and middle layer SOC within Ref and Cov were calculated by using straightforward quadrature sum. Significant differences between the two sites for soil and soil respired CO_2 , F^{14}C values, C stocks, C loss rates, hypothetical C stocks, heterotrophic soil respiration

rates, hypothetical non-drainage layer thickness, subsidence, soil temperature, soil moisture and the contribution of fresh C, topsoil C, and middle layer SOC were determined by using a t-Test. The error probability was chosen as $p < 0.05$. Significant differences of $F^{14}C$ of soil respiration among the three sampling dates were determined by using ANOVA. In case of a significant effect, a Tukey HSD test was performed for multiple pairwise-comparison between the different sampling dates. Results are always reported as mean \pm 1 standard error (se).

3 Results

3.1 Soil C stock and C loss

3.1.1 C stock

The mineral soil coverage (Cov) topsoil (0 – -12.5 cm) had significantly ($p < 0.01$) higher bulk density ($1.11 \pm 0.05 \text{ g cm}^{-3}$) than the original peat surface underneath the mineral soil coverage ($0.61 \pm 0.07 \text{ g cm}^{-3}$) and the surface (0 – -12.5 cm) of the drained site without mineral soil coverage (Ref) ($0.49 \pm 0.02 \text{ g cm}^{-3}$). Underneath the mineral soil layer, differences in soil bulk density between the two sites were less pronounced (Fig. 2A). Owing to the coverage with carbon-poor mineral soil, Cov had lower ($p < 0.05$) topsoil C concentrations and C/N ratios ($2.71 \pm 0.55 \%$ and 9.8 ± 0.3) than Ref ($17.63 \pm 0.67 \%$ and 12.8 ± 0.4) (Figs. 2B and C). Below c. 50 cm depth, C/N ratios and C concentrations of the two sites were similar. At Cov, however, we identified a layer with lower C concentrations and C/N ratios but higher bulk densities at c. -100 – -112.5 cm depth.

In the upper 50 cm of soil, Ref stored significantly ($p < 0.01$) more C ($36.42 \pm 2.90 \text{ kg C m}^{-2}$) as compared to Cov ($25.07 \pm 1.55 \text{ kg C m}^{-2}$). This pattern was maintained over the whole profile with significantly more ($p < 0.05$) C accumulated down to 200 cm depth at Ref ($124.47 \pm 8.06 \text{ kg C m}^{-2}$) than Cov ($112.54 \pm 3.40 \text{ kg C m}^{-2}$) (Fig. 2D). The higher carbon stock at Ref was mainly caused by the different C concentrations between the surface mineral soil and the peat soil, which was not compensated by higher bulk densities of the mineral soil coverage at Cov.

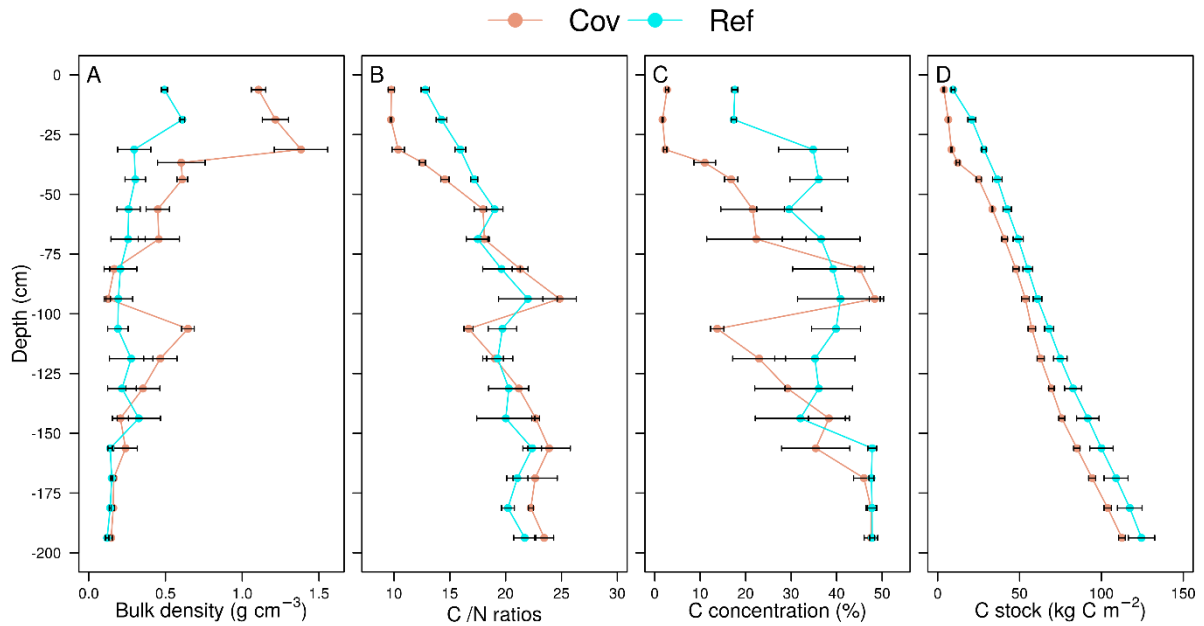


Fig. 2. Soil bulk density (A), C/N ratio (B), organic carbon concentration (C) and cumulative carbon stock (D) (mean \pm se, $n=3$) for the site with (Cov) and without mineral soil cover (Ref), plotted based on the middle segment depth.

3.1.2 C stock above the reference layer with same radiocarbon age and historical carbon accumulation

To allow a comparison of C stocks which is not biased by differences in soil bulk densities, the deeper layers of each core were normalized to a depth with the same $F^{14}C$, which represents a layer of same age, above which carbon accumulated since then. The core with the highest $F^{14}C$ value (among the deep soil layers) of 0.4642 ± 0.0015 (calibrated radiocarbon age 7071 ± 91 years cal yr BP, segment -175.0 – -187.5 cm) was chosen for calculating the layer of the same radiocarbon age for the other five soil cores. The corresponding soil depths with the same $F^{14}C$ value varied between -173 cm to -181 cm and the C stock younger than 7071 ± 91 cal yr BP ranged from 84 kg C m^{-2} to 112 kg C m^{-2} (Table 1). At Ref, significantly higher ($p < 0.05$) C stocks were observed ($107 \pm 8 \text{ kg C m}^{-2}$) compared to Cov ($87 \pm 6 \text{ kg C m}^{-2}$) above the reference layer (Fig. 3). The C accumulation rate at both sites varied from $21.0 \text{ g C m}^{-2} \text{ a}^{-1}$ to $27.5 \text{ g C m}^{-2} \text{ yr}^{-1}$. Neither the C accumulation rates ($21.9 \pm 1.1 \text{ g C m}^{-2} \text{ yr}^{-1}$ and $23.3 \pm 2.7 \text{ g C m}^{-2} \text{ yr}^{-1}$ for Cov and Ref, respectively), the hypothetical non-drainage C stocks ($155 \pm 5 \text{ kg C m}^{-2}$ and $164 \pm 15 \text{ kg C m}^{-2}$ for Cov and Ref, respectively) nor the hypothetical non-drainage layer thickness ($227.3 \pm 4.7 \text{ cm}$ and $265.4 \pm 15.7 \text{ cm}$ for Cov and Ref, respectively) differed significantly between Cov and Ref (Table 1, Fig. 3).

Table 1. Summary of radiocarbon age peat and C accumulation rate and carbon storage of all soil profiles at drained peatland with (Cov) and without mineral soil cover (Ref), numbers 1, 2, 3 indicate the replicates within Cov and Ref.

Indicator	Cov			Ref		
	Cov1	Cov2	Cov3 ^a	Ref1	Ref2	Ref3
0 – 12.5 cm (cal yr BP)	617±55	499±23	703±27	1623±77	1679±59	2181±125
37.5 – 50 cm (cal yr BP)	2149±145	3594±98	3508±56	5623±39	5877±115	5139±153
175 – 187.5 cm (cal yr BP)	7217±54	7344±79	7071±91	7171±95	7074±92	7294±124
Soil depth of same age ^b (cm)	176 ± 4	173 ± 5	181 ± 2	178 ± 6	181 ± 6	173 ± 8
C stock above same age ^c (kg C m ⁻²)	90 ± 5	84 ± 4	87 ± 1	103 ± 4	107 ± 4	112 ± 6
Hypothetical non-drainage layer thickness L_0 (cm)	235.81	226.36	219.64	251.32	248.23	296.77
Subsidence (cm)	69.11	56.86	50.14	51.32	48.23	96.77
Hypothetical peat accumulation rate (mm yr ⁻¹)	0.309±0.002	0.291±0.003	0.293±0.004	0.333±0.004	0.333±0.004	0.389±0.007
Hypothetical C accumulation rate (g C m ⁻² yr ⁻¹)	23.4±0.2	21.0±0.2	21.3±0.3	21.4±0.3	20.9±0.3	27.5±0.5

a. the reference soil profile.

b. for Cov the carbon stock above the reference layer is shown without the carbon contained in the mineral soil cover.

c. the radiocarbon age of the reference layer is 7071 ± 91 cal yr BP

3.2 C loss due to drainage in the long-term

The comparison of the measured C stock above the reference layer (same radiocarbon age) and the hypothetical C stock as determined by the C accumulation rate revealed that the measured C stock was smaller than the hypothetical carbon stock, indicating C loss since onset of drainage. The C loss was not significantly different between sites (Cov, $67 \pm 4 \text{ kg C m}^{-2}$; Ref, $57 \pm 10 \text{ kg C m}^{-2}$) (Fig. 3) and corresponded to annual C loss rates of $0.49 - 0.58 \text{ kg C m}^{-2} \text{ yr}^{-1}$ and $0.31 - 0.63 \text{ kg C m}^{-2} \text{ yr}^{-1}$ for Cov and Ref, respectively, for an onset of peat drainage in 1890 CE.

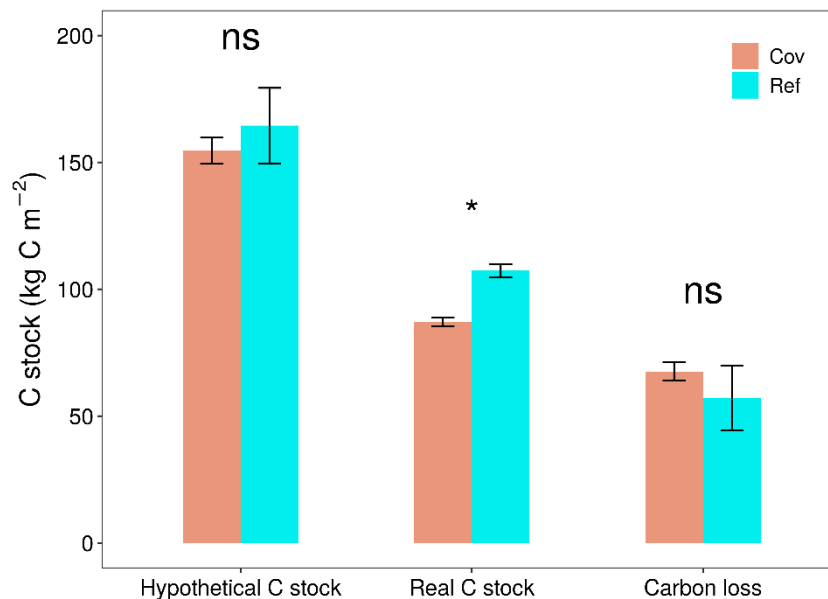


Fig. 3. Soil organic carbon stocks and carbon losses (mean \pm se, $n = 3$) determined relative to a reference layer (the same $F^{14}C$ and calibrated radiocarbon age) in organic layers from drained peatland with (Cov) and without mineral soil cover (Ref). A significant difference (t-test) between two sites is indicated with a star ($p < 0.05$), “ns” indicates no significant differences.

3.3 Environmental parameters and soil Rh

Soil groundwater levels, soil temperature, and soil water filled pore space at the three sampling dates are provided in Table 2. Neither the soil temperature nor the soil moisture (water filled pore space) were significantly different between two sites over three gas sampling dates whereas the groundwater level was always closer to the surface at Ref.

The amount of evolved CO_2 was in the same order of magnitude for both sites and at any date. In detail, the amount of respired CO_2 was significant higher ($p < 0.05$) at Ref ($16.16 \pm 1.81 \text{ g CO}_2 \text{ m}^{-2} \text{ day}^{-1}$) than Cov ($10.83 \pm 1.52 \text{ g CO}_2 \text{ m}^{-2} \text{ day}^{-1}$) on July 16. On August 18, significantly more CO_2 was respired at Cov ($16.49 \pm 2.72 \text{ g CO}_2 \text{ m}^{-2} \text{ day}^{-1}$) than Ref ($10.92 \pm 2.69 \text{ g CO}_2 \text{ m}^{-2} \text{ day}^{-1}$) ($p < 0.05$), whereas no difference between sites was found at September 16 ($13.33 \pm 1.73 \text{ g CO}_2 \text{ m}^{-2} \text{ day}^{-1}$ and $12.38 \pm 1.56 \text{ g CO}_2 \text{ m}^{-2} \text{ day}^{-1}$ for Cov and Ref, respectively) (Fig. 4).

Table 2. Summary of soil temperature, water filled pore space, and groundwater level at drained peatland with (Cov) and without mineral soil cover (Ref) at the three gas sampling dates.

Date	Soil temperature (°C)		Water filled pore space (%)		Groundwater level (m)	
	Cov	Ref	Cov	Ref	Cov	Ref
16.07.2019	20.8 ± 0.2	20.3 ± 0.3	56.1 ± 4.5	60.0 ± 1.5	- 0.96	- 0.61
18.08.2019	21.5 ± 0.3	20.9 ± 0.1	65.4 ± 3.0	69.5 ± 0.8	- 0.75	- 0.39
16.09.2019	19.0 ± 0.1	18.9 ± 0.2	65.4 ± 3.3	68.6 ± 1.5	- 0.72	- 0.50

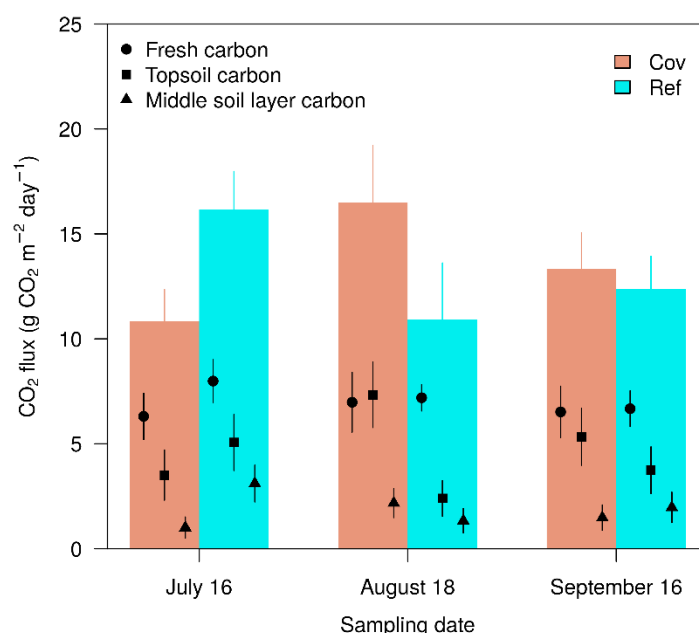


Fig. 4. Calculated sources of soil heterotrophic respiration (mean ± se, n = 3) from drained peatland with (Cov) and without mineral soil cover (Ref), using a Bayesian stable isotope mixing model comprising fresh residues, topsoil C and middle layer SOC as sources (see detailed data in Table S2).

3.4 Radiocarbon signature of soil and heterotrophic soil respiration

The F¹⁴C of SOC declined steadily with depth at both sites (Fig. 5A). It was significantly higher ($p < 0.05$) at Cov (0.92 ± 0.02 and 0.70 ± 0.06) than Ref (0.79 ± 0.02 and 0.55 ± 0.02) in the topsoil (0 cm to -12.5 cm) and subsoil (-37.5 cm to -50 cm), respectively, whereas no significant difference was recorded in the deepest (-175.0 cm to -187.5 cm) soil layer (0.46 ± 0.004 and 0.46 ± 0.003 for Cov and Ref, respectively).

The fraction of $^{14}\text{CO}_2$ of soil Rh was higher ($p < 0.01$), i.e., CO_2 younger, in Cov than Ref in July and September, but it was not significantly different in August (Fig. 5B). No difference in $F^{14}\text{C}$ of the CO_2 was found at Cov among the three sampling dates. For Ref, the $F^{14}\text{C}$ was higher ($p < 0.05$) in August than in July, but no difference was found when comparing September to August and July. Mean $F^{14}\text{C}$ values from the three sampling dates were significantly higher ($p < 0.01$) in Cov (0.93 ± 0.01) than Ref (0.86 ± 0.02).

At Ref, averaged over the three sampling dates, the relative contribution of topsoil C to the respired CO_2 was higher ($p < 0.01$) than the relative contribution of middle layer soil C (16.6 % – 38.9 % vs 11.1 % – 22.4 %). Similarly, a higher share ($p < 0.01$) of topsoil organic carbon from covered mineral soil compared to the middle peat layer to the overall respiration was observed for Cov at all the sampling dates (21.8 % – 49.2 % vs 7.6 % – 14.0 %). In addition, at all the sampling dates the contribution of peat C to the total CO_2 release was higher at Ref (27.7 % – 56.6 %) ($p < 0.01$) than Cov (7.6 % – 14.0 %). The contribution of the fresh plant residue to the overall respiration showed no difference between Cov and Ref (37.6% – 70.1% and 43.4% – 72.3% for Cov and Ref, respectively) (Fig. 4).

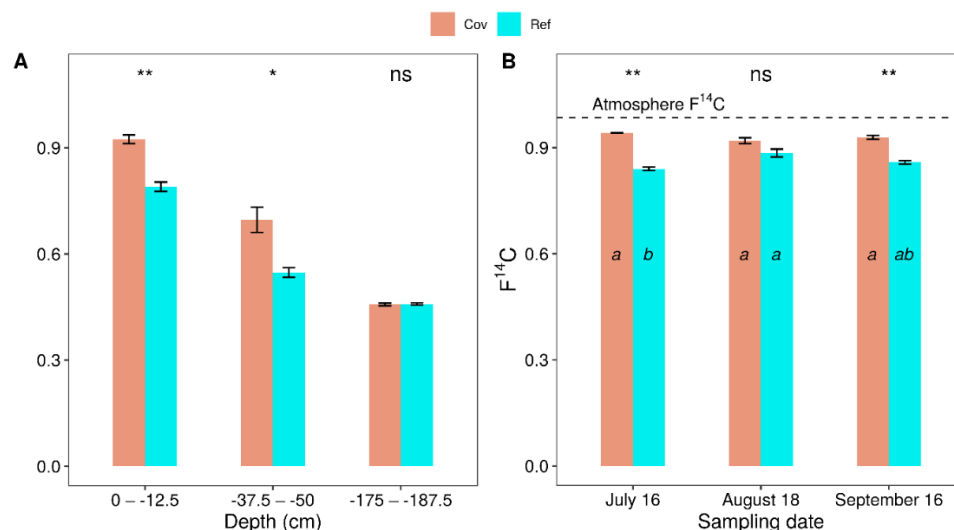


Fig. 5. $F^{14}\text{C}$ (mean \pm se, $n = 3$) of soil organic carbon (A) and heterotrophic soil respiration (B) from drained peatland with (Cov) and without mineral soil cover (Ref). Significant differences between two sites are indicated with stars (t-test, “***” $p < 0.01$, “*” $p < 0.05$, “ns” indicate no significant differences). Significant differences among three sampling dates are indicated with letters (ANOVA and Tukey Honest Significant Differences) separately for both sites.

4 Discussion

4.1 Soil properties and peat composition

Our results indicate that the differences of soil bulk densities, C/N ratios and C concentrations in the surface layer of Cov and Ref were attributed to the mineral soil coverage. The topsoil (0 – 12.5 cm)

C/N ratios (12.8 ± 0.4) at Ref were in the range of managed organic soils used for grassland in Europe (Liimatainen *et al.*, 2018; Leifeld *et al.*, 2020). In comparison, the topsoil (0 – -12.5 cm) C/N ratios (9.8 ± 0.3) at Cov were similar to the soil C/N ratios in mineral topsoil managed as grassland (de Vries *et al.*, 2012; Zhou *et al.*, 2018). The C/N ratios from Ref were smaller in the topsoil and increased with depth, in line with previous research from drained peatland (Kuhry and Vitt, 1996). This pattern is related to the stronger microbial transformation of drained peat in the topsoil and a preferential loss of C over N during decomposition, as well as owing to the input of fertilizer nitrogen (Pinsonneault *et al.*, 2016). The soil C/N ratios are therefore considered a reliable indicator of peat decomposition and degradation in drained peatlands (Krüger *et al.*, 2015a). The relatively smaller surface soil C/N ratios from Ref (as compared to the deeper layers) therefore indicated that the upper 50 cm of peat was strongly degraded. This was confirmed by the higher bulk density ($0.26 - 0.61 \text{ g cm}^{-3}$) in the surface layer of Ref as compared to the deeper layers. These bulk densities belong to the classes of high and extreme degradation as defined by Liu *et al.* (2019), who classified peat soil degradation into four categories (pristine peat, $\text{BD} \leq 0.05 \text{ g cm}^{-3}$; moderate degradation, $0.05 \text{ g cm}^{-3} < \text{BD} \leq 0.20 \text{ g cm}^{-3}$; high degradation, $0.20 \text{ g cm}^{-3} < \text{BD} \leq 0.40 \text{ g cm}^{-3}$ and extreme degradation, $\text{BD} \geq 0.40 \text{ g cm}^{-3}$).

At Cov, between -100 and -112.5 cm, soil bulk density and C concentrations were different to the soil layers above and underneath. We interpret this as indicative for the presence of a sediment layer with higher bulk density and lower SOC concentration deposited at the time of peat formation. No such layer was found at Ref in our study, indicating natural variability of the peatland.

4.2 Carbon loss due to long-term drainage

Our calculated hypothetical non-drainage C accumulation rates for Cov and Ref showed no difference, suggesting that the environmental conditions during formation of this formerly large peatland complex were similar. Our experimental site had an average C accumulation rate of $22.6 \text{ g C m}^{-2} \text{ yr}^{-1}$, close to the average C accumulation rate of $23 \text{ g C m}^{-2} \text{ yr}^{-1}$ calculated by Loisel *et al.* (2014) for northern peatlands during the Holocene.

Although we found no difference in the drainage-induced C loss the C stock in peat above the ^{14}C dated reference layer was significantly higher at Ref than at Cov. This may be related to two factors. Firstly, drainage may have induced stronger soil subsidence and carbon loss at Cov; therefore, mineral soil coverage was applied to compensate soil subsidence. Secondly, at the experimental site, drainage has commenced more than 130 years ago, but mineral soil coverage only 13 years ago. Considering that the carbon loss rate from old peat only changes gradually, its possible effect will not yet be detectable in the profile record. Our result indicate that long-term drainage caused an annual carbon loss of $0.49 - 0.58 \text{ kg C m}^{-2} \text{ a}^{-1}$ at Cov and $0.31 - 0.63 \text{ kg C m}^{-2} \text{ a}^{-1}$ at Ref. These rates are in the same range as former studies on the carbon loss from drained organic soils in Europe. Using profile based methods, Leifeld *et*

al. (2011) reported annual carbon loss rates from drained temperate fens in Switzerland of 0.25 – 0.55 kg C m⁻² a⁻¹; and Rogiers *et al.* (2008a) estimated a carbon loss of 0.50 – 0.91 kg C m⁻² a⁻¹ from managed grassland on fen peat in the pre-Alps. Fell *et al.* (2016) found a loss rate of 0.56 kg C m⁻² a⁻¹ for a grassland on drained fens in northeast Germany, and Krüger *et al.* (2015b) calculated carbon losses of 0.63 and 0.88 kg C m⁻² a⁻¹ for extensively and intensively managed bog drained for grassland in northwest Germany. In comparison to our site, flux-based methods revealed slightly higher average annual carbon loss rates of 0.84 ± 0.47 kg C m⁻² a⁻¹ from 25 different fen peat site managed as grassland in Germany (Tiemeyer *et al.*, 2016). Also IPCC reported slightly higher carbon losses from deep-drained and nutrient-rich grassland of on average of 0.61 (0.50 – 0.73) kg C m⁻² a⁻¹ (IPCC, 2014a). In our opinion, the slightly lower average loss rates revealed by profile based methods such as the one applied here are related to the time span integrated by the method, which includes different intensities of drainage. At our study site, intensive melioration of the drainage system with drainage pipes and pump was built only in 1973, whereas between 1890 and 1973 drainage ditches, which are less efficient, were used. Correspondingly, recent estimates underpin that C loss rates from agriculturally managed organic soils in Switzerland increased over time (Wüst-Galley *et al.*, 2020).

In conclusion, the comparison of C accumulation and loss rates with former studies indicate that the method for estimating a hypothetical non-drainage C stock in combination with the measurement of actual stocks seems to be a robust way for quantifying long-term C losses from drained organic soil.

4.3 Effect of mineral soil coverage on the soil's radiocarbon signature and the source of Rh

The F¹⁴C of the peat profile decreased with depth (Fig. 5A), corresponding to an increasing age, as older peat is depleted in ¹⁴C due to radioactive decay. The calibrated radiocarbon age of the surface (0 – -12.5 cm) soil at Ref was much older than the contemporary atmospheric CO₂. It was also old in comparison to the radiocarbon age of surface peat from natural peatlands, which is in general modern (Pontevedra-Pombal *et al.*, 2019; Bunsen and Loisel, 2020). Old radiocarbon ages were also previously observed for degraded surface organic soils (Krüger *et al.*, 2016; Bader *et al.*, 2017), indicating that after drainage the relatively young and recent peat decomposes, exposing older peat to the soil's surface. In contrast, the radiocarbon age of the surface mineral soil (0 – -12.5 cm) at Cov was younger than the surface peat from Ref but still much older than the contemporary atmospheric CO₂ (Fig. 5B). The age of the mineral topsoil coverage was also much higher than the radiocarbon age of surface mineral soils used for agriculture in Switzerland, where F¹⁴C values close to one have been reported (Leifeld and Mayer, 2015). The relatively old age of the mineral soil coverage could be related to various factors: First, the covered mineral soil contained old carbon. Second, there might be a contribution of older dissolved organic carbon from the peat underneath the mineral layer. This carbon might contribute to the organic carbon formation in the covered mineral soil due to the upwelling groundwater (Chasar *et al.*, 2000). Third,

plant roots might directly take up organic nutrients released from decomposing soil organic matter in deeper layers and release some of this carbon to the soil surface as dead plant residues (Jones *et al.*, 2009; Roberts and Jones, 2012). Finally, surface peat might have been mixed with the mineral soil cover during field application of the material, thereby diluting the initial signature of the cover material. Our results showed that the $F^{14}CO_2$ values of heterotrophic soil respiration were lower than those of fresh plant residues (atmosphere $F^{14}C$) (Fig. 5B), but higher than the topsoil's signature on almost any sampling date, implying that the CO_2 originated from a mixture of old SOC and recently accumulated plant residues. The more detailed analysis revealed that old carbon from the middle soil layer (peat layer) also contributed to the overall heterotrophic soil respiration (Fig. 4). These results suggest that decomposition of old peat contributes substantially to the evolved CO_2 in both treatment (Cov and Ref) and leads to the above described C loss from the soil in the long term. These results align with former research where it has been shown that not only the younger plant residues contributed to the emitted CO_2 , but also older peat (Wright *et al.*, 2011).

It is worth to recall that the original surface soil (~5 cm) was removed before gas and soil sampling in order to reduce the influence of fresh roots and litter on the $^{14}CO_2$ and soil ^{14}C signature. With this pre-treatment, both the age of the surface soil carbon and the CO_2 shift towards older signatures. However, we consider this not to systematically affect the difference between the two sites.

4.4 Potential of peat preservation with mineral soil coverage

With mineral soil coverage, the groundwater table was deeper (Table 2), implying that a larger soil volume was exposed to oxygen for SOM decomposition. This potentially leads to a higher soil CO_2 release due to the positive correlation between water table depth and soil respiration in organic soils (Musarika *et al.*, 2017; Evans *et al.*, 2021). However, taking into account the groundwater level (Table 2) and the thickness of the mineral soil cover, the volume of aerated peat above the groundwater was smaller at Cov. Also compaction of the peat underneath the mineral soil coverage (-30.5 – 62.5 cm), as visible in the soil bulk densities (Fig. 2A), might have further reduced oxygen availability for SOM decomposition. Correspondingly, the old peat contributed less to the overall CO_2 release with mineral soil coverage, whereas the newly added carbon in the mineral cover material became an extra C source for soil Rh (Fig. 4), resulting in a similar overall Rh at the two sites. At Ref, differences in soil Rh between the three sampling events followed groundwater table depth, supporting the hypothesis that the aerated peat stock is an important driver for peat mineralization (Tiemeyer *et al.*, 2016). A possible reduction in the decomposition rate of old peat must not be in contradiction to the observed long-term loss rates which were not different between Cov and Ref, considering that a gradual change in the loss rate of old peat will not be immediately visible in the profile record.

5 Conclusions

In our study, decadal drainage of organic soil for agriculture caused large SOC losses and substantial subsidence due to the decomposition and compaction of the peat. Correspondingly, the carbon sources of soil Rh were a mixture of fresh plant residues and soil C. Carbon from peat decomposition contributed around half to the total heterotrophic CO₂ from soil in drained peatland without mineral soil coverage, partially stemming also from carbon stored in the subsoil. Coverage of this drained organic soil with mineral material seems not to decrease in the amount of C loss, but to shift the source of soil Rh from the surface peat to recent assimilates. This may move the system towards a reduced peat loss in the future, and hence a more sustainable management, but further long-term and multiply field ¹⁴CO₂ observations are needed to support this interpretation.

Acknowledgements

We appreciated the help of Stefan Gloor, Robin Giger at Agroscope and Michael Battaglia at the University of Bern during field sampling and lab analysis. We thank Bernhard Schneider for collaboration on his farm. This work was supported by the China Scholarship Council (NSCIS 201806350221), and the Swiss Federal Office for the Environment (contract number 06.0091.PZ/R261-2425).

References

- Agarwal T, Bucheli TD. Adaptation, validation and application of the chemo-thermal oxidation method to quantify black carbon in soils. *Environmental Pollution* 2011; 159: 532-538
<https://doi.org/10.1016/j.envpol.2010.10.012>.
- Bader C, Müller M, Schulin R, Leifeld J. Amount and stability of recent and aged plant residues in degrading peatland soils. *Soil Biology and Biochemistry* 2017; 109: 167-175
<https://doi.org/10.1016/j.soilbio.2017.01.029>.
- Bader C, Müller M, Szidat S, Schulin R, Leifeld J. Response of peat decomposition to corn straw addition in managed organic soils. *Geoderma* 2018; 309: 75-83
<https://doi.org/10.1016/j.geoderma.2017.09.001>.
- Berhanu TA, Szidat S, Brunner D, Satar E, Schanda R, Nyfeler P, et al. Estimation of the fossil fuel component in atmospheric CO₂ based on radiocarbon measurements at the Beromünster tall tower, Switzerland. *Atmospheric Chemistry and Physics* 2017; 17: 10753-10766
<https://doi.org/10.5194/acp-17-10753-2017>.
- Bragg O, Lindsay R, Risager M, Silvius M, Zingstra H. Strategy and action plan for mire and peatland conservation in central Europe: Central European Peatland Project (CEPP). *Wetlands International*, Wageningen, 2013.
- Bunsen MS, Loisel J. Carbon storage dynamics in peatlands: Comparing recent- and long-term accumulation histories in southern Patagonia. *Global Change Biology* 2020; 26: 5778-5795
<https://doi.org/10.1111/gcb.15262>.
- Chasar LS, Chanton JP, Glaser PH, Siegel DI, Rivers JS. Radiocarbon and stable carbon isotopic evidence for transport and transformation of dissolved organic carbon, dissolved inorganic carbon, and CH₄ in a northern Minnesota peatland. *Global Biogeochemical Cycles* 2000; 14: 1095-1108 <https://doi.org/10.1029/1999gb001221>.
- Clymo RS, Bryant CL. Diffusion and mass flow of dissolved carbon dioxide, methane, and dissolved organic carbon in a 7-m deep raised peat bog. *Geochimica et Cosmochimica Acta* 2008; 72: 2048-2066 <https://doi.org/10.1016/j.gca.2008.01.032>.
- de Vries FT, Bloem J, Quirk H, Stevens CJ, Bol R, Bardgett RD. Extensive management promotes plant and microbial nitrogen retention in temperate grassland. *PLoS One* 2012; 7: e51201
<https://doi.org/10.1371/journal.pone.0051201>.
- Dioumaeva I, Trumbore S, Schuur EAG, Goulden ML, Litvak M, Hirsch AI. Decomposition of peat from upland boreal forest: Temperature dependence and sources of respired carbon. *Journal of Geophysical Research Atmospheres* 2002; 108: WFX 3-1-WFX 3-12
<https://doi.org/10.1029/2001jd000848>.

- Espic C, Liechti M, Battaglia M, Paul D, Röckmann T, Szidat S. Compound-specific radiocarbon analysis of atmospheric methane: a new preconcentration and purification setup. *Radiocarbon* 2019; 61: 1461-1476 <https://doi.org/10.1017/rdc.2019.76>.
- Evans CD, Peacock M, Baird AJ, Artz RRE, Burden A, Callaghan N, et al. Overriding water table control on managed peatland greenhouse gas emissions. *Nature* 2021; 593: 548-552 <https://doi.org/10.1038/s41586-021-03523-1>.
- Ewing JM, Vepraskas MJ. Estimating primary and secondary subsidence in an organic soil 15, 20, and 30 years after drainage. *Wetlands* 2006; 26: 119-130 [https://doi.org/10.1672/0277-5212\(2006\)26\[119:Epassi\]2.0.Co;2](https://doi.org/10.1672/0277-5212(2006)26[119:Epassi]2.0.Co;2).
- Fell H, Roßkopf N, Bauriegel A, Zeitz J. Estimating vulnerability of agriculturally used peatlands in north-east Germany to carbon loss based on multi-temporal subsidence data analysis. *Catena* 2016; 137: 61-69 <https://doi.org/10.1016/j.catena.2015.08.010>.
- Ferré M, Muller A, Leifeld J, Bader C, Müller M, Engel S, et al. Sustainable management of cultivated peatlands in Switzerland: Insights, challenges, and opportunities. *Land Use Policy* 2019; 87: 104019 <https://doi.org/10.1016/j.landusepol.2019.05.038>.
- Gallego-Sala AV, Charman DJ, Brewer S, Page SE, Prentice IC, Friedlingstein P, et al. Latitudinal limits to the predicted increase of the peatland carbon sink with warming. *Nature Climate Change* 2018; 8: 907-913 <https://doi.org/10.1038/s41558-018-0271-1>.
- Hemes KS, Chamberlain SD, Eichelmann E, Anthony T, Valach A, Kasak K, et al. Assessing the carbon and climate benefit of restoring degraded agricultural peat soils to managed wetlands. *Agricultural and Forest Meteorology* 2019; 268: 202-214 <https://doi.org/10.1016/j.agrformet.2019.01.017>.
- Hicks Pries CE, Schuur EA, Crummer KG. Thawing permafrost increases old soil and autotrophic respiration in tundra: partitioning ecosystem respiration using $\delta^{13}\text{C}$ and $\Delta^{14}\text{C}$. *Global Change Biology* 2013; 19: 649-661 <https://doi.org/10.1111/gcb.12058>.
- IPCC. 2013 Supplement to the 2006 IPCC Guidelines for National greenhouse gas inventories: Wetlands, 2014.
- Jones DL, Nguyen C, Finlay RD. Carbon flow in the rhizosphere: carbon trading at the soil–root interface. *Plant and Soil* 2009; 321: 5-33 <https://doi.org/10.1007/s11104-009-9925-0>.
- Kalbitz K, Schwesig D, Rethemeyer J, Matzner E. Stabilization of dissolved organic matter by sorption to the mineral soil. *Soil Biology and Biochemistry* 2005; 37: 1319-1331 <https://doi.org/10.1016/j.soilbio.2004.11.028>.
- Kareksela S, Haapalehto T, Juutinen R, Matilainen R, Tahvanainen T, Kotiaho JS. Fighting carbon loss of degraded peatlands by jump-starting ecosystem functioning with ecological restoration. *Science of the Total Environment* 2015; 537: 268-76 <https://doi.org/10.1016/j.scitotenv.2015.07.094>.

- Knox SH, Sturtevant C, Matthes JH, Koteen L, Verfaillie J, Baldocchi D. Agricultural peatland restoration: effects of land-use change on greenhouse gas (CO₂ and CH₄) fluxes in the Sacramento-San Joaquin Delta. *Global Change Biology* 2015; 21: 750-765
<https://doi.org/10.1111/gcb.12745>.
- Krüger JP, Alewell C, Minkinen K, Szidat S, Leifeld J. Calculating carbon changes in peat soils drained for forestry with four different profile-based methods. *Forest Ecology and Management* 2016; 381: 29-36 <https://doi.org/10.1016/j.foreco.2016.09.006>.
- Krüger JP, Leifeld J, Glatzel S, Alewell C. Soil carbon loss from managed peatlands along a land use gradient – a comparison of three different methods. *BGS Bulletin* 2015a; 36: 45-50
<https://doi.org/10.5451/unibas-ep40217>.
- Krüger JP, Leifeld J, Glatzel S, Szidat S, Alewell C. Biogeochemical indicators of peatland degradation - a case study of a temperate bog in northern Germany. *Biogeosciences* 2015b; 12: 2861-2871 <https://doi.org/10.5194/bg-12-2861-2015>.
- Kuhry P, Vitt DH. Fossil carbon/nitrogen ratios as a measure of peat decomposition. *Ecology* 1996; 77: 271-275 <https://doi.org/10.2307/2265676>.
- Kwon MJ, Natali SM, Hicks Pries CE, Schuur EAG, Steinhof A, Crummer KG, et al. Drainage enhances modern soil carbon contribution but reduces old soil carbon contribution to ecosystem respiration in tundra ecosystems. *Global Change Biology* 2019; 25: 1315-1325
<https://doi.org/10.1111/gcb.14578>.
- Lähteenoja O, Reátegui YR, Räsänen M, Torres DDC, Oinonen M, Page S. The large Amazonian peatland carbon sink in the subsiding Pastaza-Marañón foreland basin, Peru. *Global Change Biology* 2012; 18: 164-178 <https://doi.org/10.1111/j.1365-2486.2011.02504.x>.
- Leifeld J, Alewell C, Bader C, Krüger JP, Mueller CW, Sommer M, et al. Pyrogenic carbon contributes substantially to carbon storage in intact and degraded northern peatlands. *Land Degradation & Development* 2018; 29: 2082-2091 <https://doi.org/10.1002/ldr.2812>.
- Leifeld J, Klein K, Wüst-Galley C. Soil organic matter stoichiometry as indicator for peatland degradation. *Scientific Reports* 2020; 10: 7634 <https://doi.org/10.1038/s41598-020-64275-y>.
- Leifeld J, Mayer J. ¹⁴C in cropland soil of a long-term field trial – experimental variability and implications for estimating carbon turnover. *Soil* 2015; 1: 537-542 <https://doi.org/10.5194/soil-1-537-2015>.
- Leifeld J, Müller M, Fuhrer J. Peatland subsidence and carbon loss from drained temperate fens. *Soil Use and Management* 2011; 27: 170-176 <https://doi.org/10.1111/j.1475-2743.2011.00327.x>.
- Leifeld J, Wüst-Galley C, Page S. Intact and managed peatland soils as a source and sink of GHGs from 1850 to 2100. *Nature Climate Change* 2019; 9: 945-947 <https://doi.org/10.1038/s41558-019-0615-5>.

- Liimatainen M, Voigt C, Martikainen PJ, Hytönen J, Regina K, Óskarsson H, et al. Factors controlling nitrous oxide emissions from managed northern peat soils with low carbon to nitrogen ratio. *Soil Biology and Biochemistry* 2018; 122: 186-195 <https://doi.org/10.1016/j.soilbio.2018.04.006>.
- Liu H, Zak D, Rezanezhad F, Lennartz B. Soil degradation determines release of nitrous oxide and dissolved organic carbon from peatlands. *Environmental Research Letter* 2019; 14: 094009 <https://doi.org/10.1088/1748-9326/ab3947>.
- Loisel J, Yu Z, Beilman DW, Camill P, Alm J, Amesbury MJ, et al. A database and synthesis of northern peatland soil properties and Holocene carbon and nitrogen accumulation. *the Holocene* 2014; 24: 1028-1042 <https://doi.org/10.1177/0959683614538073>.
- Musarika S, Atherton CE, Gomersall T, Wells MJ, Kaduk J, Cumming AMJ, et al. Effect of water table management and elevated CO₂ on radish productivity and on CH₄ and CO₂ fluxes from peatlands converted to agriculture. *Science of the Total Environment* 2017; 584-585: 665-672 <https://doi.org/10.1016/j.scitotenv.2017.01.094>.
- Page SE, Wüst RAJ, Weiss D, Rieley JO, Shotyk W, Limin SH. A record of Late Pleistocene and Holocene carbon accumulation and climate change from an equatorial peat bog (Kalimantan, Indonesia): implications for past, present and future carbon dynamics. *Journal of Quaternary Science* 2004; 19: 625-635 <https://doi.org/10.1002/jqs.884>.
- Parnell AC, Phillips DL, Bearhop S, Semmens BX, Ward EJ, Moore JW, et al. Bayesian stable isotope mixing models. *Environmetrics* 2013; 24: 387-399 <https://doi.org/10.1002/env.2221>.
- Pinsonneault AJ, Moore TR, Roulet NT. Effects of long-term fertilization on peat stoichiometry and associated microbial enzyme activity in an ombrotrophic bog. *Biogeochemistry* 2016; 129: 149-164 <https://doi.org/10.1007/s10533-016-0224-6>.
- Pontevedra-Pombal X, Castro D, Souto M, Fraga I, Blake WH, Blaauw M, et al. 10,000 years of climate control over carbon accumulation in an Iberian bog (southwestern Europe). *Geoscience Frontiers* 2019; 10: 1521-1533 <https://doi.org/10.1016/j.gsf.2018.09.014>.
- Ramsey CB. Bayesian analysis of radiocarbon dates. *Radiocarbon* 2009; 51: 337-360 <https://doi.org/10.1017/S003382200033865>.
- Reimer PJ, Austin WEN, Bard E, Bayliss A, Blackwell PG, Bronk Ramsey C, et al. The IntCal20 Northern Hemisphere Radiocarbon Age Calibration Curve (0–55 cal kBP). *Radiocarbon* 2020; 62: 725-757 <https://doi.org/10.1017/rdc.2020.41>.
- Roberts P, Jones DL. Microbial and plant uptake of free amino sugars in grassland soils. *Soil Biology and Biochemistry* 2012; 49: 139-149 <https://doi.org/10.1016/j.soilbio.2012.02.014>.
- Rogiers N, Conen F, Furger M, Stöckli R, Eugster W. Impact of past and present land-management on the C-balance of a grassland in the Swiss Alps. *Global Change Biology* 2008; 14: 2613-2625 <https://doi.org/10.1111/j.1365-2486.2008.01680.x>.
- Schothorst CJ. Subsidence of low moor peat soils in the western Netherlands. *Geoderma* 1977; 17: 265-291 [https://doi.org/10.1016/0016-7061\(77\)90089-1](https://doi.org/10.1016/0016-7061(77)90089-1).

- Schuur EAG, Trumbore SE. Partitioning sources of soil respiration in boreal black spruce forest using radiocarbon. *Global Change Biology* 2006; 12: 165-176 <https://doi.org/10.1111/j.1365-2486.2005.01066.x>.
- Smith LC, MacDonald GM, Velichko AA, Beilman DW, Borisova OK, Frey KE, et al. Siberian peatlands a net carbon sink and global methane source since the early Holocene. *Science* 2004; 303: 353-356 <https://doi.org/10.1126/science.1090553>.
- Szidat S, Salazar Quintero GA, Vogel E, Battaglia M, Wacker L, Synal HA, et al. ¹⁴C analysis and sample preparation at the new Bern Laboratory for the Analysis of Radiocarbon with AMS (LARA). *Radiocarbon* 2014; 56: 561-566 <https://doi.org/10.7892/boris.59263>.
- Tanneberger F, Moen A, Joosten H, Nilsen N. The peatland map of Europe. *Mires and Peat* 2017; 19: 22 <https://doi.org/10.19189/MaP.2016.OMB.264>.
- Tiemeyer B, Albiac Borraz E, Augustin J, Bechtold M, Beetz S, Beyer C, et al. High emissions of greenhouse gases from grasslands on peat and other organic soils. *Global Change Biology* 2016; 22: 4134-4149 <https://doi.org/10.1111/gcb.13303>.
- Tolonen K, Turunen J. Accumulation rates of carbon in mires in Finland and implications for climate change. *The Holocene* 1996; 6: 171-178 <https://doi.org/10.1177/095968369600600204>.
- Torn MS, Swanston CW, Castanha C, Trumbore SE. Storage and Turnover of Organic Matter in Soil. *Biophysico-Chemical Processes Involving Natural Nonliving Organic Matter in Environmental Systems*, 2009, pp. 219-272 <https://doi.org/10.1002/9780470494950.ch6>.
- Trumbore S. Age of soil organic matter and soil respiration: radiocarbon constraints on belowground C dynamics. *Ecological Applications* 2000; 10: 399-411 [https://doi.org/10.1890/1051-0761\(2000\)010\[0399:AOSOMA\]2.0.CO;2](https://doi.org/10.1890/1051-0761(2000)010[0399:AOSOMA]2.0.CO;2).
- Vardy SR, Warner BG, Turunen J, Aravena R. Carbon accumulation in permafrost peatlands in the Northwest Territories and Nunavut, Canada. *The Holocene* 2000; 10: 273-280 <https://doi.org/10.1191/095968300671749538>.
- von Lützw M, Kogel-Knabner I, Ekschmitt K, Matzner E, Guggenberger G, Marschner B, et al. Stabilization of organic matter in temperate soils: mechanisms and their relevance under different soil conditions – a review. *European Journal of Soil Science* 2006; 57: 426-445 <https://doi.org/10.1111/j.1365-2389.2006.00809.x>.
- Worrall F, Evans MG, Bonn A, Reed MS, Chapman D, Holden J. Can carbon offsetting pay for upland ecological restoration? *Science of the Total Environment* 2009; 408: 26-36 <https://doi.org/10.1016/j.scitotenv.2009.09.022>.
- Wright EL, Black CR, Cheesman AW, Drage T, Large D, Turner BL, et al. Contribution of subsurface peat to CO₂ and CH₄ fluxes in a neotropical peatland. *Global Change Biology* 2011; 17: 2867-2881 <https://doi.org/10.1111/j.1365-2486.2011.02448.x>.
- Wüst-Galley C, Grünig A, Leifeld J. Land use-driven historical soil carbon losses in Swiss peatlands. *Landscape Ecology* 2020; 35: 173-187 <https://doi.org/10.1007/s10980-019-00941-5>.

Yu Z, Loisel J, Brosseau DP, Beilman DW, Hunt SJ. Global peatland dynamics since the Last Glacial Maximum. *Geophysical Research Letters* 2010; 37: L13402

<https://doi.org/10.1029/2010gl043584>.

Zhou Y, Boutton TW, Wu XB. Soil C:N:P stoichiometry responds to vegetation change from grassland to woodland. *Biogeochemistry* 2018; 140: 341-357 <https://doi.org/10.1007/s10533-018-0495-1>.

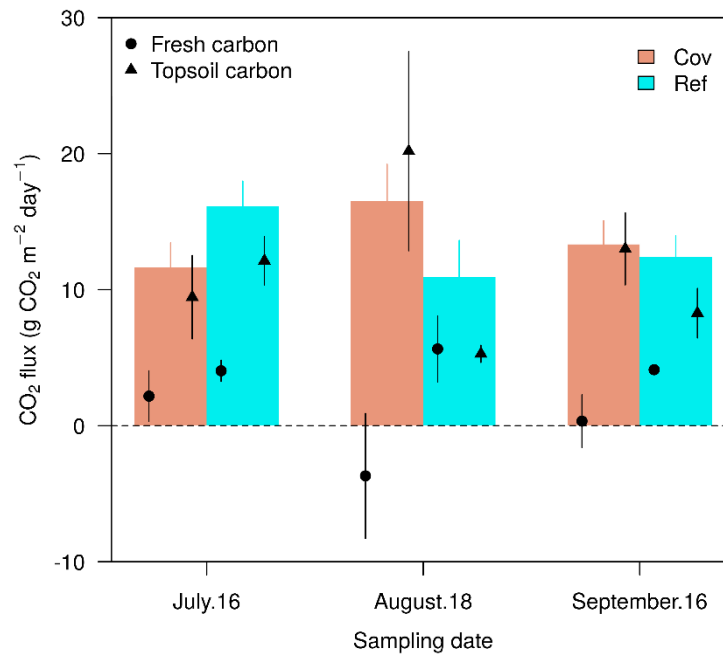
Supplemental Information

Determination of the source of soil heterotrophic respiration by a two – carbon source model

The fraction of the relative contribution of soil carbon (f_{soil} , %) and fresh residues (f_{fresh} , %) to the total CO₂ respired from soil were estimated with a two carbon source model. The measured soil F¹⁴C value ($F^{14}C_{soil}$) of the surface (0 – 12.5 cm) soil of Cov and Ref, and the atmosphere F¹⁴C value ($F^{14}C_{atm}$), which here represents the radiocarbon signature of fresh plant residues, were used to calculate f_{soil} and f_{fresh} .

$$f_{fresh} = \frac{(F^{14}C_{resp} - F^{14}C_{soil})}{(F^{14}C_{atm} - F^{14}C_{soil})} \quad (1)$$

$$f_{soil} = 1 - f_{fresh} \quad (2)$$



Supplemental Fig. 1. Calculated sources of soil heterotrophic respiration (mean \pm se, n = 3) from drained peatland with (Cov) and without mineral soil cover (Ref), using a two carbon source model comprising fresh residues, topsoil C as sources.

Supplemental Table 1. Data from heterotrophic soil respired CO₂ and soil analyzed at the AMS lab in the University of Bern

Lab Code	*Sampling date	Sample label	Fraction modern	\pm Fraction modern	**Age (yr BP)	\pm (yr BP)
BE-11451.1.1	16/07/2019	BG_CO ₂	0.9893	0.0022	86	18
BE-11452.1.1	16/07/2019	Cov 1_CO ₂	0.9442	0.0022	461	19
BE-11456.1.1	16/07/2019	Cov 2_CO ₂	0.9459	0.0022	447	19
BE-11453.1.1	16/07/2019	Cov 3_CO ₂	0.9464	0.0022	442	19
BE-11457.1.1	16/07/2019	Ref 1_CO ₂	0.8550	0.0020	1258	19
BE-11455.1.1	16/07/2019	Ref 2_CO ₂	0.8412	0.0020	1389	19
BE-11454.1.1	16/07/2019	Ref 3_CO ₂	0.8503	0.0020	1302	19
BE-11602.1.1	18/08/2019	Ref 1_CO ₂	0.8763	0.0021	1060	20
BE-11603.1.1	18/08/2019	Ref 2_CO ₂	0.8991	0.0022	855	20
BE-11604.1.1	18/08/2019	Ref 3_CO ₂	0.9072	0.0022	782	19
BE-11605.1.1	18/08/2019	Cov1_CO ₂	0.9342	0.0022	547	19
BE-11606.1.1	18/08/2019	Cov2_CO ₂	0.9280	0.0022	600	19
BE-11607.1.1	18/08/2019	Cov3_CO ₂	0.9099	0.0022	759	19
BE-11699.1.1	16/09/2019	Ref 1_CO ₂	0.8740	0.0021	1082	19
BE-11697.1.1	16/09/2019	Ref 2_CO ₂	0.8706	0.0021	1113	19
BE-11698.1.1	16/09/2019	Ref 3_CO ₂	0.8569	0.0021	1240	19
BE-11700.1.1	16/09/2019	Cov1_CO ₂	0.9333	0.0022	555	19
BE-11701.1.1	16/09/2019	Cov2_CO ₂	0.9406	0.0022	492	19
BE-11702.1.1	16/09/2019	Cov3_CO ₂	0.9234	0.0022	640	19
BE-11703.1.1	16/09/2019	BG_CO ₂	0.9796	0.0023	166	19
BE-12486.1.1	04/12/2019	Cov1_0 – 12.5 cm	0.9194	0.002	675	22
BE-12487.1.1	04/12/2019	Cov2_0 – 12.5 cm	0.9470	0.002	437	21
BE-12488.1.2	04/12/2019	Cov3_0 – 12.5 cm	0.9057	0.003	796	22
BE-12489.1.1	04/12/2019	Ref 1_0 – 12.5 cm	0.8062	0.002	1730	23
BE-12490.1.1	04/12/2019	Ref 2_0 – 12.5 cm	0.7995	0.002	1797	22
BE-12491.1.1	04/12/2019	Ref 3_0 – 12.5 cm	0.7640	0.002	2163	23
BE-12492.1.1	04/12/2019	Cov1_37.5 – 50 cm	0.7670	0.002	2131	22
BE-12493.1.1	04/12/2019	Cov2_37.5 – 50 cm	0.6574	0.002	3369	24
BE-12494.1.1	04/12/2019	Cov3_37.5 – 50 cm	0.6648	0.002	3280	23
BE-12495.1.1	04/12/2019	Ref 1_37.5 – 50 cm	0.5439	0.002	4892	25
BE-12496.1.1	04/12/2019	Ref 2_37.5 – 50 cm	0.5266	0.002	5152	26
BE-12497.1.1	04/12/2019	Ref 3_37.5 – 50 cm	0.5723	0.002	4483	25
BE-12498.1.1	04/12/2019	Cov1_175 – 187.5 cm	0.4565	0.002	6299	27
BE-12499.1.1	04/12/2019	Cov2_175 – 187.5 cm	0.4507	0.002	6401	29
BE-12500.1.1	04/12/2019	Cov3_175 – 187.5 cm	0.4642	0.002	6164	26
BE-12501.1.1	04/12/2019	Ref 1_175 – 187.5 cm	0.4584	0.002	6266	27
BE-12502.1.1	04/12/2019	Ref 2_175 – 187.5 cm	0.4636	0.002	6174	27
BE-12503.1.1	04/12/2019	Ref 3_175 – 187.5 cm	0.4531	0.002	6359	28

* Format of the date: day/month/year.

** Uncalibrated radiocarbon age.

Supplemental table 2. Analysis result based on Bayesian stable isotope mixing model

Sample label	Sampling date*	Fraction	Mean (%)	Standard deviance (%)
Cov 1	16/07/2019	Fresh	59.7	11.4
Cov 1	16/07/2019	Top	28.8	16.1
Cov 1	16/07/2019	Middle	11.5	4.8
Cov 1	18/08/2019	Fresh	49.1	15.0
Cov 1	18/08/2019	Top	37.1	21.2
Cov 1	18/08/2019	Middle	13.8	6.3
Cov 1	16/09/2019	Fresh	47.6	15.3
Cov 1	16/09/2019	Top	38.4	21.7
Cov 1	16/09/2019	Middle	14.0	6.4
Cov 2	16/07/2019	Fresh	46.6	24.8
Cov 2	16/07/2019	Top	45.9	28.0
Cov 2	16/07/2019	Middle	7.6	3.2
Cov 2	18/08/2019	Fresh	41.3	22.7
Cov 2	18/08/2019	Top	45.9	25.6
Cov 2	18/08/2019	Middle	12.8	3.0
Cov 2	16/09/2019	Fresh	45.5	24.5
Cov 2	16/09/2019	Top	45.6	27.6
Cov 2	16/09/2019	Middle	8.9	3.2
Cov 3	16/07/2019	Fresh	70.1	9.6
Cov 3	16/07/2019	Top	21.8	12.6
Cov 3	16/07/2019	Middle	8.1	3.1
Cov 3	18/08/2019	Fresh	37.6	19.9
Cov 3	18/08/2019	Top	49.2	26.4
Cov 3	18/08/2019	Middle	13.2	6.5
Cov 3	16/09/2019	Fresh	52.8	15.1
Cov 3	16/09/2019	Top	35.9	20.0
Cov 3	16/09/2019	Middle	11.3	4.9
Ref 1	16/07/2019	Fresh	50.3	11.3
Ref 1	16/07/2019	Top	31.6	18.9
Ref 1	16/07/2019	Middle	18.1	7.7
Ref 1	18/08/2019	Fresh	54.2	9.3
Ref 1	18/08/2019	Top	31.1	15.5
Ref 1	18/08/2019	Middle	14.7	6.3
Ref 1	16/09/2019	Fresh	48.5	11.6
Ref 1	16/09/2019	Top	35.0	19.4
Ref 1	16/09/2019	Middle	16.5	7.8
Ref 2	16/07/2019	Fresh	43.4	12.9
Ref 2	16/07/2019	Top	38.9	21.6
Ref 2	16/07/2019	Middle	17.7	8.7

Ref 2	18/08/2019	Fresh	65.4	6.9
Ref 2	18/08/2019	Top	22.8	11.5
Ref 2	18/08/2019	Middle	11.8	4.6
Ref 2	16/09/2019	Fresh	56.7	9.0
Ref 2	16/09/2019	Top	29.1	15.0
Ref 2	16/09/2019	Middle	14.2	6.1
Ref 3	16/07/2019	Fresh	54.4	7.1
Ref 3	16/07/2019	Top	23.3	15.1
Ref 3	16/07/2019	Middle	22.4	8.1
Ref 3	18/08/2019	Fresh	72.3	4.1
Ref 3	18/08/2019	Top	16.6	8.7
Ref 3	18/08/2019	Middle	11.1	4.7
Ref 3	16/09/2019	Fresh	58.7	6.1
Ref 3	16/09/2019	Top	24.2	13.0
Ref 3	16/09/2019	Middle	17.1	7.0

* Format of the date: day/month/year.

Paper II

Reduced nitrous oxide emissions from drained temperate agricultural peatland after coverage with mineral soil

Yuqiao Wang ^{1,2}, Sonja M. Paul ¹, Markus Jocher ¹, Christine Alewell ², Jens Leifeld ¹

¹ Climate and Agriculture Group, Agroscope, Reckenholzstrasse 191, 8046 Zürich, Switzerland

² Environmental Geosciences, University of Basel, Bernoullistrasse 30, 4056 Basel, Switzerland

Published as: Wang, Y., Paul, S. M., Jocher, M., Alewell, C., Leifeld, J. (2022). Reduced nitrous oxide emissions from drained temperate agricultural peatland after coverage with mineral soil. *Frontiers in Environmental Science*, 157. <https://doi.org/10.3389/fenvs.2022.856599>

Abstract

Peatlands drained for agriculture emit large amounts of nitrous oxide (N₂O) and thereby contribute to global warming. In order to counteract soil subsidence and sustain agricultural productivity, mineral soil coverage of drained organic soil is an increasingly used practice. This management option may also influence soil-borne N₂O emissions. Understanding the effect of mineral soil coverage on N₂O emissions from agricultural peatland is necessary to implement peatland management strategies which sustain agricultural productivity but also reduce N₂O emissions. With this study, we aimed to quantify the N₂O emissions from an agriculturally managed peatland in Switzerland and to evaluate the effect of mineral soil coverage on these emissions. The study was conducted over two years on a grassland on drained nutrient rich fen in the Swiss Rhine Valley which was divided into two parts, both with identical management. One site was not covered with mineral soil (reference 'Ref'), and the other site had a ~ 40 cm thick mineral soil cover (coverage 'Cov'). The grassland was intensively managed, cut 5-6 times per year and received c. 230 kg N ha⁻¹ yr⁻¹ of nitrogen fertilizer. N₂O emissions were continuously monitored using an automatic time integrating chamber (ATIC) system. During the experimental period, site Ref released 20.5 ± 2.7 kg N ha⁻¹ yr⁻¹ N₂O-N, whereas the N₂O emission from Cov was only 2.3 ± 0.4 kg N ha⁻¹ yr⁻¹. Peak N₂O emissions were mostly detected following fertilizer application and lasted for 2-3 weeks before returning to the background N₂O emissions. At both sites, N₂O peaks related to fertilization events contributed more than half of the overall N₂O emissions. However, not only the fertilization induced N₂O peaks, but also background N₂O emissions were lower with mineral soil coverage. Our data suggest a strong and continued reduction in N₂O emissions with mineral soil cover from the investigated organic soil. Mineral soil coverage, therefore, seems to be a promising N₂O mitigation option for intensively used drained organic soils when a sustained use of the drained peatland for intensive agricultural production is foreseen and potential rewetting and restoration of the peatland is not possible.

Keywords: Organic soil, mineral soil coverage, peatland management, fertilizer, GHG mitigation

1 Introduction

Nitrous oxide (N₂O) is the third most important long-lived greenhouse gas (GHG) and also an important reactant with stratospheric ozone (Ravishankara *et al.*, 2009; Prather *et al.*, 2015). In the last centuries, N₂O emission increased from ~12 Tg N yr⁻¹ in the preindustrial period to ~19 Tg N yr⁻¹ (Syakila and Kroeze, 2011). To a large extent, the rapid raise of N₂O emissions is driven by soil-borne N₂O, which raised from ~6.3 Tg N yr⁻¹ to ~10 Tg N yr⁻¹ over the same period, accounting for ~53% of the total N₂O increase (Tian *et al.*, 2019). Lowering soil N₂O emission is therefore of great importance for global N₂O mitigation, and consequently for meeting the climate target.

Peatlands only account for 3% of the terrestrial land surface, but store around 644 Gt organic carbon (C) (Yu *et al.*, 2010). Peatlands are also an important pool of organic nitrogen (N) of 8 – 15 Gt N (Leifeld and Menichetti, 2018). To date, more than 10 % of the global peatland areas have been drained for agriculture and forestry, with a much higher share in some European countries, where around half of the peatlands are artificially drained to enhance agricultural and forest productivity in Europe, and even ~90% in Switzerland (Bragg *et al.*, 2013; Wüst-Galley *et al.*, 2015; Kasimir *et al.*, 2018). However, long-term drainage causes peatland subsidence due to physical processes and mineralization of the surface peat. These processes cause soil degradation and induce very high GHG emissions, which turned the global peatland biome from a net GHG sink to a net source. It has been estimated that with ongoing peatland degradation c. 2.3 Gt N will be released globally (Leifeld and Menichetti, 2018). In Europe, peatland management induces N₂O emission of c. 145 Gg N yr⁻¹ (Liu *et al.*, 2020). Full peatland restoration or other steps involving rewetting decrease the peat oxidation by re-raising the water table (Blodau, 2002) and might save substantial parts of the N mineralization and also halt peatland subsidence (Knox *et al.*, 2015; Hemes *et al.*, 2019). However, with rewetting, intensive agricultural production is in many cases not possible anymore. Hence, there is a trade-off between environmental goals and agricultural production demands, that creates challenges to implementing peatland restoration (Ferré *et al.*, 2019). Therefore, peatland management strategies, which could not only sustain the productive use of organic soil but also counterbalance soil subsidence and reduce N₂O emission, are urgently needed. It has been reported that artificial mineral soil coverage with thicknesses of 0.2 – 0.5 m is becoming an increasingly used practice in Switzerland and other European countries (Schindler and Müller, 1999; Ferré *et al.*, 2019). Mineral soil coverage may have two main impacts on N and C transformation and N₂O emissions. First, it changes the topsoil properties of drained organic soil and influences substrate availability for N₂O production. As the soil depth from which emitted N₂O originates is only 0.7 – 2.8 cm, the most upper soil properties are particularly relevant for N₂O emission (Neftel *et al.*, 2000). After mineral soil coverage, the topsoil contains much less organic matter than the degrading peat. With this, carbon and nitrogen availability for denitrification might become limiting, thereby also influencing soil N₂O production (Stehfest and Bouwman, 2006; Flechard *et al.*, 2007).

Second, mineral soil coverage alters soil hydraulic properties and soil aeration due to the changing pore sizes distribution. Soil moisture and concomitantly the amount of oxygen are important regulators for microbial activity, thus affecting nitrification, denitrification, and subsequent N loss as N₂O (Davidson *et al.*, 2000).

In Switzerland, peatlands covered an area of ca. 1000 – 1500 km² in preindustrial times. Today, most of the former organic soils are already lost with only ~280 km² left. Ninety percent of the remaining organic soils are still drained for agriculture (Wüst-Galley *et al.*, 2020) and continuously contribute to the national economic values of agriculture output. It is estimated that these soils emit around 1.2 – 7.9 kg N₂O-N ha⁻¹ yr⁻¹ (Leifeld, 2018), corresponding to an annual N₂O emission of c. 65 kt CO₂-eq, or ~ 10% of the national GHG emissions from drained organic soil (FOEN, 2021). However, hitherto neither N₂O flux measurements from organic soil do exist for Switzerland nor are experimental data available to quantify the impact of mineral soil coverage on N₂O emissions from drained peatland.

In this study, we utilized an automatic time integrating chamber system (ATIC) to determine the N₂O emission from long-term intensively managed temperate drained peatland with (Cov) and without (Ref) mineral soil coverage. Our specific objectives were to: 1) quantify the N₂O emission from a drained, nutrient-rich managed peat meadow in the Swiss Rheine valley, 2) explore the effect of mineral soil coverage on N₂O fluxes from this soil.

2 Material and methods

2.1 Study site

The measurements were carried out in the Swiss Rhine Valley, at the site Rüthi (47°17' N, 9°32' E), a drained fen with a peat thickness of ~10 m. The site has a cool temperate-moist climate with mean annual 1297 mm annual precipitation and a mean annual temperature of 10.1 °C (1981 – 2010, <https://www.meteoswiss.admin.ch>). Drainage with ditches commenced before 1890 (<https://map.geo.admin.ch>). An integral drainage system with drainage pipes (depth 1 m, distance between pipes 14 m) and pump was built in 1973, at the same time the site was used as pasture until 2013, and since then as an intensively managed meadow with mineral and slurry fertilization and 5 to 6 grass cuts per year. In 2006 to 2007, one part of the field (1.7 ha) was covered with mineral soil material (thickness around 40 cm, see details in Table 1) to improve the trafficability and agriculture usability by raising the soil surface and counterbalancing peat subsidence. We established our field experiment at this mineral soil coverage site (Cov) and used the adjacent drained organic soil without mineral soil coverage as the reference (Ref, see details in Figure S1). Both sites have the identical farming practice and similar vegetation. Dominant grass species are *Lolium perenne*, *Alopecurus pratensis*, *Festuca*

arundinacea, *Trifolium spec.* and *Festuca pratensis*. The atmospheric N deposition at the study site as estimated for 2015 is 20 – 30 kg N ha⁻¹ yr⁻¹ (Rihm and Künzle, 2019).

Table 1. Surface (0 – 10 cm) soil properties of drained organic soil with (Cov) and without (Ref) mineral soil coverage (n = 11).

Parameter	Cov	Ref
Bulk density (g cm ⁻³) ^a	1.1 ± 0.04	0.5 ± 0.01
pH	7.3	5.2
Sand (%) ^a	31.8	0.6
Silt (%) ^a	52.3	67.3
Clay (%) ^a	15.9	32.1
Total pore volume (%) ^a	58.4 ± 1.5	75.1 ± 0.5
Field capacity (%) ^a	51.4 ± 0.9	57.9 ± 0.6
Total N (%)	0.30 ± 0.03	1.46 ± 0.04
SOC (%)	3.57 ± 0.52	17.68 ± 0.47
C to N ratio	11.68 ± 1.15	12.12 ± 0.16
NH ₄ ⁺ (N mg kg ⁻¹ dry soil) ^b	2.62 ± 0.96	37.33 ± 12.07
NO ₃ ⁻ (N mg kg ⁻¹ dry soil) ^b	2.81 ± 1.21	5.16 ± 1.13

a. Measured at depth of 3 – 8 cm, n = 12.

b. n = 8.

2.2 N₂O flux measurements

2.2.1 Automatic Time Integrating Chamber (ATIC) system

The here used ATIC system was developed based on the automatic chamber system design introduced by Flechard *et al.* (2005), and the air sampling follows the system introduced by Ambus *et al.* (2010). The ATIC is operated as a non-steady-state flow-through chamber with a main loop that recirculates the headspace chamber air (Figure 1). The lid of the chamber closes automatically for 15 min. During this period, four headspace gas samples are collected (at 3.50 min, 7.25 min, 11.50 min and 14.25 min after chamber closure) for 15 s and flushed into four different foil gas bags through a valve manifold. The use of the ATIC system allows flux measurements at relatively high frequency (like for online automatic chamber systems) but reduces the frequency of gas analysis and avoids the use of online trace gas analysis, which lowers the cost and energy consumption in the field. The ATIC runs with battery (12V) or power line, the latter used in our experiment. It consist of three parts, i) a stainless steel chamber ($L = l = 300$ mm, $H = 220$ mm) with pump (Thomas, Germany), CO₂ sensor (Senseair, Sweden), flow sensor (McMillan, USA), lid inclinometer sensor (DIS Sensors, Netherland) and motor connected with the lid of the chamber through pulley and rope (Figure 1A, unit 2); ii) an associated controller system, including the main control module (Siemens, Germany), and the data logger (Onset, USA) for the sensors attached with the chamber (Figure 1A, unit 1); iii) 4 replaceable foil gas bags (Supelco, Germany;

Figure 1A, unit 3). The controlling system opens and closes the chamber lid through the motor. Each chamber was placed on a PVC frame, inserted 5 cm into the soil. Flexible silicone attached below the chamber and the foam sealing above the chamber was used to achieve gas tightness of the chamber.

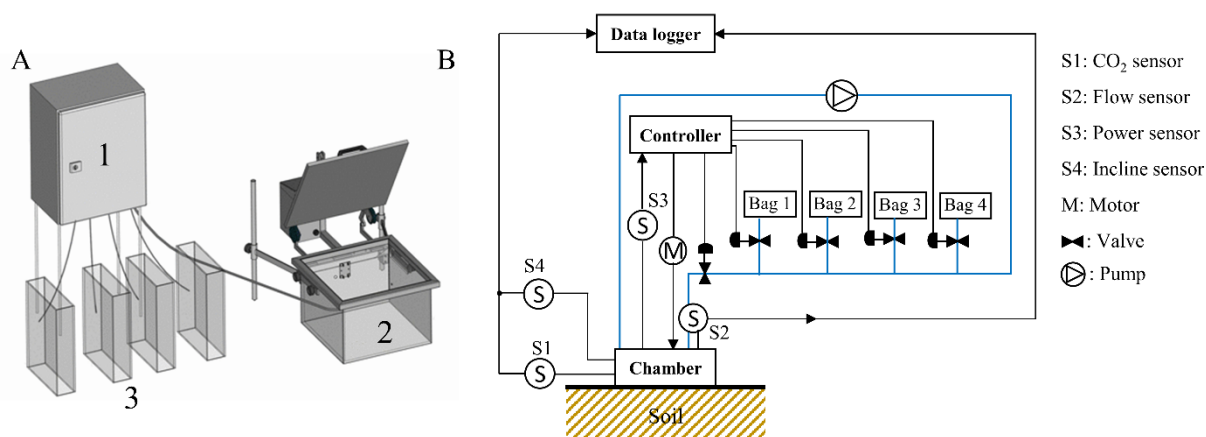


Figure 1. Brief overview of the automatic time integrating chamber system ATIC (A) and basic outline of ATIC gas sampling (B), black line indicate the control signal pathway, blue line indicates the sample gas pathway.

2.2.2 N₂O sample accumulation and analysis

N₂O fluxes were measured quasi-continuously for two entire years from 28 February 2019 to 02 March of 2021. Here we designate the first sampling year period (from 28 February 2019 to 28 February 2020) as the first year, and the second sampling year period (from 28 February 2020 to 02 March 2021) as the second year. In the study site, the ATIC systems (four on Cov, four on Ref) were installed at 13 February 2019 for testing. At 28 February 2019, eight ATIC systems (four on Cov, four on Ref) started to collect gas samples with a frequency (time between measurement cycles) of 3 – 9 hours per individual chamber, differing between growing season and non-growing season. Here, we define a measurement cycle as a lid closing phase of 15 minutes with sequential gas sampling into each of the four foil gas bags.

The bags were filled 3.50, 7.25, 11.50, 14.25 minutes after chamber closure, respectively, and the gas samples from individual cycles accumulated in these four foil gas bags. The final bag samples represented an average over a time period of 3 to 14 days (hereafter referred to as ‘sampling period’), depending on the sampling frequency and the total number of measurement cycles. Usually, gas samples accumulated in the bags over 30 – 40 cycles, which was limited by the volume of the foil gas bag (10 L) and the flow rate of the pump (1L min⁻¹). After that sampling period, the foil gas bags were replaced with empty ones, and the filled gas bags were transferred to the lab to determine their gas concentration by the gas analyzer (G2308, Picarro, USA). Overall, each ATIC system was working for ~ 3200 cycles during the two entire years. The foil gas bags have been tested and proved to be suitable for long term storage of N₂O near ambient concentrations in air (Figure S2).

2.2.3 N₂O flux calculation

For static (non-steady-state) chamber measurement, the increase in headspace gas concentration is widely thought to be linear during a short closure time (Charteris *et al.*, 2020). The analysis of the gas bags as described in the previous section resulted in four average concentrations $\bar{C}_1 \dots \bar{C}_4$ for each chamber and sampling period. Calculating a linear regression of the four concentrations against their sampling times (3.50, 7.25, 11.50, 14.25 min after chamber closure) yielded the regression slope $\partial\bar{C}/\partial t$ (mg m⁻³ min⁻¹) from which the average flux of the sampling period was derived as:

$$F = \frac{V}{A} \times \frac{\partial\bar{C}}{\partial t} \quad (1)$$

V and A are the volume (m³) and the covered area (m²) of the static chamber, 0.02 m³ and 0.09 m². Since each average bag concentration \bar{C}_a is the arithmetic average of the respective concentrations in each cycle ($C_{a,b}$), where a ($a = 1, 2, 3, 4$) is the number of bag, b is the number of cycles, the average slope $\partial\bar{C}/\partial t$ also represents the average of the individual concentration increases of each measurement cycle ($\partial C_b/\partial t$) in the sampling period. Therefore, F (Eq. 1) represents the average gas flux of each sampling period.

The multiplication of gas fluxes during each individual sampling period F (mg N m⁻² day⁻¹) and the duration of each sampling period T (days) yielded the cumulative gas fluxes of each individual sampling period. Finally the annual cumulative N₂O fluxes (F_a , kg N ha⁻¹) were calculated from the cumulative gas fluxes of each individual sampling period as below:

$$F_a = \sum_{i=1}^{i=n} F_i * T_i \quad (2)$$

F_i is the N₂O emission (mg N m⁻² day⁻¹) from sampling period i , and T_i is the duration of each sampling period i (days).

N₂O fluxes resulted from fertilization induced N₂O peaks (F-peak) and background N₂O emissions. The comparison of N₂O emissions before and after a fertilization event allowed for the detection and quantification of F-peak N₂O emissions. Quantifying background N₂O emissions after fertilization event is challenging, and we here use mean N₂O emissions one week before fertilization to represent the background N₂O emissions during the fertilization event and for further analysis of the F-peaks. Only when the observed N₂O emissions during a fertilization event was higher than the background N₂O emissions, we consider this as F-peak induced by the fertilization event.

2.2.4 Data quality control and gap filling

Data quality control

The accuracy of the ATIC system was accessed by the CO₂ and inclinometer sensors inside the chamber. The measurement of the real-time headspace chamber CO₂ concentration and the incline angle between the lid and chamber allowed us to detect any operational chamber problem (eg. leakage, power failure). The CO₂ fluxes during each chamber closure time was evaluated by linear regression, and an overall $R^2 \geq 0.9$ was taken as indicator for a fully functional ATIC within the sampling period. With the comparison between the average CO₂ fluxes during each chamber closure time and the CO₂ fluxes from the ATIC system within each individual sampling period we determined whether the gas fluxes from the ATIC system represented the average gas fluxes within the sampling period (Figure S3). N₂O fluxes calculated from the concentration gradient from the four foil gasbags were selected for post-processing after fulfilling certain quality criteria. Firstly, the R^2 of CO₂ fluxes calculated from the regression lines of the four bags had to exceed 0.9, indicating that within the sampling days the ATIC worked properly. $R^2 \leq 0.9$ indicated a failure of gas sampling within the sampling days, which lead to a rejection of the N₂O flux data. Secondly, a $R^2 > 0.9$ of the N₂O regression lines was used as critical to accept the data for further analysis. However, low fluxes ($\pm 0.5 \text{ mg N m}^{-2} \text{ day}^{-1}$, calculated based on the detection limit of the Picarro) were accepted regardless of the R^2 . With low fluxes, the random error of the measurement could be larger than the N₂O concentration difference between different sampling points, which could result in a low R^2 , and therefore rejection of the N₂O emission based on the low R^2 would lead to an underestimation of the overall fluxes. After two-year's continuous field observation, the N₂O data could cover ~86% of the sampling days, i.e. a data gap of ~14%.

Gap filling

For any missing N₂O emissions outside the fertilization event (background N₂O emissions), ie. values missing owing to a failure of ATIC systems or a rejection of data, a look-up table approach with two parameters (soil moisture and soil temperature) was used to fit the missing values ($RMSE = 0.62 \text{ mg N m}^{-2} \text{ day}^{-1}$, $R^2 = 0.60$), and tested by the available background N₂O values through cross validation. For each individual chamber, background N₂O emissions were divided into 16 classes based on soil moisture (0–25th percentile, > 25th percentile–median, > median–75th percentile, > 75th percentile), and soil temperature (0–25th percentile, > 25th percentile–median, > median–75th percentile, > 75th percentile). With the assumption that without extra fertilizer input, background N₂O should respond similar to similar soil temperature and moisture conditions at each site, the mean N₂O fluxes from each class was used to fit the missing value under the same soil temperature and moisture condition. To check the sensitivity of the N₂O gap filling method for the background fluxes, two other methods were compared with the look-up table approach, 1) linear interpolation ($RMSE = 0.65 \text{ mg N m}^{-2} \text{ day}^{-1}$, $R^2 = 0.51$) to bridge the missing values, 2) taking mean values from the properly operating chambers for each site ($RMSE = 1.3 \text{ mg N m}^{-2} \text{ day}^{-1}$, $R^2 = 0.36$). For a N₂O gap caused by a power failure during the fertilization event at 30 August 2019 (site Ref), data were linearly interpolated to fill the data gap. For the failure of individual chambers ($n = 6$) during fertilization events, mean values from the properly operating chambers at each site were used to fill the data gap.

2.3 Additional measurements

2.3.1 Environmental variables

Air temperature was measured with a Vaisala weather Transmitter (WXT520, Finland) and continuously logged every 10 minutes on a CR1000 data logger (Campbell Scientific, UK). Rainfall data and missing air temperature (27 December 2020 to 2 February 2021) was filled with data from a nearby meteorological station operated by MeteoSwiss (<https://www.meteoswiss.admin.ch>). For both sites soil temperature and soil moisture (GS3 and 5TE decagon devices, NE Hopkins Court, USA) was continuously recorded half hourly at depth of 5 cm for Cov ($n = 3$) and Ref ($n = 3$). At 4 December 2019, 24 additional soil temperature sensors (UA-001-64 devices, Onset, USA) were installed near each chamber at three depth 0 cm, 2.5 cm and 5 cm for recording surface soil temperature in winter. These sensors were taken out at 21 April 2020 for reading out the data, and the same process was followed for the winter 2020/2021. Close to the chambers, the soil volumetric water contents at -5 cm depth were consistently recorded every 10 minutes with soil moisture sensor (EC-5, decagon devices, NE Hopkins Court, USA). Missing soil temperature data – due to a failure of a data logger between November to December 2019 and April to May 2020 (site Cov) was fitted using linear regression between temperatures of the two sites with similar temperature range ($RMSE = 0.07$ °C, $R^2 = 0.98$).

2.3.2 Soil properties and fertilizer nutrient

To determine the soil pore volume, at 12 April 2019, 72 undisturbed cylindrical soil samples (100 cm^3) were collected at three depth (3 – 8 cm, 18 – 23 cm, 58 – 63 cm) with 12 replications each site, and transferred to the lab. In the laboratory, different pore diameters were measured following the approach from (Keller *et al.*, 2019). For this, samples were saturated from below and then drained to soil matric potentials of -30, -60, -100, -300, -1500 kPa.

Air porosity was calculated based on the difference between volumetric water content (VWC) and total pore volume. The relative gas diffusion coefficient (D_p/D_0) was calculated based on air-filled porosity by following the approach from Keller *et al.* (2019). A D_p/D_0 of 0.02 has been suggested as the critical threshold for adequate soil aeration, and D_p/D_0 value lower than 0.02 indicate insufficient soil aeration (Schjønning *et al.*, 2003). The water filled pore space was determined by the ratio of volumetric water content and total pore volume; and field capacity was determined by water retention at -30 kPa. Here, we used the threshold of 80 % of the field capacity for each site to roughly distinguish dry and wet conditions separately for Cov and Ref. A soil moisture of below 80 % of the field capacity was designated as dry, and > 80% of the field capacity as wet.

For soil organic carbon (C) and total nitrogen (N) content measurement, 22 soil samples were taken at year 2018, with 11 replications each site. Soil samples were dried at 105 °C for 72 h, ground with mortar

and pestle, and then milled in a ball mill (Retsch, MM 400, Germany) at 25-rotation s^{-1} for 3 min. Samples containing carbonate (soil surface from Cov) were fumigated with hydrochloric acid overnight in a desiccator before being analyzed by elemental analysis (Hekatech, Germany). For soil pH, (unground) soil was suspended 10 g in 0.01 M calcium chloride ($CaCl_2$), shaken at 160 cycles min^{-1} for 15 min, and left overnight before measuring the soil pH with a flat surface electrode (pH3310, WTW, Germany). For ammonium and nitrate measurements, 16 soil samples were taken at July 2021, with 8 replications each site. Soil N was extracted from 20 g field-moist soil with 0.01 M $CaCl_2$ solution and filtered. The filtrate was analyzed by segmented flow injection analysis (Skalar Analytical B.V., Breda, The Netherlands). The C and N content in slurry was determined in a central laboratory (Labor für Boden und Umweltanalytik, Eric Schweizer AG, Thun, Switzerland. For details about N application rate and frequency, please see Table 2).

2.4 Data analysis

Plots and statistical analysis were performed using open sources software R (version 3.6.0, The R Project, 2014). N_2O emissions as measured by the ATIC systems were calculated based on linear regression in R. Environmental parameters including soil temperature, soil moisture, air filled porosity, and D_p/D_0 were calculated and plotted as daily means. A Multiple linear regression (MLR) model with unstandardized explanatory variables was used to evaluate the drivers for the F-peak and daily background N_2O emissions, with soil temperature, water filled pore space and nitrogen (N) input as explanatory variables. For each of those variables, its statistical significance to the MLR model was chosen as $p < 0.05$. The adjusted coefficient of determination (R^2_{adj}), is then given by the number of driving variables and the sample size, and is used to describe the explained variation of the dependent variable. For the daily background N_2O emissions, the minimum N_2O flux plus one (which was determined by the minimum observed N_2O emission data) was added to N_2O fluxes separately for the two sites and log transformed before applying to the MLR model. Difference in soil temperature, soil moisture, air-filled porosity, daily N_2O emission, annual N_2O emission, daily N_2O emission from fertilization events (daily F-peak N_2O), fertilization induced N_2O peaks, daily background N_2O emission and cumulative background N_2O emission were analyzed for statistical difference between Cov and Ref by using a t-Test. An error probability of $p < 0.05$ was chosen. Results are always reported as mean \pm 1 standard error (se).

For the annual N_2O emission from Cov and Ref, we calculated the standard error based on the spatial variability between the four ATIC systems for both sites. The annual cumulative se of each N_2O flux calculation by linear regression within each chamber contributed only 0.1% to the se derived from the spatial variability of the four replicates. Therefore, we believe that the se deriving from spatial variability covers the overall se inherent to our N_2O flux calculations.

3 Results

3.1 Environmental conditions

The two sampling years had a mean annual air temperature of 10.7 °C (Figure 2A) and annual precipitation of 1535 mm. The latter, was higher in the first (1690 mm) than the second year (1380 mm, Figure 2B). The two years and two sites had similar daily mean soil temperature on average. At both sites 5 cm soil temperature was continuously above 0 °C for both sites during the two sampling years despite frequent winter frost (Figure 2A). In the second year, spring and summer were moister with ~10.9 % and ~11.4 % higher ($p < 0.01$) soil water filled pore space (WFPS) during March to June and June to August than in the first year. Soil WFPS was not different between sites, but more variable for Cov (30.8 % – 91.6 %) than Ref (24.2 % – 76.4 %, Figure 2B). During spring and summer of year 2019, air filled porosity was higher ($p < 0.05$) than in 2020 by ~ 3.9 % and ~ 5.4 %. Air filled porosity was almost continuously higher ($p < 0.01$) at Ref than Cov (Figure 2C). Consequently, the relative gas diffusion coefficient of Ref exceeded that of Cov ($p < 0.01$). At Cov, the relative gas diffusion coefficient was lower than critical threshold for adequate soil aeration (0.02) at 172 days, whereas it never passed the critical threshold at Ref (Figure 2D).

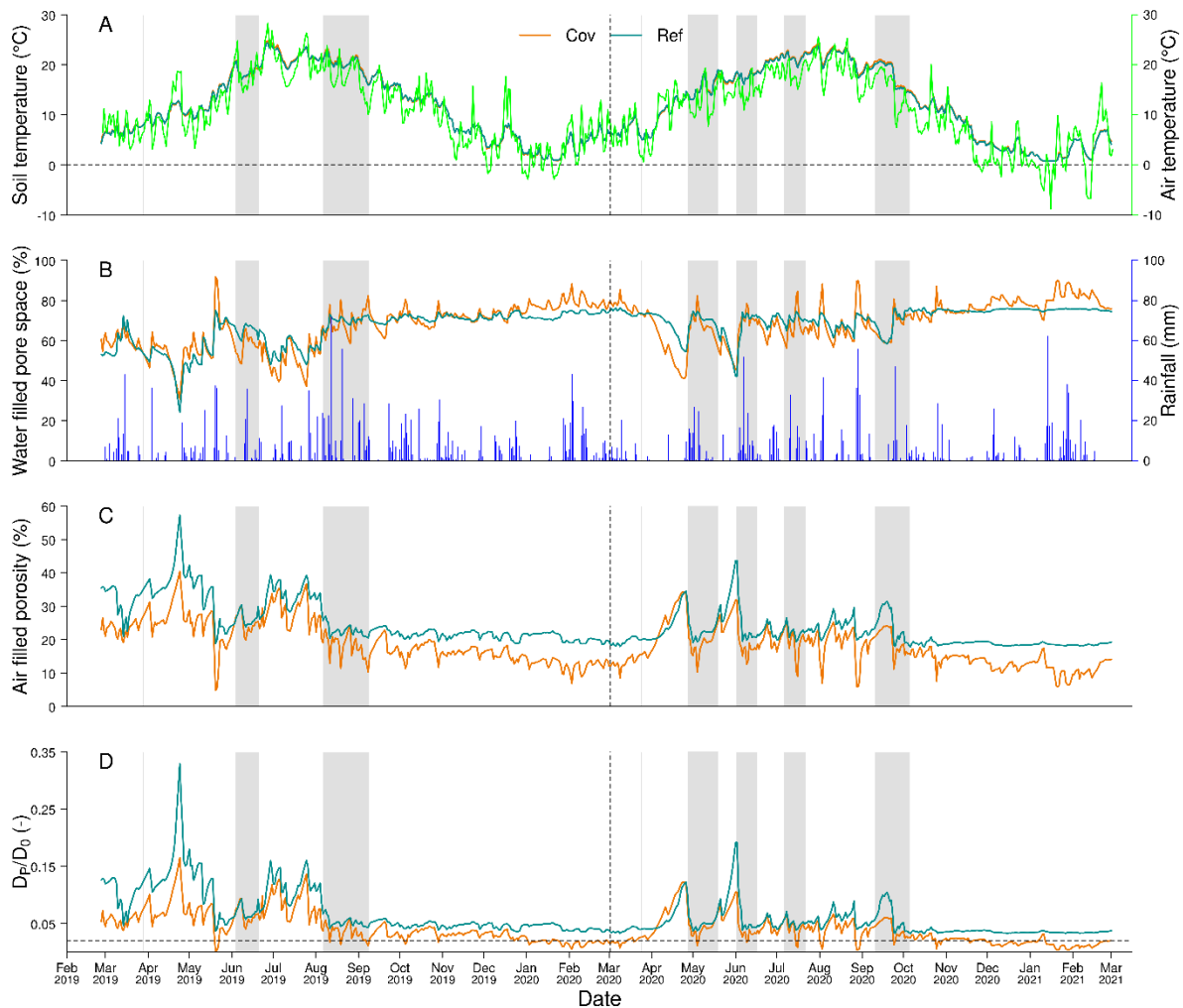


Figure 2. Daily mean soil (dark green and orange lines are overlaying because of high similarity of soil temperature at Cov and Ref) and air (light green) temperature (A), soil water filled pore space and rainfall (B), air filled porosity (C) and relative gas diffusion coefficient (D_p/D_0 , D) from drained peatland with (Cov) and without (Ref) mineral soil coverage at 5 cm depth. The horizontal dashed line in panel D indicate the critical threshold for adequate soil aeration, which was set at 0.02 by Schjønning et al. (2003). Vertical dashed line separate the first year (28.02.2019 to 28.02.2020) and the second year (28.02.2020 to 02.03.2021). The shaded areas indicate time periods influenced by fertilization events.

3.2 N₂O emissions

The N₂O emissions integrated over two year's continuous field measurement from Ref exceeded that of Cov by a factor of 9 (Figure 3). Daily N₂O emissions showed a larger variability during the first year, ranging from -0.02 to 242.01 mg N m⁻² day⁻¹ for Ref, and from -0.04 to 22.08 mg N m⁻² day⁻¹ for Cov. During the second year, daily N₂O emission ranged from -0.04 to 18.41 mg N m⁻² day⁻¹ for Ref and from -0.04 to 2.80 mg N m⁻² day⁻¹ for Cov (Figure 3). At Ref, the average daily N₂O emissions during the first year was 8.98 ± 1.03 mg N m⁻² day⁻¹, which was higher ($p < 0.01$) than Cov (0.86 ± 0.10 mg N m⁻² day⁻¹, see Figure 4C).

Overall, N₂O emissions differed largely both between the two sites and the two years. At Ref, emissions were ~ 4 times higher during the first year, than during the second year. At Cov the first year emissions were ~ 2 times higher than the second year ones. The annual N₂O fluxes for the two years were different for both sites, but the N₂O emissions from Ref was still clearly higher ($p < 0.01$) than Cov. In the first year, the cumulative annual N₂O flux from Ref was $32.71 \pm 3.87 \text{ kg N ha}^{-1} \text{ yr}^{-1}$, around 11 times higher than Cov ($3.18 \pm 0.35 \text{ kg N ha}^{-1} \text{ yr}^{-1}$; Figure 4A). In the second year, the annual N₂O fluxes from Ref was $8.28 \pm 1.77 \text{ kg N ha}^{-1} \text{ yr}^{-1}$ (Figure 4B), which was around 6 times higher than Cov ($1.33 \pm 0.23 \text{ kg N ha}^{-1} \text{ yr}^{-1}$). The difference of N₂O emissions between the sites was not only related to higher ($p < 0.01$) fertilization induced peak N₂O emissions from Ref ($42.48 \pm 3.34 \text{ mg N m}^{-2} \text{ day}^{-1}$) than Cov ($3.41 \pm 0.54 \text{ mg N m}^{-2} \text{ day}^{-1}$), but also driven by higher ($p < 0.05$) background N₂O emissions from Ref ($1.63 \pm 0.46 \text{ mg N m}^{-2} \text{ day}^{-1}$) than Cov ($0.27 \pm 0.04 \text{ mg N m}^{-2} \text{ day}^{-1}$, see Figure 4C). A similar pattern was seen in the second year (Figure 4D).

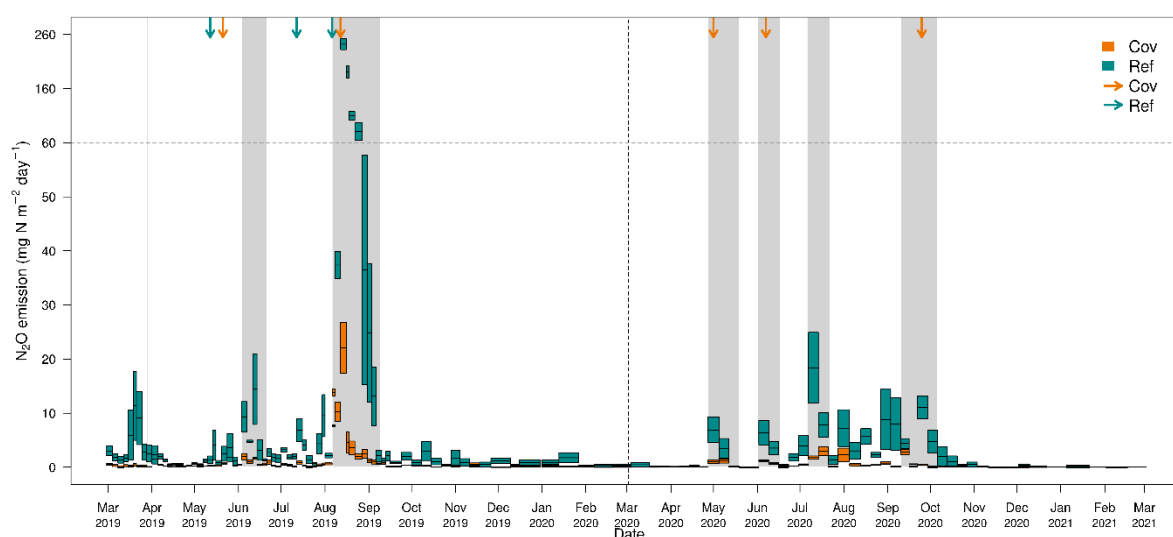


Figure 3. Comparison of gap-filled N₂O emissions (mean \pm se, $n = 4$) from drained organic soil with (Cov) and without (Ref) mineral soil coverage for the period 28.02.2019 to 02.03.2021. The width of the box represent the length of each individual sampling period. Each individual box shows the mean \pm se ($n = 4$) value of N₂O emissions from four chambers per sites. The shaded areas indicate time periods influenced by fertilization events. Arrows on the top indicate when field conditions changed from long term dry to wet. The vertical black dashed line separates the first year (28.02.2019 to 28.02.2020) from the second year (28.02.2020 to 02.03.2021). For better readability, the scale of the y-axis is expanded ten times for N₂O emission higher than $60 \text{ mg N m}^{-2} \text{ day}^{-1}$, indicating by a grey dashed line.

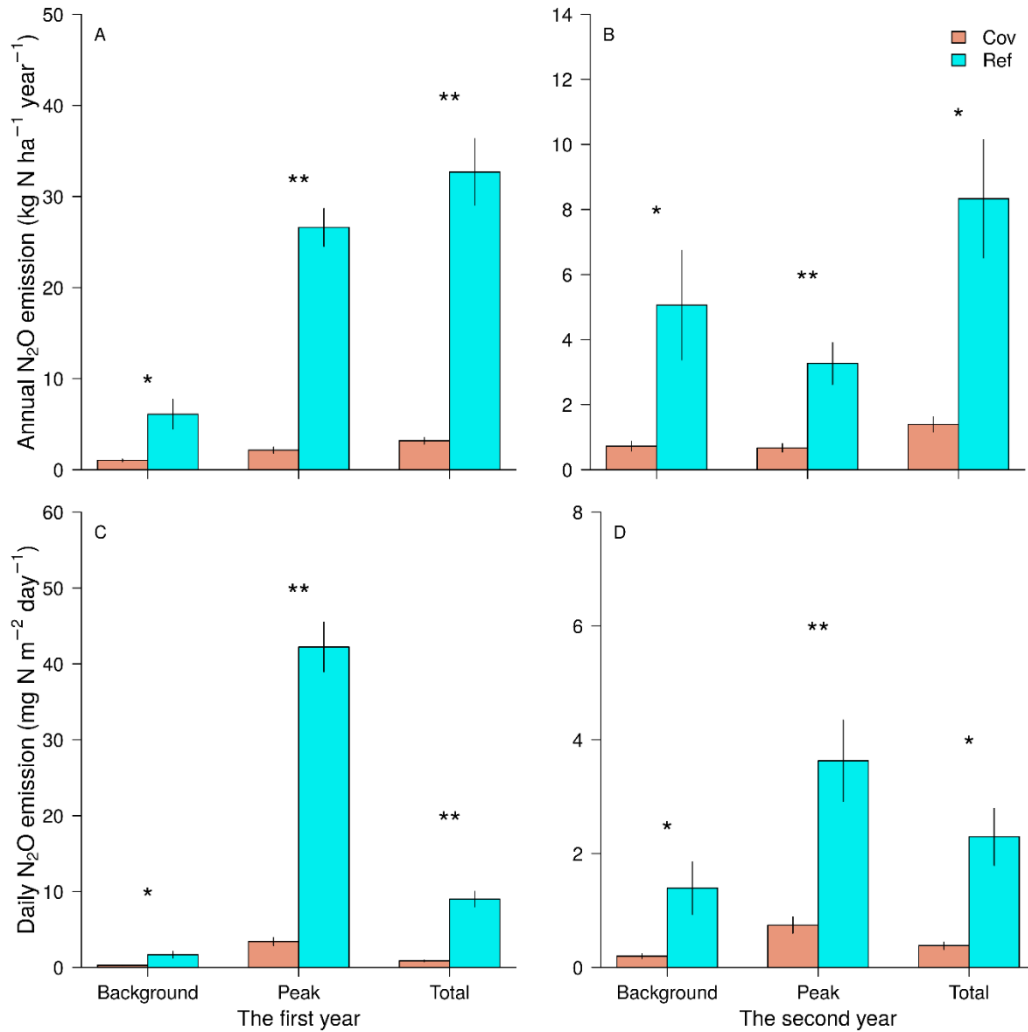


Figure 4. Cumulative N₂O emissions (mean ± se, $n = 4$) and contribution of the emission types to the overall field N₂O emission from drained organic soil with (Cov) and without (Ref) mineral soil coverage during the first year (A) and the second year (B); and average daily N₂O emission (mean ± se, $n = 4$) for two emission types during the first year (C) and the second year (D). Significant differences between two sites are indicated with asterisks (“***” $p < 0.01$, “**” $p < 0.05$).

3.3 Main driving factors of N₂O emissions

3.3.1 Fertilization effect

At both sites, high N₂O emission peaks were primarily triggered by fertilization events (F-peak), and lasted for 2 – 3 weeks before returning to background N₂O emissions (Figure 3). There were eight fertilization events during the experimental period, but we only observed six F-peaks during summer and autumn when the soil temperature was high (Table 2). To further explore the influence of N input on N₂O emissions, we defined a corresponding fraction of N loss as the ratio of the N₂O emissions during each F-peak and the corresponding fertilizer N input. We found the fraction of N loss to be higher at Ref than at Cov ($p < 0.01$) for each of the six individual F-peaks. In the first year, F-peaks contributed

~78 % to the annual N₂O emissions at Ref, corresponding to 25.56 ± 2.15 kg N ha⁻¹. At Cov, F-peaks contributed ~ 64 % to the annual N₂O emissions, corresponding to 2.02 ± 0.32 kg N ha⁻¹ (Figure 4A). For the second year, at both sites F-peak fluxes only contributed ~ 43 % to the annual N₂O emissions, corresponding to 3.51 ± 0.84 kg N ha⁻¹ for Ref and 0.57 ± 0.11 kg N ha⁻¹ for Cov (Figure 4B). It need to be noted that during the fertilizer event in August 2019, we observed a relatively high peak at both sites (Figure 3), which extended over 25 days (8 sampling periods). The N₂O emissions from this high peak contributed ~78 % to the annual N₂O emissions to Ref, and ~ 64 % to Cov.

Table 2. Fertilization event induced nitrous oxides (N₂O) fluxes (mean \pm se, $n = 4$) and associated environmental parameters, soil temperature (T_{soil}) and water filled pore space (WFPS) from drained organic soil with (Cov) and without (Ref) mineral soil coverage.

Date	Fertilization (kg N ha ⁻¹)		F-peak N ₂ O flux(kg N ha ⁻¹)		Fraction of N loss* (%)		T_{soil} (°C)		WFPS(%)	
	Cov	Ref	Cov	Ref	Cov	Ref	Cov	Ref	Cov	Ref
28.Mar.19 ^a	0	0	0	0	0	0	8.0	8.1	53.7	53.6
03.Jun.19 ^b	0.01 \pm 0.009	0.07 \pm 0.02	0.03 \pm 0.02	0.22 \pm 0.04	0.03 \pm 0.02	0.22 \pm 0.04	18.6	18.8	57.8	65.6
06.Aug.19 ^a	2.01 \pm 0.32	25.50 \pm 2.15	2.37 \pm 0.38	30.04 \pm 2.53	2.37 \pm 0.38	30.04 \pm 2.53	20.8	20.3	67.6	69.0
24.Mar.20 ^a	0	0	0	0	0	0	5.8	5.5	73.3	73.4
27.Apr.20 ^a	0.16 \pm 0.05	0.77 \pm 0.31	0.25 \pm 0.07	1.18 \pm 0.47	0.25 \pm 0.07	1.18 \pm 0.47	15.0	14.8	67.6	69.7
02.Jun.20 ^b	0.13 \pm 0.008	0.70 \pm 0.23	0.50 \pm 0.03	2.69 \pm 0.88	0.50 \pm 0.03	2.69 \pm 0.88	17.8	17.7	67.1	69.4
07.Jul.20 ^b	0.28 \pm 0.07	1.43 \pm 0.56	1.08 \pm 0.27	5.50 \pm 2.16	1.08 \pm 0.27	5.50 \pm 2.16	21.4	20.9	66.9	70.3
10.Sep.20 ^a	0.003 \pm 0.005	0.62 \pm 0.16	0.004 \pm 0.007	0.84 \pm 0.21	0.004 \pm 0.007	0.84 \pm 0.21	20.6	19.8	61.1	62.9

* Equivalent fraction of fertilization induced N₂O emission and the fertilizer N input, mean \pm SE (n = 4).

a. Nitrogen (N) inputs as slurry.

b. Nitrogen (N) inputs as synthetic fertilizer.

3.3.2 Environmental parameters

In order to identify the main driving factors for N₂O emissions, regression analysis were applied separately on fertilization induced and background N₂O emissions. For fertilization induced N₂O emissions, the regression analysis was performed on each individual fertilization induced F- peak. We found that 50 % to 60 % of the variation in F-peak N₂O emissions could be explained by the multiple linear regression model with soil temperature, soil water filled pore space and amount of N input as explanatory variables (Table 3). At both sites, the variability of F-peak emission was mainly driven by soil temperature and N inputs ($p < 0.05$; $p < 0.01$), and the two parameters were positive drivers for F-peak N₂O emissions. In addition, the average WFPS during the fertilization events also contributed significantly to the variability of the F-peak N₂O emissions at both sites. For background N₂O emissions, the variation in N₂O emissions explained by the MLR model was low with R^2 of 0.10 (Cov) and 0.16 (Ref). The impact of the two potentially driving parameters soil temperature and soil WFPS differed between Cov and Ref. Overall, soil temperature was a significant driver for background N₂O emissions at both sites ($p < 0.01$), but the effect of soil WFPS on background N₂O emissions was not significant (Table 3). A threshold of 80% of the field capacity was used to define dry and wet conditions in the field. At Ref, soil WFPS was a positive driver for background N₂O emissions during dry conditions in the field whereas it was negative under wet conditions ($p < 0.01$). At Cov, soil WFPS only exerted limited influence on background fluxes.

Table 3. Regression analysis using log-transformed background N_2O fluxes, and fertilization induced N_2O fluxes from each individual chamber as dependent variable and soil temperature (T_{soil}), water filled pore space (WFPS) and nitrogen input (N input) as explanatory variables. In the analysis, the linear model $y = ax_1 + bx_2 + cx_3 + d$ was used for multiply linear regression. The error probability is indicated by asterisks (“***” $p < 0.01$, “**” $p < 0.05$).

Site	Parameters	R^2 (R^2_{adj})	a (T_{soil})	b(WFPS)	c(N input)	d(intercept)
<i>Log transferred background N_2O fluxes</i>						
Cov ($n = 392$)	Overall	0.11(0.10)**	0.007**	0.0006	-	-0.17**
	WFPS ≥ 80 % field capacity	0.28(0.28)**	0.015**	0.01**	-	-1.04**
	WFPS < 80 % field capacity	0.03(0.02) *	0.004**	0.001	-	-0.15*
Ref ($n = 392$)	Overall	0.16(0.15)**	0.02**	-0.003	-	0.19
	WFPS ≥ 80 % field capacity	0.26(0.25)**	0.019**	-0.022**	-	1.62**
	WFPS < 80 % field capacity	0.11(0.09)**	0.007**	0.013**	-	-0.45*
<i>Cumulated peak N_2O fluxes ($kg N ha^{-1}$)</i>						
Cov ($n = 48$)	N_2O fluxes	0.67(0.60)**	0.11*	0.04**	0.02**	-6.32**
	N_2O fluxes	0.61(0.53)**	1.80*	0.69*	0.24**	-91.11**

4 Discussion

4.1 Magnitude of N₂O fluxes from the two sites

Our continuous two-year's field N₂O observation showed that the drained nutrient rich fen (Ref) emitted 20.5 ± 2.7 kg N ha⁻¹ yr⁻¹. This was substantially higher than the IPCC default value and its 95% confidence interval, 8.2 (4.9 – 11) kg N ha⁻¹ yr⁻¹ (IPCC, 2014). Moreover, the study site also emitted substantially more N₂O than 25 measured fen peats in Germany (average 2.9 ± 2.7 kg N ha⁻¹ yr⁻¹; (Tiemeyer *et al.*, 2016), and also more than the average from drained grassland organic soils from 217 annual budgets across Europe (5.8 ± 10.3 kg N ha⁻¹ yr⁻¹; Leppelt *et al.*, 2014). However, the annual N₂O emissions from the study site were lower than the N₂O emissions from drained fens with high organic carbon in Slovenia (37.1 ± 0.2 kg N ha⁻¹ yr⁻¹; (Danevčič *et al.*, 2010). In our opinion, these differences in the N₂O emissions from drained fens between our site and the bulk of measurements from temperate grasslands is mainly driven by climate conditions and the amount of fertilizer input. Compared with the overall peatland distribution across Europe (Tanneberger *et al.*, 2017), our site and the Slovenian site of Danevčič *et al.* (2010) are situated in regions with relatively high soil temperatures, particularly during summer. This may foster higher N₂O emissions, owing to the normally positive correlation between soil temperature and N₂O emission that we found, in line with previous studies (Marushchak *et al.*, 2011; Parn *et al.*, 2018). Regarding fertilizer input, our site received c. 230 kg N ha⁻¹ yr⁻¹, which is much above the average rate of ~ 44 kg N ha⁻¹ yr⁻¹ for drained grassland organic soils across Europe (Leppelt *et al.*, 2014), and ~ 52 kg N ha⁻¹ yr⁻¹ of drained fens managed as grassland in Germany (Tiemeyer *et al.* 2016). Moreover, for some of the study sites from Tiemeyer *et al.* (2016), where fertilizer input was higher than 300 kg N ha⁻¹ yr⁻¹ these authors also reported higher N₂O emissions of 6.4 – 27.2 kg N ha⁻¹ yr⁻¹.

With mineral soil coverage, the N₂O emissions were strongly reduced (2.3 ± 0.4 kg N ha⁻¹ yr⁻¹) and also lower than the IPCC emission factor for managed deeply drained nutrient rich grassland on organic soil (8.2 kg N ha⁻¹ yr⁻¹; IPCC, 2014). It is not possible to compare the N₂O emission from Cov with former studies, because no N₂O emission data from drained peatland with artificial mineral soil coverage exist up to date. The observed N₂O emissions from Cov were in the range of N₂O emissions from mineral grassland soils in Switzerland. These have been reported to be 1.0 – 2.6 kg N ha⁻¹ yr⁻¹ N₂O-N from an intensively used grassland in the temperate Swiss Central Plateau with a fertilization rate of ~200 kg N yr⁻¹ (Flechard *et al.*, 2005); 2.2 – 7.4 kg N ha⁻¹ yr⁻¹ from another intensively used grassland in the Swiss Central Plateau during year 2010 to 2011 and year 2013 to 2014 with extra total N inputs of ~ 350 kg N yr⁻¹ (Merbold *et al.*, 2021); and 3.9 – 5.9 kg N ha⁻¹ yr⁻¹ from an intensively used grassland in the Swiss Plateau during year 2013 to 2016 with extra total N inputs of ~ 270 kg N yr⁻¹ (Fuchs *et al.*, 2020). Based on IPCC (2006), a fertilizer N input of c. 45 kg N ha⁻¹ yr⁻¹ mineral and c. 185 kg N ha⁻¹ yr⁻¹ organic fertilizer nitrogen (N) as in our study site would induce a N₂O emission of 0.8 – 2.9 kg N ha⁻¹ yr⁻¹, and

the average rate measured in Cov is within the range. It therefore seems that with mineral soil coverage, the drained organic soil of our site behaves like a mineral soil in term of its N₂O release.

4.2 Drivers of N₂O emissions and effects of mineral soil coverage

4.2.1 Drivers of N₂O emissions for the two sites

In our study, soil temperature, soil water filled pore space and N input could explain more than half of the variance of fertilization induced N₂O emissions (F-peak; Table 3). Higher F-peaks were found with warm temperatures, and lower with cold temperatures (Table 2), most likely due to the reduced soil microbial activity (Holtan-Hartwig and Bakken, 2002). The fertilizer N inputs and the high WFPS did not compensate for the effect of cold temperatures (Table 2), indicating that in our field high N₂O peaks only occur if all the driving variables (soil temperature, soil water content, N availability) are supporting high N₂O production. Previous research also highlighted that peak N₂O emissions were not observed if one driving factor was below thresholds for soil temperature and moisture (Holtan-Hartwig and Bakken, 2002; Meng *et al.*, 2005). In turn, if these driving factors were above the threshold, a fertilization event will lead to very high N₂O emissions. In the first year, we observed a very high F-peak after fertilization in August, which contributed more than half to the annual N₂O emissions for both sites and even 78% for Ref. This led to a significantly higher annual N₂O release in the first year compared to the second year. One explanation might be the timeline of the dry summer period followed by a wetting event together with the fertilizer application (Figure 3). This interpretation is supported by a large body of former researches that after dry and wet cycles for both mineral soils and organic soils, a greater amount of N₂O is emitted from grassland owing to the enhanced availability of C and N as related to soil organic matter mineralization (Priemé and Christensen, 2001; Beare *et al.*, 2009; Harrison-Kirk *et al.*, 2013). The differences in fertilization induced N₂O emissions under different soil temperature and soil WFPS suggest that as one N₂O mitigation option for the study site, fertilizer application should be avoided in hot summer period or during frequent precipitation.

4.2.2 Drivers of N₂O reduction after mineral soil coverage

Despite receiving the same amount of N input and having similar soil temperature and WFPS, as well as the same agricultural management, Ref had much higher N₂O emissions after fertilization. The different N₂O release after fertilization might be related to various mechanisms. First, exogenous N inputs might prime the mineralization of SOM, thereby influencing N₂O production differently in Cov and Ref. Priming effects are defined as short-term changes of SOM mineralization in response to external stimuli, e.g. exogenous N addition, and they alter the subsequent N₂O production from SOM-N (Kuznyakov *et al.*, 2000; Daly and Hernandez-Ramirez, 2020; Thilakarathna and Hernandez-Ramirez, 2021). Priming may effect N₂O emissions positively or negatively, depending on soil moisture and SOM content (Roman-Perez and Hernandez-Ramirez, 2020). Former studies revealed positive N₂O priming

effects to be associated with wetter soil conditions (WFPS > 60 %) and higher SOM content (Schleusner *et al.*, 2018; Thilakarathna and Hernandez-Ramirez, 2021). In our study site, soil moisture for Cov and Ref were similar during the fertilization events (Table 2), but SOC content in surface soil of Ref was 5 times higher than Cov (Table 1), which might have induced a stronger priming by adding N, subsequently leading also to higher N₂O emissions for Ref (Perveen *et al.*, 2019). For the background N₂O emissions, soil temperature was still a significant driver at both sites, but the influence of the soil water filled pore space was limited (Table 3). Moreover, the variance of background N₂O emissions explained by the MLR model with soil temperature and soil water content was low, indicating that for both sites, the influence of soil temperature and soil moisture on background N₂O emission was limited. In our study, background N₂O emissions were also significantly reduced ($p < 0.05$) with mineral soil coverage, indicating that the higher N₂O emission from Ref was not only directly related to fertilization, but also to the properties of the surface soil itself, e.g. soil pH and soil N availability. Surface soil properties are of particular relevance for the amount of N₂O release as it has been shown that the soil depth from which emitted N₂O originates is only 0.7 – 2.8 cm (Neftel *et al.*, 2000).

Second, surface soil pH raised from 5.2 to 7.3 (Table 1) with mineral soil coverage in our study site. It has been reported that the net production of N₂O from denitrification is strongly dependent on soil pH (Nadeem *et al.*, 2020), N₂O emissions are negatively correlated with soil pH in organic soil, due to the decreased N mineralization with rising soil pH under aerobic condition of peat (Chapin *et al.*, 2003; Weslien *et al.*, 2009), and the possible enhancement of the synthesis of functional N₂O reductase from denitrification (Liu *et al.*, 2014), resulting in a higher share of N₂. Hence, the relatively high soil pH at Cov may have contributed to the lower background N₂O emissions.

Third, the two topsoils differed in soil N content and soil N availability (Table 1). Soil available N from SOM mineralization is considered to be the main source for background N₂O production (Lampe *et al.*, 2006). Our study site revealed a carbon loss of 3100 – 6300 kg C ha⁻¹ yr⁻¹ from peat oxidation after drainage based on a former study using a radiocarbon approach to estimate the soil carbon loss (Wang *et al.*, 2021). Considering the C to N ratios of ~ 25 (at a depth of 2 m) as representative for the nitrogen stored in peat without fertilization, the study site has a N mineralization potential of 120 – 250 kg N ha⁻¹ yr⁻¹. This relatively high soil N supply at Ref, as also indicated by higher available soil N (Table 1), become available for microbial processing and consequently N₂O production. After mineral soil coverage with a thickness of ~ 40 cm, N release from peat mineralization of topsoil SOM as an N source for N₂O formation is no longer available. Instead, mineralization of SOM from the mineral soil coverage, whose soil N content and the corresponding soil available N are much lower (Table 1), becomes a major N source. The decreased surface soil N availability due to mineral soil coverage for nitrification and denitrification may then restrain the N₂O production (Senbayram *et al.*, 2012). As one consequence for

management, the high soil N supply in drained peatland suggests that compared with mineral grassland soils, the fertilization demand for organic grassland soils might be substantially lower.

Fourth, although the organic soil at site Cov still has the potential to produce N₂O, the mineral soil coverage might have pushed the organic soil underneath into a deeper zone with higher soil moisture and lower oxygen availability as compared to the organic topsoil at site Ref. Higher soil moisture could influence the exchange of N₂O between the site of production and the aerated pore space, thereby affecting the balance between N₂O production and consumption. With high soil moisture, a reduction of N₂O emission is expected owing to the higher consumption of N₂O when gas diffusion is slow (Harris *et al.*, 2021; Kuang *et al.*, 2019). Moreover, under strongly anaerobic conditions, N₂ as the end product of denitrification will be produced preferentially (Davidson *et al.*, 2000). Thus the amount of formed N₂O from the organic soil underneath might be reduced at site Cov via enhanced dissolution in soil water (Clough *et al.*, 2006; Goldberg *et al.*, 2008) or full denitrification before escaping into the atmosphere (Davidson *et al.*, 2000). These effects are further pronounced by the lower gas diffusivity of the surface soil of Cov compared to Ref (Figure 2D). We suppose these effects in combination lead to lower N₂O emissions after mineral soil coverage.

4.3 Potential of N₂O reduction by mineral soil coverage

Based on two year's continuous field observation, the results from our study site showed that mineral soil coverage as a management option for organic soils induced a strong reduction of N₂O emissions from drained organic soil in the Swiss Rheine valley. In Switzerland, ~ 250 km² organic soils are still drained for agricultural production (Wüst-Galley *et al.*, 2020), and N₂O release contributes by ~ 10% to the overall c. 650 kt CO₂ -eq yr⁻¹ GHG emissions from these soils (FOEN, 2021). Globally, c. 2.7 × 10⁵ km² peatlands are drained for agricultural (grassland and cropland) production, those areas are estimate to result in c. 1046 Mt CO₂ -eq yr⁻¹ GHGs emissions, and N₂O release contributes by ~ 24 % to it (FAOSTAT, 2019; Evans *et al.*, 2021). Rewetting has been suggested as key to reducing those GHG emissions from drained organic soils (Hemes *et al.*, 2019; Günther *et al.*, 2020; Ojanen and Minkkinen, 2020). However, in many areas, rewetting of all of those areas will be difficult to achieve. Firstly, for some countries, cultivation on drained organic soils is continuously making significant contributions to the economic development, therefore rewetting on those areas might cause economic losses. Secondly, global demand for food and feed production and pressure on land is continuously increasing (FAO, 2017). This set barriers for full rewetting of drained agricultural organic soil, despite the need for GHG reduction (Biancalani and Avagyan, 2014). Thus, in situation for which full rewetting is not possible, mineral soil coverage might become a promising building block for GHG mitigation and at the same time, counterbalance soil subsidence and maintain the productivity of drained organic soil.

5 Conclusions

Draining organic soil for intensive agricultural production induced N_2O emissions of $20.5 \pm 2.7 \text{ kg N ha}^{-1} \text{ yr}^{-1}$ at our study site, which were reduced to $2.3 \pm 0.4 \text{ kg N ha}^{-1} \text{ yr}^{-1}$ by mineral soil coverage. Most of the N_2O emissions were related to fertilization, and a single fertilization event under suitable soil temperature and soil moisture may contribute by more than half to the annual N_2O emissions in our study site, underpinning the need for high frequency flux measurements. Mineral soil coverage of drained organic soil could significantly reduce both, fertilization induced N_2O emission, and background N_2O emissions. The large potential of N_2O reduction after mineral soil coverage, which itself is a measure applied by farmers to counterbalance soil subsidence, provides an opportunity for not only reducing the environmental footprint of using drained organic soils but also for maintaining their agricultural productivity and hence, farmers income. We are not aware of any management options apart from peatland restoration and rewetting that has the potential to substantially reduce N_2O emissions from organic soils. Mineral soil coverage of intensively used drained peatlands, which are not suitable for rewetting owing to soil conditions or socio-economic constraints, may therefore be a prospective management strategy for the sustained use of these soils. Our findings encourage further research on this measure, particularly for tropical conditions where drained peatlands are GHG hotspots and contribute the most to the overall emissions from managed organic soils (Dommain *et al.*, 2018; Leifeld and Menichetti, 2018).

Funding

The research was supported by funding received from the Swiss Federal Office for the Environment (contract number 06.0091.PZ/R261-2425), and the China Scholarship Council (NSCIS 201806350221).

Acknowledgement

We appreciate the help of Stefan Gloor, Robin Giger, Urs Zihlmann and Marlies Sommer at Agroscope during field sampling and lab analysis. We are thankful for many useful discussions with Christof Ammann and Karl Voglmeier, Agroscope. We thank Bernhard Schneider for collaboration on his farm.

References

- Ambus, P., Skiba, U., Drewer, J., Jones, S.K., Carter, M.S., Albert, K.R., Sutton, M.A., 2010. Development of an accumulation-based system for cost-effective chamber measurements of inert trace gas fluxes. *Eur. J. Soil Sci.* 61, 785-792. <https://doi.org/10.1111/j.1365-2389.2010.01272.x>.
- Beare, M.H., Gregorich, E.G., St-Georges, P., 2009. Compaction effects on CO₂ and N₂O production during drying and rewetting of soil. *Soil Biol. Biochem.* 41, 611-621. <https://doi.org/10.1016/j.soilbio.2008.12.024>.
- Biancalani, R., Avagyan, A., 2014. *Towards climate-responsible peatlands management series*. Food and Agriculture Organization of the United Nations, Italy, Rome.
- Blodau, C., 2002. Carbon cycling in peatlands - A review of processes and controls. *Environ. Rev.* 10, 111-134. <https://doi.org/10.1139/a02-004>.
- Bragg, O., Lindsay, R., Risager, M., Silvius, M., Zingstra, H., 2013. *Strategy and action plan for mire and peatland conservation in central Europe*: Central European Peatland Project (CEPP). Wetlands International, Wageningen.
- Chapin, C.T., Bridgham, S.D., Pastor, J., Updegraff, K., 2003. Nitrogen, phosphorus, and carbon mineralization in response to nutrient and lime additions in peatlands. *Soil Sci.* 168, 409-420. <https://doi.org/10.1097/01.ss.0000075286.87447.5d>.
- Charteris, A.F., Chadwick, D.R., Thorman, R.E., Vallejo, A., de Klein, C.A.M., Rochette, P., Cardenas, L.M., 2020. Global research alliance N₂O chamber methodology guidelines: recommendations for deployment and accounting for sources of variability. *J Environ Qual* 49, 1092-1109. <https://doi.org/10.1002/jeq2.20126>.
- Clough, T.J., Kelliher, F.M., Wang, Y.P., Sherlock, R.R., 2006. Diffusion of ¹⁵N-labelled N₂O into soil columns: a promising method to examine the fate of N₂O in subsoils. *Soil Biol. Biochem.* 38, 1462-1468. <https://doi.org/10.1016/j.soilbio.2005.11.002>.
- Daly, E.J., Hernandez-Ramirez, G., 2020. Sources and priming of soil N₂O and CO₂ production: Nitrogen and simulated exudate additions. *Soil Biol. Biochem.* 149, 107942. <https://doi.org/10.1016/j.soilbio.2020.107942>.
- Danevčič, T., Mandić-Mulec, I., Stres, B., Stopar, D., Hacin, J., 2010. Emissions of CO₂, CH₄ and N₂O from Southern European peatlands. *Soil Biol. Biochem.* 42, 1437-1446. <https://doi.org/10.1016/j.soilbio.2010.05.004>.
- Davidson, E.A., Keller, M., Erickson, H.E., Verchot, L.V., Veldkamp, E., 2000. Testing a conceptual model of soil emissions of nitrous and nitric oxides: using two functions based on soil nitrogen availability and soil water content, the hole-in-the-pipe model characterizes a large fraction of the observed variation of nitric oxide and nitrous oxide emissions from soils. *Bioscience* 50, 667-680. [https://doi.org/10.1641/0006-3568\(2000\)050\[0667:TACMOS\]2.0.CO;2](https://doi.org/10.1641/0006-3568(2000)050[0667:TACMOS]2.0.CO;2).

- Dommain, R., Frohling, S., Jeltsch-Thommes, A., Joos, F., Couwenberg, J., Glaser, P.H., 2018. A radiative forcing analysis of tropical peatlands before and after their conversion to agricultural plantations. *Glob. Chang. Biol.* 24, 5518-5533. <https://doi.org/10.1111/gcb.14400>.
- Evans, C.D., Peacock, M., Baird, A.J., Artz, R.R.E., Burden, A., Callaghan, N., Chapman, P.J., Cooper, H.M., Coyle, M., Craig, E., Cumming, A., Dixon, S., Gauci, V., Grayson, R.P., Helfter, C., Heppell, C.M., Holden, J., Jones, D.L., Kaduk, J., Levy, P., Matthews, R., McNamara, N.P., Misselbrook, T., Oakley, S., Page, S.E., Rayment, M., Ridley, L.M., Stanley, K.M., Williamson, J.L., Worrall, F., Morrison, R., 2021. Overriding water table control on managed peatland greenhouse gas emissions. *Nature* 593, 548-552. <https://doi.org/10.1038/s41586-021-03523-1>.
- FAO, 2017. The future of food and agriculture – Trends and challenges., Rome.
- FAOSTAT, 2019. Drained organic soils, Food and Agriculture Organisation of the United Nations.
- Ferré, M., Muller, A., Leifeld, J., Bader, C., Müller, M., Engel, S., Wichmann, S., 2019. Sustainable management of cultivated peatlands in Switzerland: Insights, challenges, and opportunities. *Land Use Policy* 87, 104019. <https://doi.org/10.1016/j.landusepol.2019.05.038>.
- Flechard, C.R., Ambus, P., Skiba, U., Rees, R.M., Hensen, A., van Amstel, A., Dasselaar, A.v.d.P.-v., Soussana, J.F., Jones, M., Clifton-Brown, J., Raschi, A., Horvath, L., Neftel, A., Jocher, M., Ammann, C., Leifeld, J., Fuhrer, J., Calanca, P., Thalman, E., Pilegaard, K., Di Marco, C., Campbell, C., Nemitz, E., Hargreaves, K.J., Levy, P.E., Ball, B.C., Jones, S.K., van de Bulk, W.C.M., Groot, T., Blom, M., Domingues, R., Kasper, G., Allard, V., Ceschia, E., Cellier, P., Laville, P., Henault, C., Bizouard, F., Abdalla, M., Williams, M., Baronti, S., Berretti, F., Grosz, B., 2007. Effects of climate and management intensity on nitrous oxide emissions in grassland systems across Europe. *Agric. Ecosyst. Environ.* 121, 135-152. <https://doi.org/10.1016/j.agee.2006.12.024>.
- Flechard, C.R., Neftel, A., Jocher, M., Ammann, C., Fuhrer, J., 2005. Bi-directional soil/atmosphere N₂O exchange over two mown grassland systems with contrasting management practices. *Glob. Chang. Biol.* 11, 2114-2127. <https://doi.org/10.1111/j.1365-2486.2005.01056.x>.
- FOEN, 2021. Switzerland's Greenhouse Gas Inventory 1990–2019: National Inventory Report, CRF-tables. Submission of April 2021 under the United Nations Framework Convention on Climate Change and under the Kyoto Protocol. Federal Office for the Environment, Bern. <http://www.climatereporting.ch>
- Fuchs, K., Merbold, L., Buchmann, N., Bretscher, D., Brilli, L., Fitton, N., Topp, C.F.E., Klumpp, K., Lieffering, M., Martin, R., Newton, P.C.D., Rees, R.M., Rolinski, S., Smith, P., Snow, V., 2020. Multimodel evaluation of nitrous oxide emissions from an intensively managed grassland. *J. Geophys. Res. Biogeosci.* 125, e2019JG005261. <https://doi.org/10.1029/2019jg005261>.
- Goldberg, S.D., Knorr, K.H., Gebauer, G., 2008. N₂O concentration and isotope signature along profiles provide deeper insight into the fate of N₂O in soils. *Isotopes Environ Health Stud* 44, 377-391. <https://doi.org/10.1080/10256010802507433>.

- Günther, A., Barthelmes, A., Huth, V., Joosten, H., Jurasinski, G., Koebisch, F., Couwenberg, J., 2020. Prompt rewetting of drained peatlands reduces climate warming despite methane emissions. *Nat. Commun.* 11, 1644. <https://doi.org/10.1038/s41467-020-15499-z>.
- Harris, E., Diaz-Pines, E., Stoll, E., Schloter, M., Schulz, S., Duffner, C., Li, K., Moore, K.L., Ingrisch, J., Reinthaler, D., Zechmeister-Boltenstern, S., Glatzel, S., Brüggemann, N., Bahn, M., 2021. Denitrifying pathways dominate nitrous oxide emissions from managed grassland during drought and rewetting. *Sci. Adv.* 7(6), eabb7118. <https://DOI: 10.1126/sciadv.abb7118>.
- Harrison-Kirk, T., Beare, M.H., Meenken, E.D., Condrón, L.M., 2013. Soil organic matter and texture affect responses to dry/wet cycles: Effects on carbon dioxide and nitrous oxide emissions. *Soil Biol. Biochem.* 57, 43-55. <https://doi.org/10.1016/j.soilbio.2012.10.008>.
- Hemes, K.S., Chamberlain, S.D., Eichelmann, E., Anthony, T., Valach, A., Kasak, K., Szutu, D., Verfaillie, J., Silver, W.L., Baldocchi, D.D., 2019. Assessing the carbon and climate benefit of restoring degraded agricultural peat soils to managed wetlands. *Agric. For. Meteorol.* 268, 202-214. <https://doi.org/10.1016/j.agrformet.2019.01.017>.
- Holtan-Hartwig, L.D., P., Bakken, L.R., 2002. Low temperature control of soil denitrifying communities: kinetics of N₂O production and reduction. *Soil Biol. Biochem.* 34, 1797-1806. [https://doi.org/10.1016/S0038-0717\(02\)00169-4](https://doi.org/10.1016/S0038-0717(02)00169-4).
- IPCC, 2019, 2019 Refinement to the 2006 IPCC Guidelines for National Greenhouse Gas Inventories, Calvo Buendia, E., Tanabe, K., Kranjc, A., Baasansuren, J., Fukuda, M., Ngarize S., Osako, A., Pyrozhenko, Y., Shermanau, P. and Federici, S. (eds). IPCC, Switzerland. <https://www.ipcc-nggip.iges.or.jp/public/2019rf/vol4.html>.
- IPCC, 2014, 2013 Supplement to the 2006 IPCC Guidelines for National Greenhouse Gas Inventories: Wetlands, Hiraishi, T., Krug, T., Tanabe, K., Srivastava, N., Baasansuren, J., Fukuda, M. and Troxler, T.G. (eds). IPCC, Switzerland. https://www.ipcc.ch/site/assets/uploads/2018/03/Wetlands_Supplement_Entire_Report.pdf.
- Kasimir, A., He, H., Coria, J., Norden, A., 2018. Land use of drained peatlands: Greenhouse gas fluxes, plant production, and economics. *Glob. Chang. Biol.* 24, 3302-3316. <https://doi.org/10.1111/gcb.13931>.
- Keller, T., Hüppi, R., Leifeld, J., 2019. Relationship between greenhouse gas emissions and changes in soil gas diffusivity in a field experiment with biochar and lime. *J. Plant Nutr. Soil Sci.* 182, 667-675. <https://doi.org/10.1002/jpln.201800538>.
- Knox, S.H., Sturtevant, C., Matthes, J.H., Koteen, L., Verfaillie, J., Baldocchi, D., 2015. Agricultural peatland restoration: effects of land-use change on greenhouse gas (CO₂ and CH₄) fluxes in the Sacramento-San Joaquin Delta. *Glob. Chang. Biol.* 21, 750-765. <https://doi.org/10.1111/gcb.12745>.

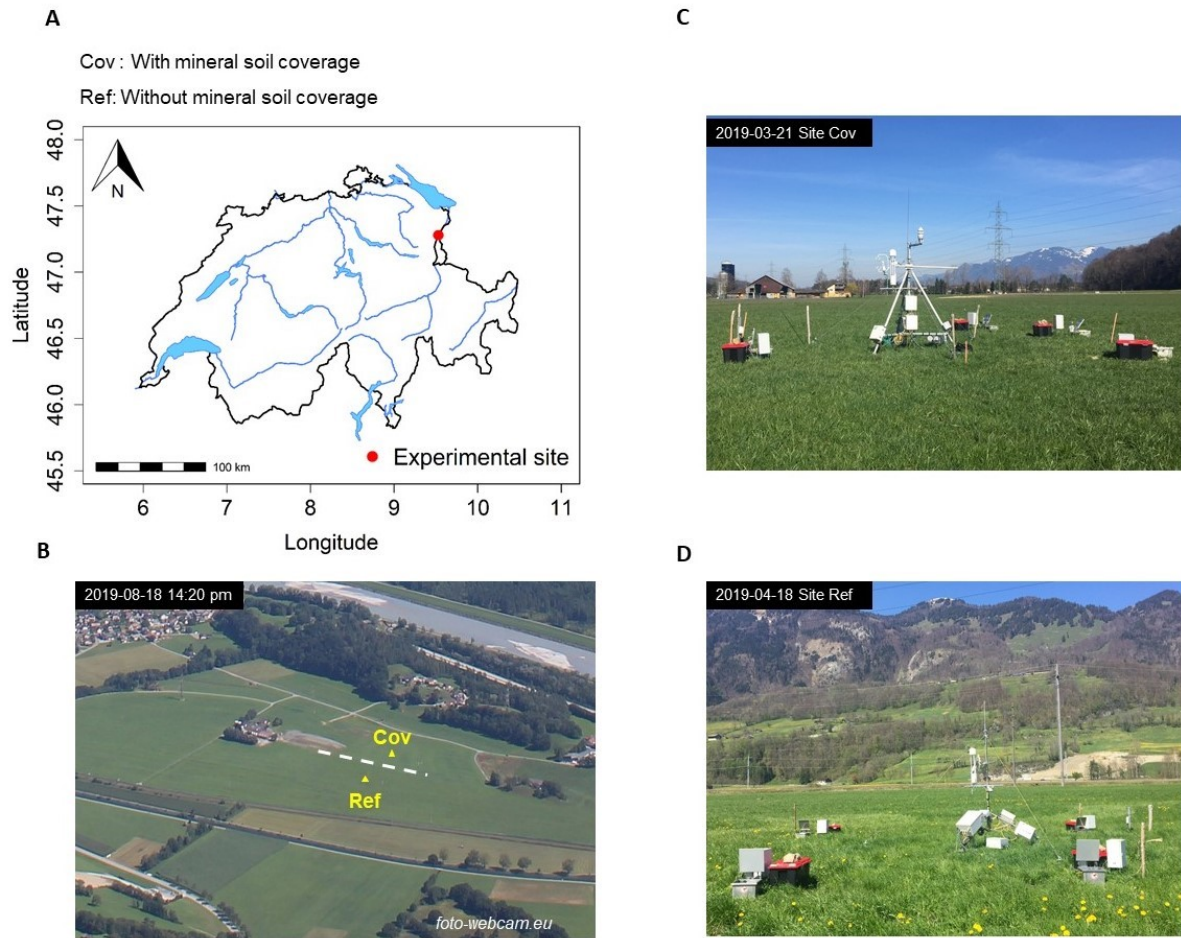
- Kuang, W., Gao, X., Tenuta, M., Gui, D., Zeng, F., 2019. Relationship between soil profile accumulation and surface emission of N₂O: effects of soil moisture and fertilizer nitrogen. *Biol. Fertil. Soils*. 55(2), 97-107. <https://doi.org/10.1007/s00374-018-01337-4>.
- Kuzyakov, Y., Friedel, J.K., K Stahr, 2000. Review of mechanisms and quantification of priming effects. *Soil Biol. Biochem.* 32, 1485-1498. [https://doi.org/10.1016/S0038-0717\(00\)00084-5](https://doi.org/10.1016/S0038-0717(00)00084-5).
- Lampe, C., Dittert, K., Sattelmacher, B., Wachendorf, M., Loges, R., Taube, F., 2006. Sources and rates of nitrous oxide emissions from grazed grassland after application of ¹⁵N-labelled mineral fertilizer and slurry. *Soil Biol. Biochem.* 38, 2602-2613. <https://doi.org/10.1016/j.soilbio.2006.03.016>.
- Leifeld, J., 2018. Distribution of nitrous oxide emissions from managed organic soils under different land uses estimated by the peat C/N ratio to improve national GHG inventories. *Sci. Total Environ.* 631-632, 23-26. <https://doi.org/10.1016/j.scitotenv.2018.02.328>.
- Leifeld, J., Menichetti, L., 2018. The underappreciated potential of peatlands in global climate change mitigation strategies. *Nat. Commun.* 9, 1071. <https://doi.org/10.1038/s41467-018-03406-6>.
- Leppelt, T., Dechow, R., Gebbert, S., Freibauer, A., Lohila, A., Augustin, J., Drösler, M., Fiedler, S., Glatzel, S., Höper, H., Järveoja, J., Laerke, P.E., Maljanen, M., Mander, Ü., Mäkiranta, P., Minkinen, K., Ojanen, P., Regina, K., Strömngren, M., 2014. Nitrous oxide emission budgets and land-use-driven hotspots for organic soils in Europe. *Biogeosciences* 11, 6595-6612. <https://doi.org/10.5194/bg-11-6595-2014>.
- Liu, B., Frostegård, Å. and Bakken, L.R., 2014. Impaired reduction of N₂O to N₂ in acid soils is due to a posttranscriptional interference with the expression of nosZ. *MBio*, 5(3), pp.e01383-14. <https://doi.org/10.1128/mBio.01383-14>.
- Liu, H., Wrage-Mönnig, N., Lennartz, B., 2020. Rewetting strategies to reduce nitrous oxide emissions from European peatlands. *Commun. Earth Environ.* 1, 1-7. <https://doi.org/10.1038/s43247-020-00017-2>.
- Nadeem, S., Bakken, L.R., Frostegård, Å., Gaby, J.C., Dörsch, P., 2020. Contingent effects of liming on N₂O-emissions driven by autotrophic nitrification. *Front. Environ. Sci.* 8:598513. <https://doi.org/10.3389/fenvs.2020.598513>.
- Marushchak, M.E., Pitkamaki, A., Koponen, H., Biasi, C., Seppala, M., Martikainen, P.J., 2011. Hot spots for nitrous oxide emissions found in different types of permafrost peatlands. *Glob. Chang. Biol.* 17, 2601-2614. <https://doi.org/10.1111/j.1365-2486.2011.02442.x>.
- Meng, L., Ding, W., Cai, Z., 2005. Long-term application of organic manure and nitrogen fertilizer on N₂O emissions, soil quality and crop production in a sandy loam soil. *Soil Biol. Biochem.* 37, 2037-2045. <https://doi.org/10.1016/j.soilbio.2005.03.007>.
- Merbold, L., Decock, C., Eugster, W., Fuchs, K., Wolf, B., Buchmann, N., Hörtnagl, L., 2021. Are there memory effects on greenhouse gas emissions (CO₂, N₂O and CH₄) following grassland restoration?. *Biogeosciences*, 18(4), 1481-1498. <https://doi.org/10.5194/bg-2020-141>.

- Neftel, A., Blatter, A., Schmid, M., Lehmann, B., Tarakanov, S.V., 2000. An experimental determination of the scale length of N₂O in the soil of a grassland. *J. Geophys. Res. Atmos.* 105, 12095-12103. <https://doi.org/10.1029/2000jd900088>.
- Ojanen, P., Minkkinen, K., 2020. Rewetting offers rapid climate benefits for tropical and agricultural peatlands but not for forestry - drained peatlands. *Glob. Biogeochem. Cycles* 34. <https://doi.org/10.1029/2019gb006503>.
- Parn, J., Verhoeven, J.T.A., Butterbach-Bahl, K., Dise, N.B., Ullah, S., Aasa, A., Egorov, S., Espenberg, M., Jarveoja, J., Jauhiainen, J., Kasak, K., Klemedtsson, L., Kull, A., Laggoun-Defarge, F., Lapshina, E.D., Lohila, A., Lohmus, K., Maddison, M., Mitsch, W.J., Muller, C., Niinemets, U., Osborne, B., Pae, T., Salm, J.O., Sgouridis, F., Sohar, K., Soosaar, K., Storey, K., Teemusk, A., Tenywa, M.M., Tournebize, J., Truu, J., Veber, G., Villa, J.A., Zaw, S.S., Mander, U., 2018. Nitrogen-rich organic soils under warm well-drained conditions are global nitrous oxide emission hotspots. *Nat. Commun.* 9, 1135. <https://doi.org/10.1038/s41467-018-03540-1>.
- Perveen, N., Barot, S., Maire, V., Cotrufo, M.F., Shahzad, T., Blagodatskaya, E., Stewart, C.E., Ding, W., Siddiq, M.R., Dimassi, B., Mary, B., Fontaine, S., 2019. Universality of priming effect: An analysis using thirty five soils with contrasted properties sampled from five continents. *Soil Biol. Biochem.* 134, 162-171. <https://doi.org/10.1016/j.soilbio.2019.03.027>.
- Prather, M.J., Hsu, J., DeLuca, N.M., Jackman, C.H., Oman, L.D., Douglass, A.R., Fleming, E.L., Strahan, S.E., Steenrod, S.D., Sovde, O.A., Isaksen, I.S., Froidevaux, L., Funke, B., 2015. Measuring and modeling the lifetime of nitrous oxide including its variability. *J. Geophys. Res. Atmos.* 120, 5693-5705. <https://doi.org/10.1002/2015JD023267>.
- Priemé, A., Christensen, S., 2001. Natural perturbations, drying–wetting and freezing–thawing cycles, and the emission of nitrous oxide, carbon dioxide and methane from farmed organic soils. *Soil Biol. Biochem.* 33, 2083-2091. [https://doi.org/10.1016/S0038-0717\(01\)00140-7](https://doi.org/10.1016/S0038-0717(01)00140-7).
- Ravishankara, A.R., Daniel, J.S., Portmann, R.W., 2009. Nitrous oxide (N₂O): the dominant ozone-depleting substance emitted in the 21st century. *Science* 326, 123-125. <https://doi.org/10.1126/science.1176985>.
- Rihm, B., Künzle, T., 2019. Mapping nitrogen deposition 2015 for Switzerland. Technical Report on the Update of Critical Loads and Exceedance, including the years 1990, 2000, 2005 and 2010, Bern, Switzerland. <https://www.bafu.admin.ch>.
- Roman - Perez, C.C., Hernandez - Ramirez, G., 2020. Sources and priming of N₂O production across a range of moisture contents in a soil with high organic matter. *J Environ Qual* 50, 94-109. <https://doi.org/10.1002/jeq2.20172>.
- Senbayram, M., Chen, R., Budai, A., Bakken, L., Dittert, K., 2012. N₂O emission and the N₂O/(N₂O+N₂) product ratio of denitrification as controlled by available carbon substrates and nitrate concentrations. *Agric Ecosyst Environ.*, 147, 4-12. <https://doi.org/10.1016/j.agee.2011.06.022>.

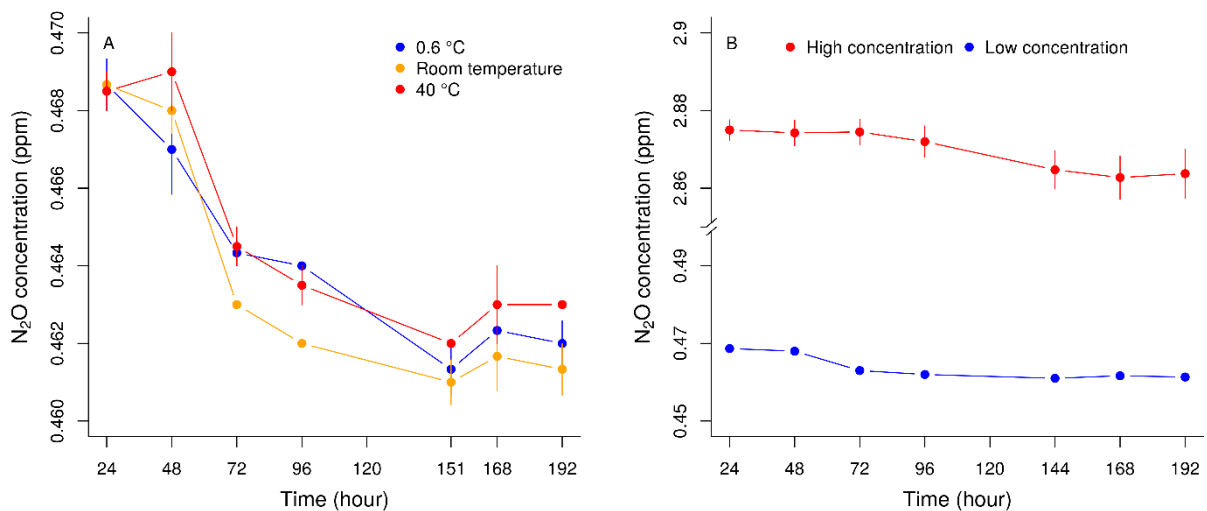
- Schindler, U., Müller, L., 1999. Rehabilitation of the soil quality of a degraded peat site. In: D.E., S., R.H., M., G.C., S. (Eds.), 10th International Soil Conservation Organization Meeting Purdue University, pp. 648-654.
- Schjøning, P., Thomsen, I.K., Moldrup, P., Christensen, B.T., 2003. Linking soil microbial activity to water - and air - phase contents and diffusivities. *Soil Sci. Soc. Am. J.* 67, 156-165. <https://doi.org/10.2136/sssaj2003.1560>.
- Schleusner, P., Lammirato, C., Tierling, J., Lebender, U., Rütting, T., 2018. Primed N₂O emission from native soil nitrogen: A ¹⁵N-tracing laboratory experiment. *J. Plant Nutr. Soil Sci.* 181, 621-627. <https://doi.org/10.1002/jpln.201700312>.
- Stehfest, E., Bouwman, L., 2006. N₂O and NO emission from agricultural fields and soils under natural vegetation: summarizing available measurement data and modeling of global annual emissions. *Nutri. Cycl. Agroecosyst.* 74, 207-228. <https://doi.org/10.1007/s10705-006-9000-7>.
- Syakila, A., Kroeze, C., 2011. The global nitrous oxide budget revisited. *Greenh. Gas Meas. Manag.* 1, 17-26. <https://doi.org/10.3763/ghgmm.2010.0007>.
- Tanneberger, F., Moen, A., Joosten, H., Nilsen, N., 2017. The peatland map of Europe. *Mires and Peat* 19, 1-17. <https://doi.org/10.19189/MaP.2016.OMB.264>.
- Thilakarathna, S.K., Hernandez-Ramirez, G., 2021. Primings of soil organic matter and denitrification mediate the effects of moisture on nitrous oxide production. *Soil Biol. Biochem.* 155, 108166. <https://doi.org/10.1016/j.soilbio.2021.108166>.
- Tian, H., Yang, J., Xu, R., Lu, C., Canadell, J.G., Davidson, E.A., Jackson, R.B., Arneeth, A., Chang, J., Ciais, P., Gerber, S., Ito, A., Joos, F., Lienert, S., Messina, P., Olin, S., Pan, S., Peng, C., Saikawa, E., Thompson, R.L., Vuichard, N., Winiwarter, W., Zaehle, S., Zhang, B., 2019. Global soil nitrous oxide emissions since the preindustrial era estimated by an ensemble of terrestrial biosphere models: Magnitude, attribution, and uncertainty. *Glob. Chang. Biol.* 25, 640-659. <https://doi.org/10.1111/gcb.14514>.
- Tiemeyer, B., Albiac Borraz, E., Augustin, J., Bechtold, M., Beetz, S., Beyer, C., Drosler, M., Ebli, M., Eickenscheidt, T., Fiedler, S., Forster, C., Freibauer, A., Giebels, M., Glatzel, S., Heinichen, J., Hoffmann, M., Hoper, H., Jurasinski, G., Leiber-Sauheitl, K., Peichl-Brak, M., Roskopf, N., Sommer, M., Zeitz, J., 2016. High emissions of greenhouse gases from grasslands on peat and other organic soils. *Glob. Chang. Biol.* 22, 4134-4149. <https://doi.org/10.1111/gcb.13303>.
- Wang, Y., Paul, S.M., Jocher, M., Espic, C., Alewell, C., Szidat, S., Leifeld, J., 2021. Soil carbon loss from drained agricultural peatland after coverage with mineral soil. *Sci. Total Environ.*, 149498. <https://doi.org/10.1016/j.scitotenv.2021.149498>.
- Weslien, P., Kasimir Klemedtsson, Å., Börjesson, G., Klemedtsson, L., 2009. Strong pH influence on N₂O and CH₄ fluxes from forested organic soils. *Eur. J. Soil Sci.* 60, 311-320. <https://doi.org/10.1111/j.1365-2389.2009.01123.x>.

- Wüst-Galley, C., Grünig, A., Leifeld, J., 2015. Locating organic soils for the Swiss greenhouse gas inventory. *Agroscope Sci*, 1-100.
- Wüst-Galley, C., Grünig, A., Leifeld, J., 2020. Land use-driven historical soil carbon losses in Swiss peatlands. *Landsc. Ecol.* 35, 173-187. <https://doi.org/10.1007/s10980-019-00941-5>.
- Yu, Z., Loisel, J., Brosseau, D.P., Beilman, D.W., Hunt, S.J., 2010. Global peatland dynamics since the Last Glacial Maximum. *Geophys. Res. Lett.* 37. <https://doi.org/10.1029/2010gl043584>.

Supplementary Material



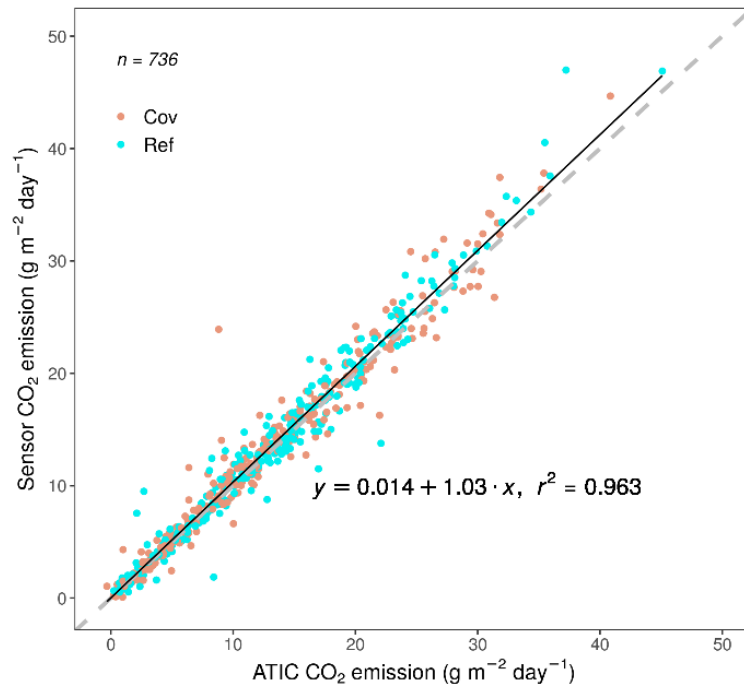
Supplementary Figure 1. The location (A) and image (B, C, D) of the experimental site.



Supplementary Figure 2. Eight days bag test for long - term storage of N_2O compounds with different temperature (A) and different N_2O concentration (B).

Comparison of CO₂ flux from ATIC and the mean CO₂ fluxes from each chamber closure time.

After entire two-year's field observation, within each individual sampling period, the discrepancy of the mean CO₂ emission from each chamber closure time and the CO₂ emission from ATIC showed similar among all the chambers for both sites (n = 736). The real - time CO₂ sensor revealed slightly higher CO₂ emission than the ATIC with a ratio of 1.03 (Figure 2), but the difference between ATIC and real - time CO₂ sensor is within 5%.



Supplemental Figure 3. Comparison of CO₂ emission from ATIC and mean CO₂ emission of each chamber closure time within each sampling period in drained peatland with (Cov) and without (Ref) mineral soil coverage during March 2019 to March 2021.

Paper III

Reduced nitrogen losses from drained temperate agricultural peatland after mineral soil coverage

Yuqiao Wang^{1,2}, **Sonja M. Paul**¹, **Christine Alewell**², **Jens Leifeld**¹

¹ Climate and Agriculture Group, Agroscope, Reckenholzstrasse 191, 8046 Zürich, Switzerland

² Environmental Geosciences, University of Basel, Bernoullistrasse 30, 4056 Basel, Switzerland

Submitted as: Wang, Y., Paul, S. M., Alewell, C., Leifeld, J. Reduced nitrogen losses from drained temperate agricultural peatland after mineral soil coverage. *Biology and Fertility of Soils* (Under review).

Abstract

Draining peatlands for agriculture induces peat decomposition, subsidence, and carbon and nitrogen losses, thereby contributing to soil degradation and climate change. To sustain the agricultural productivity of these organic soils, coverage with mineral soil material has increasingly been used. This practice may change the nitrogen fluxes within the plant–soil system. To evaluate this, we conducted a ^{15}N tracer experiment on a drained peatland in Switzerland that was managed as an intensive meadow. This peatland was divided into two parts, either without (reference ‘Ref’) or with ~ 40 cm mineral soil cover (coverage ‘Cov’). We applied $^{15}\text{NH}_4^{15}\text{NO}_3$ on field plots to follow the recovery of ^{15}N in grass, root, and soil over 11 months. The ^{15}N that was not recovered was designated as lost via leaching or gaseous emissions. Nitrogen mineralization was measured in a laboratory incubation. The field experiment showed that the total ^{15}N loss from Cov was lower ($p < 0.05$) than from Ref, even though plant ^{15}N uptake did not vary between the two sites. However, the lower net N loss from the Cov site was accompanied by higher soil ^{15}N retention in the soil. The laboratory incubation revealed a ~ 3 times higher nitrogen mineralization at Ref than at Cov, whereas, the specific release per unit soil nitrogen was around two times higher at Cov than at Ref, suggesting a faster SOM turnover rate at Cov. Overall, the mineral soil cover increased the retention of fertilizer-N in the soil, thus reducing the system N losses.

Keywords: Organic soil, ^{15}N recovery, N mineralization, Intensively managed grassland

1 Introduction

Peatlands are an essential soil organic matter (SOM) pool. While they only cover approximately 3 % of the terrestrial surface area, peatlands store 8 – 14 Gt N globally (Yu *et al.*, 2010; Loisel *et al.*, 2014; Leifeld and Menichetti, 2018). However, long-term drainage for agricultural production has already resulted in ~51 Mha degraded peatlands worldwide, with the highest share occurring in tropical and temperate regions, where around half of the initial peatland surface has been disturbed due to agricultural production, forestry, or peat extraction (Kasimir *et al.*, 2018; Leifeld and Menichetti, 2018). Peatland degradation is typically associated with peat decomposition, which result in carbon (C) and, to a smaller extent, in nitrogen (N) losses, as well as strong soil subsidence. As a consequence, soil carbon to nitrogen (C/N) ratios decrease (Klemedtsson *et al.*, 2005; Leifeld, 2018). The decomposition of peat is a substantial contributor to the N supply for agricultural production in drained peatlands. Therefore, the soil N supply and plant N uptake from drained peatlands might be higher than in mineral soil.

Around 30 % of the agriculturally used peatland is managed as grassland globally (Leifeld and Menichetti, 2018; Evans *et al.*, 2021). For the temperate zone, plant N uptake in grasslands has been widely explored in both mineral soils and organic soils. It has been reported from grasslands on mineral soil that plant biomass accumulated up to ~130 kg N ha⁻¹ yr⁻¹ nitrogen without fertilization in Germany (Bessler *et al.*, 2012). Müller *et al.* (2011) found that, based on a 38-year field observation in Germany, the aboveground grass N uptake ranges from 50 – 200 kg N ha⁻¹ yr⁻¹ with N application of ~ 200 kg N ha⁻¹. In a study on grasslands on organic soil, Sonneveld and Lantinga (2011) reported an aboveground grass N uptake of 342 kg N ha⁻¹ based on a 3-year field experiment in drained peatland without fertilization in the Netherlands. Schothorst (1977) even reported an aboveground grass N uptake of ~400 kg N ha⁻¹ from a non-fertilized drained peatland in the Netherlands. These data tentatively suggest that plant N uptake in drained organic soil might be generally higher than in mineral soil, which might be related to the higher soil N supply in drained peatland through organic matter decomposition. Higher soil N mineralization often leads to a supply of N exceeding grass uptake, which consequently results in greater N losses to the environment of grass produced on drained organic soil as compared to production on mineral soil (Pijlman *et al.*, 2020). It has been estimated that with the ongoing agricultural use of degraded peatland, c. 2.3 Gt N will be released to the environment cumulatively (Leifeld and Menichetti, 2018). Therefore, it is vitally important to evaluate how the N losses from drained peatland can be reduced.

In order to compensate for continued soil subsidence of drained organic soils and thereby to maintain agricultural productivity, adding mineral soil as a cover fill with a thicknesses of 0.2 – 0.5 m on the surface of organic soil has increasingly been adopted by farmers' working in Switzerland and other European countries (Schindler and Müller, 1999; Ferré *et al.*, 2019). With mineral soil cover, the soil N

balance of drained peatlands may change due to various factors. First, the smaller surface soil C and N content in the mineral soil cover material supports smaller microbial biomass and microbial activity (Wardle, 1998). This may result in lower SOM mineralization rates with mineral soil coverage compared with the surface soil from non-covered drained organic soil. Second, mineral soil cover might increase fertilizer N retention in drained peatland owing to its overall smaller N content. Third, a cover fill may also change other physical-chemical soil properties (e.g. clay content, soil pore volume, and soil cation exchange capacity) that feedback into soil N dynamics (Barrett and Burke, 2002). Finally, for the peat layer underneath the mineral soil coverage, the addition of mineral soil material may compress the peat layer and push it deeper into zones with lower oxygen availability, thereby reducing the mineralization of easily degradable N in drained peat layers. A prior study conducted at the same site proved that mineral soil cover induced a substantial reduction of N₂O emissions (Wang *et al.*, 2022), underpinning a strong influence of mineral soil coverage on the N balance in the soil-plant system of the drained peatland. However, a mechanistic understanding of the impact of mineral soil cover on the N cycling in the plant-soil system of drained organic soils is still outstanding.

In this study, we examined the gross N dynamic, plant N uptake, and N losses in a drained peatland under grassland use both with and without mineral soil coverage. We did so by using isotopically labeled ¹⁵N fertilizer in combination with measurements of the corresponding nitrogen pools in soil, roots, and harvests. The application of ¹⁵N-enriched fertilizer is considered a useful and targeted tool for tracing the fate of applied N in plant-soil systems (Rahman and Parsons, 1999; Wesselsperelo *et al.*, 2006; Sebilo *et al.*, 2013; Rowlings *et al.*, 2016; Kalu *et al.*, 2021). The specific objectives of this study were to 1) determine the fertilizer N recovery and fertilizer allocation in the plant-soil system in drained peatland with and without mineral soil coverage; 2) assess the soil mineral N (N_{r_min}) release in drained peatland with and without mineral soil coverage; and 3) quantify the impact of mineral soil cover on the total N losses from drained peatland.

2 Materials and methods

2.1 Field site

The field experiment was carried out in the Swiss Rhine Valley, at the site Rüthi (47°17' N, 9°32' E), a drained fen with a peat thickness of ~10 m. The site has a cool temperate-moist climate with a mean annual precipitation of 1297 mm and a mean annual temperature of 10.1 °C (1981–2010, <https://www.meteoswiss.admin.ch>; for precipitation and temperature during the experimental period please see Fig. S2). The site was drained with ditches before 1890 (<https://map.geo.admin.ch>). In 1973, an intensive drainage system with pumps and pipes was built. The site was used as pasture, and since 2013 as an intensively managed meadow. From 2006 to 2007, one part of the field (~ 2 ha) was covered with mineral soil material (without mixing) to improve the agricultural usability. We established the field

experiment at this mineral soil coverage site (Cov) and used the adjacent drained organic soil without mineral soil coverage as the reference (Ref). The basic soil properties for both sites are provided in Table 1. Both sites have similar vegetation and identical farming practices with 5–6 cuts per year and ~230 kg N ha⁻¹ fertilizer application, both as slurry and as mineral fertilizer. The atmospheric N deposition at the study site for 2015 is 20 – 30 kg N ha⁻¹ yr⁻¹ (Rihm and Künzle, 2019). Dominant grass species are *Lolium perenne*, *Alopecurus pratensis*, *Festuca arundinacea*, *Trifolium spec.* and *Festuca pratensis*.

Table 1 Surface soil properties (0 – 5 cm) of drained organic soil with (Cov) and without (Ref) mineral soil coverage ($n = 16$).

Parameter	Cov	Ref
Sand (%) ^a	31.8	0.6
Silt (%) ^a	52.3	67.3
Clay (%) ^a	15.9	32.1
Total pore volume (%) ^a	58.4 ± 1.5	75.1 ± 0.5
pH, 0 – 25 cm ^b	7.2	5.2
pH, 25 – 50 cm ^b	7.0	5.1
pH, 50 – 75 cm ^b	5.8	4.7
NH ₄ ⁺ (N mg kg ⁻¹ dry soil) ^a	2.62 ± 0.96	37.33 ± 12.07
NO ₃ ⁻ (N mg kg ⁻¹ dry soil) ^a	2.81 ± 1.21	5.16 ± 1.13
Bulk density (g cm ⁻³)	0.7 ± 0.09	0.3 ± 0.06
N stock, 0 – 15 cm (t ha ⁻¹) ^c	6.5 ± 0.03	14.4 ± 0.5
Total N content cm (%) ^c	0.36 ± 0.02	1.4 ± 0.09
C to N ratios ^c	18.5 ± 0.7	18.2 ± 5.0

a. Data from Wang *et al.* (2022).

b. Soil pH was determined based on the samples from Wang *et al.* (2021);

c. Total N content, total N content, and C to N ratios down to 60 cm are provided in Supplementary Table S1.

2.2 Experimental design and field management

The study was conducted from July 2020 to July 2021. In July 2020, eight separate plots (four for Cov, four for Ref; size, 3.5 m × 1.5m) were randomly distributed on the experimental site. Each plot was divided into two subplots (1.5 m × 1.5m, Fig. S1.A), and the distance between the two subplots was 0.5 m. At each plots, one subplot received ¹⁵N double-labeled ammonium nitrate (¹⁵NH₄¹⁵NO₃) as a treatment plot and the other one received the same amount of non-labelled ammonium nitrate (NH₄NO₃) as a control plot. For these treatment plots, ¹⁵NH₄¹⁵NO₃ was dissolved in water and the salt solution was applied in three campaigns at the same time the farmer fertilized the overall field. We dissolved 1.35 g, 1.35 g and 0.8 g 98 atom %¹⁵N ¹⁵NH₄¹⁵NO₃ in 2.25L water for each each application, which is equivalent

to 1 mm precipitation for each application. The control plot (i.e., the plot without a label) always received the same amount of NH_4NO_3 solution. The additional N input rate was chosen based on the typical field fertilizer N application. A total extra ^{15}N input of 0.57 g N m^{-2} for each plot was chosen; this was equivalent to $\sim 2.5 \%$ of the regular field fertilizer N input, and it was assumed that this small extra dose would not cause a major disturbance in the N cycle of the ecosystem. The plot received the same regular fertilizer as the overall field. Extra $^{15}\text{NH}_4^{15}\text{NO}_3$ salt solution was sprayed directly onto the ground on 10 September 2020, 25 March 2021, and 13 May 2021. In order to spread the salt solution homogeneously, each subplot was divided into 15 units ($0.3 \text{ m} \times 0.5 \text{ m}$, Fig. S1.B), and the same amount of the salt solutions was applied to each unit.

2.3 Plant and soil sample collection and analysis

During the experimental period, soil and plant samples were taken one day before the regular field harvest events in October of year 2020, May, June, and July of year 2021. In addition, extra soil samples were taken on August 2020 and August 2021. Soil samples from the first sampling were used to determine the background ^{15}N signature over all experimental plots, and those from the last sampling were used to determine the soil bulk density from 0 – 5 cm and 5 – 15 cm. For each subplot, composite soil samples from 3 units were collected by using a 6.5 cm-diameter corer for 0 – 20 cm depth, and a 2.6 cm-diameter corer for 20 – 60 cm depth. Those samples were divided into 4 layers, 0 – 5 cm, 5 – 15 cm, 15 – 30 cm and 30 – 60 cm. The samples from Cov were additionally divided at the boundary of mineral soil cover and underlying peat. After sampling, soil samples were stored at $4 \text{ }^\circ\text{C}$ in a cooling room overnight, and visible root and stones were removed from composite soil samples the next day. Soil samples were then dried at $105 \text{ }^\circ\text{C}$ for 72 h, ground with mortar and pestle, milled in a ball mill (Retsch, MM 400, Germany) at $25\text{-rotation s}^{-1}$ for 3 minutes and finally loaded in a tin capsule to determine the soil N and ^{15}N content via elemental analysis isotope ratio mass spectrometry (EA-IRMS) (vario PYRO cube, Elementar, Germany and isoprime precisION, Elementar, Germany).

For each subplot, aboveground grass samples from three units were harvested by grass clippers to a height of 3 cm. At the same unit, root samples were collected by taking soil cores with a 6.5 cm-inner-diameter corer down to a depth of 20 cm. Composited grass samples were dried at $60 \text{ }^\circ\text{C}$ in the oven for 72 h to determine the dry biomass. Dried plant samples were cut into small pieces, milled in a ball mill (Retsch, MM 400, Germany) at $25\text{-rotation s}^{-1}$ for 3 minutes and then loaded into a tin capsule to determine the grass N and ^{15}N content with elemental analysis isotope ratio mass spectrometry (EA-IRMS) (vario PYRO cube, Elementar, Germany and isoprime precisION, Elementar, Germany). Roots were extracted from each soil core in the lab. To do so, soil material from the soil core was removed by hand, and the remaining root from the removed soil material was picked out. The left soil core and the roots that were picked out from the soil were submerged in distilled water for 2 – 3 hours, and then put on a fine mesh screen to be washed with a gentle water shower until the residual soil material was

removed. The bare roots were dried at 60 °C in the oven until the constant weight (~48 h); then the root N and ¹⁵N content was determined by following the same procedure described above.

2.4 Laboratory incubation

To determine the net soil N mineralization rate for the two sites, the 0 – 5 cm and 5 – 15 cm soil samples, which were collected in October 2020, were incubated for 28 days. Five duplicated (n = 160) soil samples equivalent to 10 g dry soils were weighted into 50 ml PET containers with soil moisture adjusted to 60 % of their water holding capacity. Water holding capacity was determined following Franzluebbers (2020). The PET containers were incubated at 25 °C, and soil moisture was adjusted every two days by adding distilled water. After 0, 7, 14, 21, and 28 days of incubation, the soil samples were suspended in 80 ml 0.01M CaCl₂ salt solution to extract soil ¹⁵N (Steffens *et al.*, 1996), shaken at 160 cycles min⁻¹ for 30 min and filtered. Total N and ¹⁵N from the soil extracts were determined by EA-IRMS (vario TOC cube, Elementar, Germany and iso TOC cube, Elementar, Germany). For each time step (e.g., 0 to 7 days), daily net N mineralization rates (N_{r_min} , mg N kg⁻¹ soil day⁻¹) from two sites and depth were calculated based on the difference of the total dissolved nitrogen between each extraction. The specific N mineralization rate (specific N_{r_min} , mg N g⁻¹ soil N day⁻¹) was calculated as the ratio of the N mineralization rate and the soil N content.

2.5 Isotope calculation and statistics

The N isotope ratios of the samples are presented by using the δ notation (Fry, 2006).

$$\delta^{15}N(\text{‰}) = \left(\frac{R_{sample}}{R_{standard}} - 1 \right) \times 1000 \quad (1)$$

Where R_{sample} and $R_{standard}$ are the ratios between ¹⁵N and ¹⁴N of the sample and the standard, respectively. Here, atmospheric N₂ is used as a standard with $R_{standard} = 0.003665$ (Mariotti, 1983).

The isotope enrichment in the sample from the treatment plot ($\delta^{15}N_{sample}$) is expressed as ¹⁵N enrichment relative to that of the control plot ($\delta^{15}N_{control}$).

$$^{15}N \text{ enrichment (‰)} = \left(\frac{\delta^{15}N_{sample} - \delta^{15}N_{control}}{\delta^{15}N_{control} + 1000} \right) \times 1000 \quad (2)$$

The recovery of the ¹⁵N fertilizer in the labeled N pools is calculated as follows:

$$^{15}N (\%) = \left(\frac{(\%^{15}N_{sample} - \%^{15}N_{control}) \times M_{pool}}{(\%^{15}N_{label} - \%^{15}N_{control}) \times M_{label}} \right) \times 1000 \quad (3)$$

Here, $\%^{15}N_{sample}$ is ¹⁵N atom percent in the soil sample from the labelled plot; $\%^{15}N_{control}$ is ¹⁵N atom percent in the corresponding control plot, M_{label} is the amount of the ¹⁵N applied to the treatment plot (g ¹⁵N m⁻²), and $\%^{15}N_{label}$ is the ¹⁵N atom percent in the labeled fertilizer, and M_{pool} is the N amount of the labeled pool (g N m⁻²). In this study, there are three labeled pools, $M_{pool,grass}$, $M_{pool,root}$ and $M_{pool,soil}$. $M_{pool,grass}$ and $M_{pool,root}$ were determined based on the dry biomass for each plot. $M_{pool,soil}$ was calculated as follows:

$$M_{pool,soil} = \sum BD_i \times L_i \times N_{sample} \quad (4)$$

BD_i is the soil bulk density (g cm^{-3}) at four different soil depths (0 – 5cm, 5 – 15 cm, 15 – 30 cm and 30 – 60 cm). Soil bulk density from 15 – 30 cm and 30 – 60 cm was determined plot wise based on the correlation between soil bulk density and the soil organic carbon from Wang et al. (2021). L_i is the thickness of each depth (cm), and N_{sample} % is the total N content of the soil sample from the labeled plot (%).

The mass balances of ^{15}N in the system were used to account for the quantitative recovery of ^{15}N in the system; any ^{15}N which was not retained in the plant and soil system was defined as losses. Plot based ^{15}N losses (N_{losses}) were calculated as the difference between ^{15}N input through ^{15}N tracer application, as well as the N output from harvest and the ^{15}N retained in soil and roots. The ^{15}N input through regular fertilizer and atmospheric ^{15}N deposition is accounted for by the ^{15}N abundance from the associated control plot. The cumulative N losses at each harvest event are calculated as follows:

$$N_{losses,i} = \sum_{i=1}^{i=n} {}^{15}N_{fer,i} - \sum_{i=1}^{i=n} {}^{15}N_{grass,i} - {}^{15}N_{root,i} - {}^{15}N_{soil,i} \quad (5)$$

$N_{losses,i}$ is the N losses after the i th harvest event, $n = 1, 2, 3, 4$, ${}^{15}N_{fer}$ is the cumulative ^{15}N input through fertilization, ${}^{15}N_{grass}$ is the cumulative ^{15}N uptake through harvest, $N_{root,i}$ and $N_{soil,i}$ is the ^{15}N retained in roots and soil at the i th harvest event, respectively.

Statistical analysis and data visualization were performed using the open source software R (version 4.1.3). Significant differences between the two sites for soil and plant N content, $\delta^{15}\text{N}$ content, ^{15}N enrichment, net N mineralization rate, ^{15}N recovery, and ^{15}N losses were determined using a t-test. Significant differences in the ratio of the specific ${}^{15}N_{r_{min}}: N_{r_{min}}$, N and ^{15}N release rate, and specific N and ^{15}N mineralization rate in soil layers 0 – 5 cm and 5 – 15 cm between the two sites were determined through ANOVA. In case of a significant effect, a Tukey HSD test was performed for multiple pairwise comparisons between different sampling dates. The error probability was set as $p < 0.05$. The results were always reported as mean \pm 1 standard error (se).

3 Results

3.1 Effect of mineral soil coverage on plant biomass, nitrogen uptake and plant ^{15}N enrichment

During the experimental period, the cumulated grass yield was not different between sites (Table 2), only in June 2021, the yield at Cov was higher ($p < 0.05$) than at Ref. The harvested grass took up $274.34 \pm 22.78 \text{ kg N ha}^{-1}$ from the mineral soil coverage (Cov) site over four harvest events, which was significantly higher than that taken up from the drained peatland (Ref) site ($229.97 \pm 10.56 \text{ kg N ha}^{-1}$). The higher grass N uptake of Cov was not observed in all harvest events; it was significant only for the

harvest in June 2021 whereas for the rest of the cuts, no significant difference between Cov and Ref was found. The ^{15}N enrichment of the grass varied largely between the different harvest events. It was higher at Ref compared to Cov in October 2020, whereas no significant differences were found for the other harvest events.

For roots, the differences in biomass, N uptake, and ^{15}N enrichment was not constant between the two sites. In June 2021, root biomass and ^{15}N enrichment were significantly higher ($p < 0.05$) at Cov than at Ref, and a significantly higher root N content was found at Ref in July 2021.

Table 2 Plant biomass, nitrogen uptake and ¹⁵N enrichment of a drained peatland with (Cov) and without mineral soil coverage (Ref). Significant differences between the two sites over the experimental period are indicated with asterisks (“***” $p < 0.01$, “**” $p < 0.05$, “ns” no significant difference).

Sample	Item	Site	October 2020	May 2021	June 2021	July 2021	Total	
Grass	Biomass (kg ha ⁻¹)	Cov	2015 ± 133	4044 ± 541	4905 ± 183	2853 ± 111	13817 ± 738	
		Ref	2144 ± 89	3755 ± 238	4063 ± 264	3049 ± 156	13011 ± 290	
	N uptake (kg N ha ⁻¹)	Cov	ns	ns	*	ns	ns	
		Ref	57.76 ± 5.86	74.82 ± 10.49	81.23 ± 5.04	54.59 ± 5.28	274.34 ± 22.78	
	¹⁵ N enrichment (‰)	Cov	61.74 ± 3.62	62.40 ± 4.34	55.26 ± 4.81	49.00 ± 3.11	229.97 ± 10.56	
		Ref	ns	ns	*	ns	*	
	Root	Biomass (kg ha ⁻¹)	Cov	1977.63 ± 124.24	2252.37 ± 170.86	2187.33 ± 193.50	705.53 ± 146.43	-
			Ref	2518.91 ± 153.99	2212.39 ± 143.02	2393.74 ± 100.52	760.24 ± 25.15	-
		N uptake (kg N ha ⁻¹)	Cov	*	ns	ns	ns	-
			Ref	4133 ± 548	4893 ± 404	5396 ± 616	3604 ± 312	-
¹⁵ N enrichment (‰)		Cov	4371 ± 576	4781 ± 442	4127 ± 322	3933 ± 224	-	
		Ref	ns	ns	*	ns	-	
Biomass (kg ha ⁻¹)		Cov	73.5 ± 10.6	53.2 ± 3.9	45.9 ± 3.7	27.7 ± 2.5	-	
		Ref	92.1 ± 12.7	53.0 ± 5.2	43.3 ± 3.9	42.8 ± 5.0	-	
¹⁵ N enrichment (‰)		Cov	ns	ns	ns	*	-	
		Ref	901.67 ± 77.97	1847.36 ± 303.83	2073.23 ± 195.26	1403.81 ± 155.81	-	
Biomass (kg ha ⁻¹)	Cov	710.57 ± 70.95	1613.24 ± 160.84	1445.56 ± 192.88	1408.22 ± 102.89	-		
	Ref	ns	ns	*	ns	-		

3.2 Effect of mineral soil coverage on soil ^{15}N enrichment

Applications of ^{15}N labeled fertilizer induced an increase in the soil ^{15}N signature. At both sites, the highest soil ^{15}N signature was found in July 2021 after the three labeling events were finished, although no ^{15}N tracer was applied directly before that sampling event. At 0 – 5 cm soil depth, the ^{15}N enrichment was 146.0 ± 13.3 ‰ at Cov and 49.4 ± 13.7 ‰ at Ref (Fig. 1D). At 5 – 15 cm soil depth, the ^{15}N enrichment was 32.7 ± 8.8 ‰ at Cov, and 7.4 ± 1.4 ‰ at Ref (Fig. 1D). The higher ^{15}N signature was only found at the surface 0 – 30 cm, below 30 cm depth, the soil ^{15}N enrichment was similar to the value prior the ^{15}N tracer application, which was near zero (Fig. 1). The surface (0 – 5 cm, 5 – 15 cm) soil ^{15}N enrichment was higher ($p < 0.05$) at Cov than at Ref, whereas below 15 cm, the difference in ^{15}N enrichment between the sites was less pronounced at any sampling date (Fig. 1).

At Cov, the ^{15}N signal moved from the surface soil to the deeper (15 – 30 cm) layer during the growing season and resulted in a slightly higher ^{15}N enrichment (49.4 ± 13.7 ‰) at 15 – 30 cm depth compared with the upper layer (32.7 ± 8.8 ‰) at the last sampling date (July 2021). However, no such trend was found for Ref (Fig. 1D).

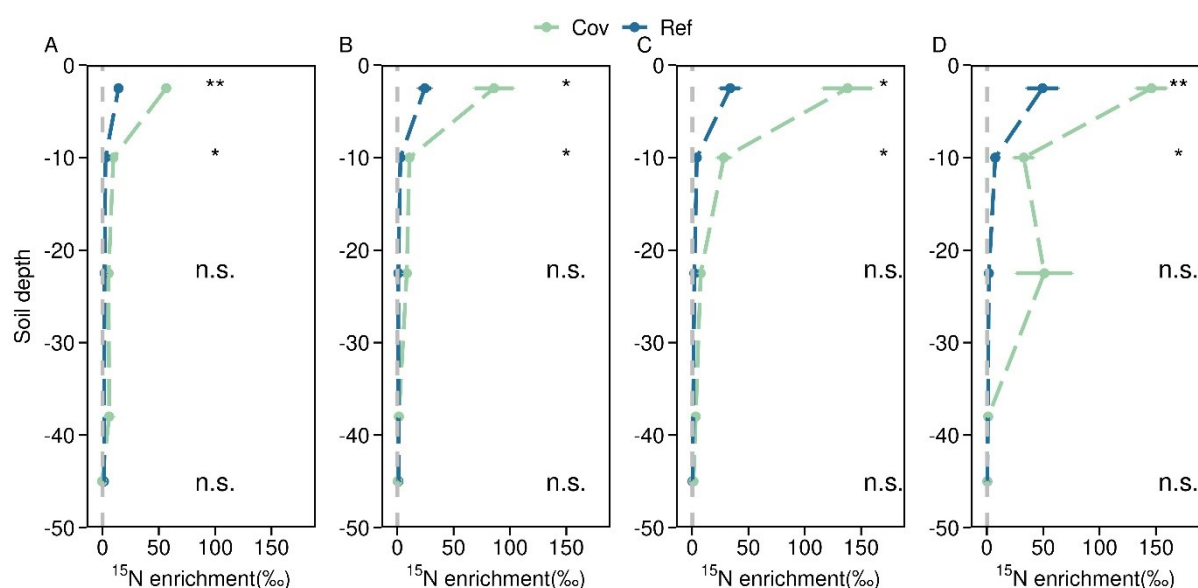


Fig. 1 Soil profile (0 – 60 cm) ^{15}N enrichment (mean \pm se, $n = 4$) at sampling dates in October 2020 (A), May 2021 (B), June 2021 (C), July 2021 (D) from the drained peatland with (Cov) and without mineral soil coverage (Ref). The symbols always denote the middle depth of each sampled segment. The dashed gray line indicates the background ^{15}N enrichment before ^{15}N application, which is zero. For each sampling date, significant differences between two sites at different soil depths are indicated with asterisks (“***” $p < 0.01$, “**” $p < 0.05$, “ns” no significant difference).

3.3 The effect of mineral soil coverage on ^{15}N recovery from drained organic soil

During the experimental period, the recovery of ^{15}N in plant biomass (grass and roots) was not different between Cov and Ref. The cumulative tracer exports through grass harvest accounted for $32.2 \pm 2.2\%$ and $30.0 \pm 0.3\%$ of the applied ^{15}N for Cov and Ref, respectively (Fig. 2A). Roots took up $2.5 \pm 0.3\%$ and $3.9 \pm 0.5\%$ of the applied ^{15}N from Cov and Ref respectively after the three labeling events were finished (Fig. 2A). Hence, a significant part of the applied ^{15}N was not used by the plants. A share of $10\% - 20\%$ was incorporated into the soil N pool. At site Cov, $19.8 \pm 2.0\%$ of the tracer remained in the soil N pool, more ($p < 0.05$) than at Ref ($9.8 \pm 3.2\%$ see Fig. 2B). Overall, site Cov showed smaller N losses ($p < 0.05$) compared to Ref. At Cov, $45.4 \pm 3.0\%$ of the applied labeled mineral fertilizer was lost outside the plant–soil system boundary of the study, whereas at Ref, the loss accounted for $56.2 \pm 3.1\%$ (Fig. 2C).

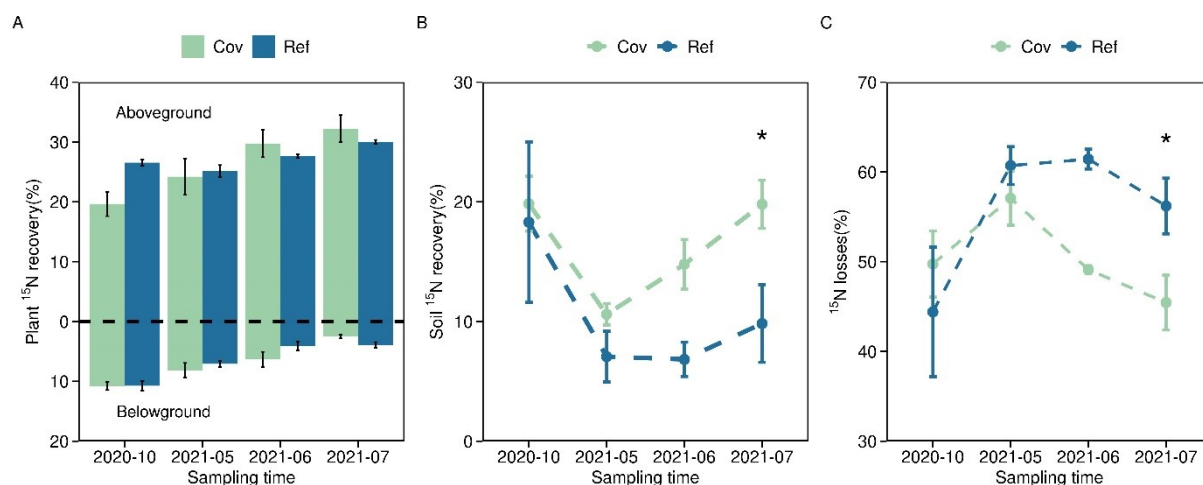


Fig. 2 Budget of ^{15}N tracer based on mass and isotope balances for plants (A), soil (B), and N losses (C) from drained peatland with (Cov) and without mineral soil coverage (Ref). Significant differences in cumulative soil ^{15}N recovery and ^{15}N losses between the two sites over the experimental period are indicated with asterisks (“***” $p < 0.01$, “**” $p < 0.05$, “ns” no significant difference) in panel (B) and (C). The dashed line in panel (A) separates the aboveground grass ^{15}N recovery and the belowground root ^{15}N recovery.

3.4 Nitrogen mineralization

The average amount of soil N_{r_min} was significantly higher ($p < 0.05$) at Ref ($6.07 \pm 0.84 \text{ mg N kg}^{-1} \text{ day}^{-1}$) than at Cov ($2.10 \pm 0.15 \text{ mg N kg}^{-1} \text{ day}^{-1}$) at the $0 - 5 \text{ cm}$ depth (Fig. 3A). In addition, in the deeper layer, the average amount of soil N_{r_min} was significantly higher ($p < 0.01$) at Ref ($5.45 \pm 0.26 \text{ mg N kg}^{-1} \text{ day}^{-1}$) compared to Cov ($1.71 \pm 0.13 \text{ mg N kg}^{-1} \text{ day}^{-1}$; Fig. 3B). A similar trend to that of the total N release was found for the average release of soil ^{15}N . Ref released ^{15}N at higher rates ($0.027 \pm 0.001 \text{ mg}$

^{15}N $\text{kg}^{-1} \text{ day}^{-1}$ at 0 – 5 cm; $0.022 \pm 0.002 \text{ mg N kg}^{-1} \text{ day}^{-1}$ at 5 – 15 cm) than at Cov ($0.009 \pm 0.001 \text{ mg N kg}^{-1} \text{ day}^{-1}$ at 0 – 5 cm; $0.005 \pm 0.0004 \text{ mg N kg}^{-1} \text{ day}^{-1}$, at 5 – 15 cm) (Fig. 3C&D).

In addition, the average amount of N and ^{15}N release showed no difference at the 0 – 5 cm depth for the two sites ($73.67 \pm 6.27 \text{ mg N m}^{-2} \text{ day}^{-1}$, $0.31 \pm 0.02 \text{ mg } ^{15}\text{N m}^{-2} \text{ day}^{-1}$ at Cov and $77.71 \pm 8.08 \text{ mg N m}^{-2} \text{ day}^{-1}$, $0.35 \pm 0.04 \text{ mg } ^{15}\text{N m}^{-2} \text{ day}^{-1}$ at Ref, respectively). However, it was significantly ($p < 0.05$) higher at Ref ($204.68 \pm 10.53 \text{ mg N m}^{-2} \text{ day}^{-1}$, $0.81 \pm 0.06 \text{ mg } ^{15}\text{N m}^{-2} \text{ day}^{-1}$) than at Cov ($155.70 \pm 15.41 \text{ mg N m}^{-2} \text{ day}^{-1}$, $0.48 \pm 0.05 \text{ mg } ^{15}\text{N m}^{-2} \text{ day}^{-1}$) at the 5 – 15 cm depth (Table 3).

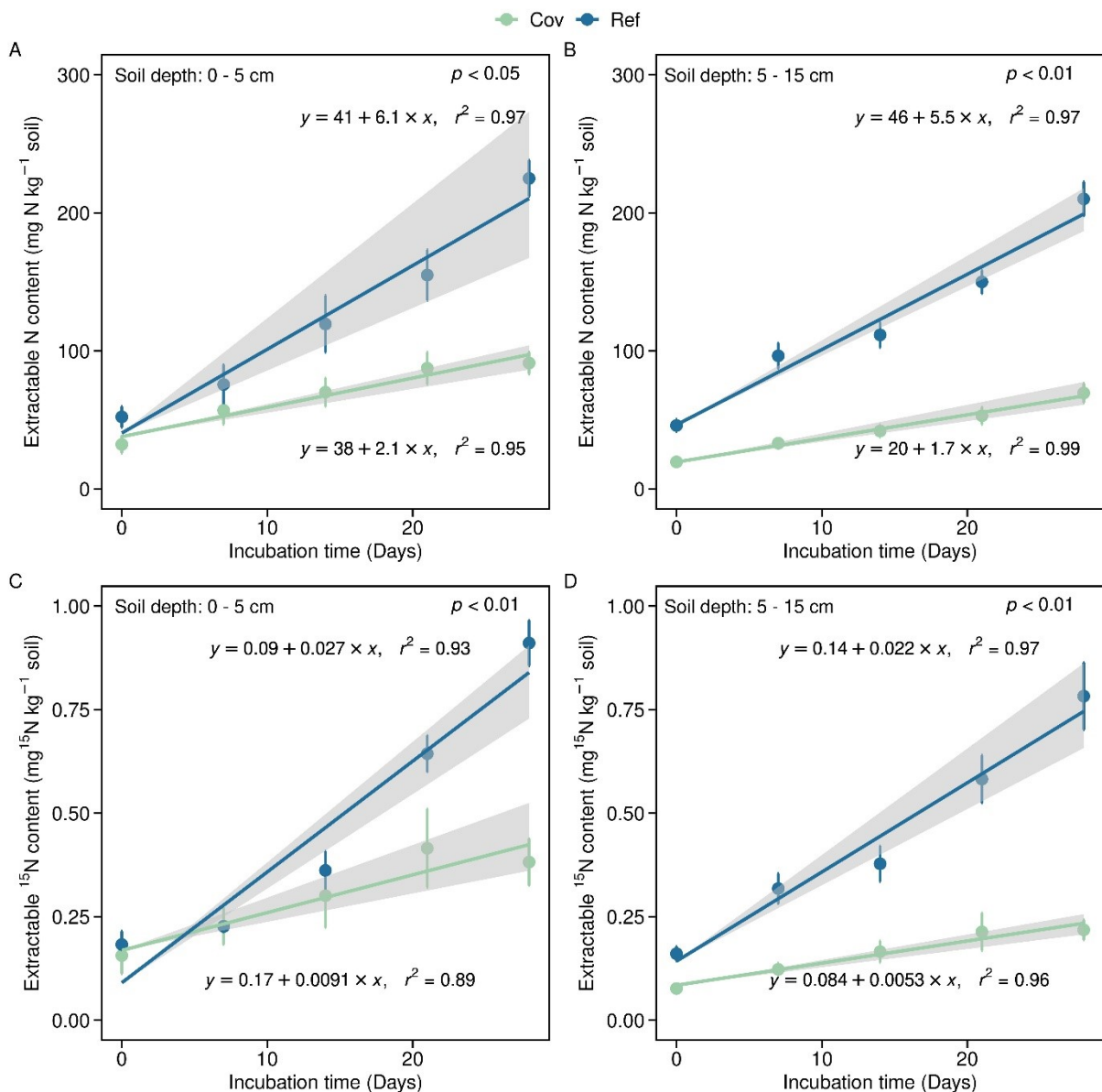


Fig. 3 Extractable soil N and ^{15}N (mean \pm se, n = 4) for different incubation days in soil layers 0 – 5 cm and 5 – 15 cm from drained peatland with (Cov) and without mineral soil coverage (Ref). The shaded area indicate the maximum and minimum rate of soil N_{r_min} and $^{15}\text{N}_{r_min}$ release from soil. The p-values indicate significant differences (t-Test) of soil N_{r_min} and $^{15}\text{N}_{r_min}$ release between the two sites.

3.5 Specific nitrogen mineralization

The specific soil N mineralization (specific soil N_{sr_min}) was significantly higher with mineral soil coverage (Table 3) for both soil layers (0 – 5 cm and 5 – 15 cm). Throughout 28 days of incubation, the specific soil N_{sr_min} at site Cov was $0.60 \pm 0.07 \text{ mg N g}^{-1} \text{ N day}^{-1}$ and $0.35 \pm 0.03 \text{ mg N g}^{-1} \text{ N day}^{-1}$ at Ref at a soil depth of 0 – 5 cm. A similar difference was also found at the 5 – 15 cm soil depth, where Cov released $0.58 \pm 0.03 \text{ mg N g}^{-1} \text{ N day}^{-1}$, significantly more than Ref ($0.36 \pm 0.03 \text{ mg N g}^{-1} \text{ N day}^{-1}$). In addition, specific soil $^{15}\text{N}_{sr_min}$ was also significantly higher with mineral soil coverage (Table 3) for both soil layers ($0.65 \pm 0.10 \text{ mg }^{15}\text{N g}^{-1} \text{ }^{15}\text{N day}^{-1}$ at 0 – 5 cm depth and $0.71 \pm 0.14 \text{ mg }^{15}\text{N g}^{-1} \text{ }^{15}\text{N day}^{-1}$ at 5 – 15 cm depth) than at Ref ($0.39 \pm 0.02 \text{ mg }^{15}\text{N g}^{-1} \text{ }^{15}\text{N day}^{-1}$ at 0 – 5 cm depth and $0.35 \pm 0.02 \text{ mg }^{15}\text{N g}^{-1} \text{ }^{15}\text{N day}^{-1}$ at 5 – 15 cm depth).

The ratio of the specific soil $^{15}\text{N}_{sr_min}$ release to the N_{r_min} release was above one for both layers and sites (Fig. 4). No difference was found between the two sites; however, the ratio of specific $^{15}\text{N}_{sr_min}$ and N_{sr_min} from the 5 – 15 cm soil layer was lower than from the 0 – 5 cm soil layer.

Table 3 Soil nitrogen release rate and specific nitrogen mineralization rate in soil layers with depths of 0 – 5 cm and 5 – 15 cm from drained peatland with (Cov) and without mineral soil coverage (Ref). Significant differences among the two soil layers and the two sites are indicated with lowercase letters (ANOVA and Tukey honest significant differences).

	Cov		Ref	
	0 - 5 cm	5 - 15 cm	0 - 5 cm	5 - 15 cm
Soil N release rate $\text{mg N m}^{-2} \text{ day}^{-1}$	73.67 ± 6.27^c	155.70 ± 15.41^b	77.71 ± 8.08^c	204.68 ± 10.53^a
Soil ^{15}N release rate $\text{mg }^{15}\text{N m}^{-2} \text{ day}^{-1}$	0.31 ± 0.02^b	0.48 ± 0.05^b	0.35 ± 0.04^b	0.81 ± 0.06^a
Specific soil N mineralization rate $\text{mg N g}^{-1} \text{ soil N day}^{-1}$	0.60 ± 0.07^a	0.58 ± 0.03^a	0.35 ± 0.03^b	0.36 ± 0.03^b
Specific soil ^{15}N mineralization rate $\text{mg }^{15}\text{N g}^{-1} \text{ soil }^{15}\text{N day}^{-1}$	0.65 ± 0.10^a	0.71 ± 0.14^a	0.39 ± 0.02^b	0.35 ± 0.02^b

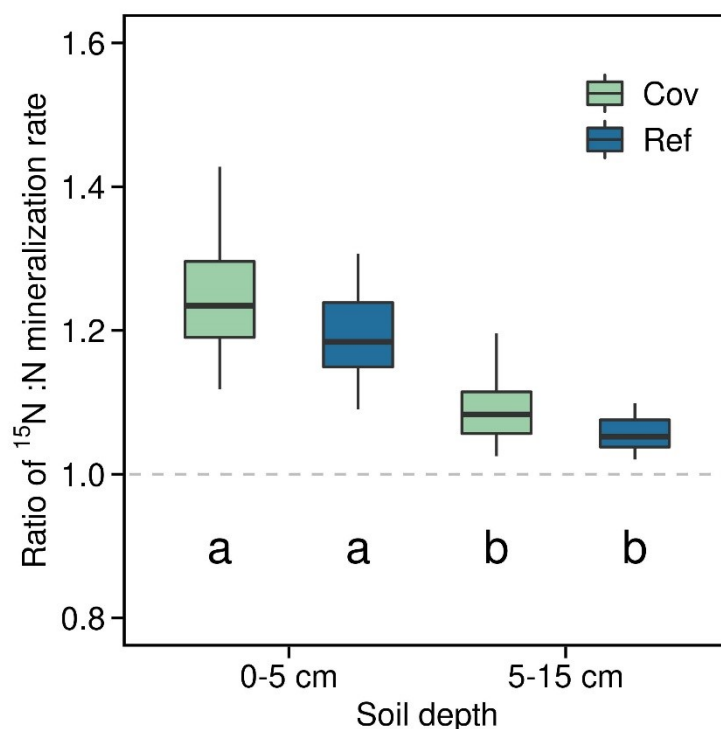


Fig. 4 The ratio of ^{15}N mineralization rate to N mineralization rate in soil layers with depth of 0 – 5 cm and 5 – 15 cm from drained peatland with (Cov) and without mineral soil coverage (Ref) for different incubation days. Significant differences among the two soil layers and the two sites are indicated with lowercase letters.

4 Discussion

4.1 The effect of mineral soil cover on soil ^{15}N retention and nitrogen mineralization

4.1.1 Soil ^{15}N retention

The field ^{15}N tracer experiment showed that of the applied ^{15}N tracer, ~10 % resided in the soil pool in the Ref site, of which more than 90 % was found in the top 30 cm of soil. This result was similar to the ^{15}N retention from the drained fen peatland reported by Augustin *et al.* (1997) who found that 10 – 20 % of the applied labeled ^{15}N fertilizer was recovered in the soil pool in a ^{15}N tracer experiment from two drained peatlands in Germany, of which more than 90 % was located at the 0 – 20 cm depth. To the best of our knowledge, soil ^{15}N recovery from drained peatland with mineral soil coverage has never been studied. Our results indicate that the soil ^{15}N recovery (~ 20 % of the applied ^{15}N tracer) from the Cov site was generally significantly higher than at Ref at the end of the study period, suggesting a better retention of the fertilizer-N though mineral soil coverage. The recovery was at the lower end of the range of data reported from ^{15}N tracer (with ^{15}N enriched fertilizer or slurry) studies in grassland on mineral soil in Europe. This included 20 – 25 % soil ^{15}N retention from a grassland in southern England

(Jenkinson *et al.*, 2004), ~ 15 % from grassland in the Netherlands (De Vries *et al.*, 2011), and 30 – 40 % from grassland in Germany (Zistl-Schlingmann *et al.*, 2020).

However, we observed a downward movement of the ^{15}N tracer to the deeper layer at Cov, whereas no such trend was found at Ref (Fig. 1D) over the course of the experiment. This indicates that, despite a higher overall recovery in the studied soil layers, fertilizer N might leach faster in the covered mineral soil material at Cov than in the drained peatland at Ref. This may, after longer periods, also change the overall recovery once the leachate leaves the investigated zone of 0 – 60 cm. The higher ^{15}N leaching from Cov may be attributed to the low absorption rate of the mineral cover material compared to the degraded peat, as the sand content of the mineral soil coverage is much higher than that of the peat at Ref (Table 1). Hence, the low adsorption potential of the sand for anions compared to organic materials with higher anion sorption capacity may have induced a higher N leaching at the mineral soil layer from Cov.

4.1.2 Soil N mineralization

The lab incubation results showed that soil $\text{N}_{\text{r_min}}$ and soil $^{15}\text{N}_{\text{r_min}}$ at 0 – 5 cm and 5 – 15 cm depth were significantly higher ($p < 0.05$) at Ref than at Cov. We attribute this higher soil N content of the surface peat as compared to the mineral soil cover material. In contrast, the specific soil $\text{N}_{\text{sr_min}}$ release was higher at Cov than at Ref (Table 3), which indicates that the surface soil organic matter (SOM) at the Cov site was more labile compared to the Ref site. By definition, the labile SOM pool decomposes very quickly and is easily accessible to plants and microbes (Dungait *et al.*, 2012; Liu *et al.*, 2017).

The higher relative lability of the SOM pool at Cov coincided with the higher soil ^{15}N recovery (Fig. 2). Higher soil ^{15}N recovery might be due to a higher gross microbial ^{15}N immobilization. Microbial N immobilization is positively correlated with soil substrate availability and soil pH (Elrys *et al.*, 2022). The higher availability of soil substrates stimulates soil microbial activity, which ultimately promotes gross N immobilization (Barrett and Burke, 2000; Booth *et al.*, 2005; Yang *et al.*, 2022). Compared with Cov, the SOM pool from Ref is larger (Table 1), but may exist in forms that the microorganism cannot easily use (Baldock and Skjemstad, 2000; Fontaine *et al.*, 2007). This may result in a lower microbial immobilization rate at Ref than at Cov. Moreover, a lower soil pH suppresses the soil microbial activity whereas higher soil pH could enhance the abundance of ammonia-oxidizers and eventually gross microbial N immobilization (Zhang *et al.*, 2017). The soil pH of the surface layers at Cov was higher than at Ref (Table 1), which may enhance soil microbial immobilization and further induce better soil ^{15}N retention at Cov than at Ref.

At both sites, the soil $^{15}\text{N}_{\text{r_min}}$ release was faster than the $\text{N}_{\text{r_min}}$ release (Fig. 4), implying that the added ^{15}N turnover rate was higher than the gross N turnover rate. This finding indicates that the newly applied

mineral N (^{15}N and ^{14}N), after incorporation into SOM, was preferably stored in the labile soil N pool. This finding is consistent with former studies found that the exogenous N input is mostly labile (Shevtsova *et al.*, 2003; Mulvaney *et al.*, 2009; Sebilo *et al.*, 2013). This part of the soil organic N pool releases available N for plant uptake in the growing season, but likewise bears the risk of N losses to the environment.

4.2 The effect of mineral soil coverage on plant ^{15}N uptake

Over the experimental period, both sites had similar grass yields; however, the plant N uptake was higher at Cov than at Ref ($p < 0.05$), suggesting that mineral soil coverage not only sustains the agricultural productivity of the drained peatland, but also increases the fertilizer N use efficiency. However, mineral soil coverage did not influence plant and root ^{15}N content. At both sites, plants took up $\sim 30\%$ of the applied ^{15}N fertilizer, similar to the results reported from a meta – analysis of ^{15}N tracer studies, which found that on average, 30% of the applied ^{15}N is taken up by plants in grassland (Templer *et al.*, 2012). It is often assumed that plant N uptake tends to be higher under higher soil N availability (Stevens *et al.*, 2005; Tatenno and Takeda, 2010). However, we found that the application of mineral soil material, which was relatively poor in N and also released an absolutely smaller amount of N in the incubation experiments, did not reduce the plant N uptake and the plant ^{15}N recovery. The similar grass biomass and ^{15}N recovery might be driven by the ample amount of N supplied at both sites and the lack of any N limitations. During the experimental period, $\sim 230\text{ kg N ha}^{-1}$ were applied equally to both sites, and the soil $\text{N}_{\text{r_min}}$ results suggest that soil mineralization could supply further N, exceeding the demand for grass production at both sites. Therefore, as N was not limited in the system, the presence of relatively N-poor mineral soil did not impair grass yields.

4.3 The effect of mineral soil coverage on N loss

4.3.1 Fertilizer N loss reduction

The two sites received $\sim 230\text{ kg N ha}^{-1}\text{ yr}^{-1}$ fertilizer N input. Together, the fertilizer N input and the soil N supply largely exceed the plant N demand and consequently lead to N losses to the environment, i.e. release into the atmosphere via ammonia volatilization and denitrification as well as via leaching to the groundwater (Robertson and Vitousek, 2009; Bowles *et al.*, 2018). At Cov, less of the applied N was lost through the experimental period, considering the storage in the 0 – 60 cm soil layer. Thus, mineral soil coverage at this site may prevent $\sim 25\text{ kg N ha}^{-1}\text{ yr}^{-1}$ fertilizer N from being lost to the environment compared with Ref if no substantial leaching below 60 cm will occur.

4.3.2 Effects on peat decomposition

The higher soil N release from Ref at 0 – 15 cm soil depth (Table 3) also implies a rapid peat decomposition and peatland degradation, as the soil N losses are closely linked to the C losses from the

SOM mineralization (Leifeld *et al.*, 2020; Klein *et al.*, 2022). However, we only have evidence for this for the topsoil and the peat underneath the mineral soil coverage was not used for determining soil N_{r_min} in the incubation experiment. At Cov, these subsoil organic layers may have a higher N_{r_min} release than the surface organic soil from Ref site due to two possible mechanisms. First, the covered mineral soil material revealed some N leaching (Fig. 1). This leachate from the mineral soil material may stimulate the decomposition of the peat underneath the mineral soil cover via positive priming (Kuzyakov *et al.*, 2000). Second, the mineral cover enhanced the soil pH of the peat layers underneath (Table 1). As SOM decomposition increases with soil pH (Sinsabaugh *et al.*, 2008), a higher potential for peat decomposition underneath the mineral soil coverage may be possible.

On the other hand, oxygen availability is vital for peat mineralization (Blodau, 2002; Tiemeyer *et al.*, 2016). For the peat layer underneath the mineral soil coverage, the oxygen availability for SOM mineralization is reduced (Jørgensen *et al.*, 2012), leading to a presumably lower N release. In addition, the absence of fresh plant residue input into the deeper layers of the organic soil underneath might limit SOM mineralization (Song *et al.*, 2018; Zhang *et al.*, 2021). Fresh plant inputs are the primary source of SOM formation, which could not only determine the chemical composition of SOM, but also impact soil microbial activities. The exclusion of fresh plant inputs may lead to a N limitation for microorganisms and further limit the N mineralization for peat underneath the mineral soil coverage (Mooshammer *et al.*, 2014). Moreover, a former study conducted at the same site found that SOC from mineral soil material contributed greatly to heterotrophic soil respiration at the Cov site (Wang *et al.*, 2021). The contribution of the peat layer underneath the mineral soil coverage was relatively small compared to the contribution of peat C at Ref (Wang *et al.*, 2021). The lower contribution of subsoil peat to C loss from Cov suggests that mineral soil cover might be able to reduce the peat decomposition rate despite incoming N leachate and a higher pH. However, further in-situ soil profile-based SOM mineralization experiments are still needed to support this interpretation.

5 Conclusion

Our findings suggest that mineral soil coverage has the potential to reduce N losses (due to higher soil N recovery) from drained peatland and, hence, may make agricultural production on drained peatland less harmful to the environment as compared to the continued direct use of drained peatland. However, we would like to point out that from a nature conservation standpoint as well as climate mitigation strategy, mineral soil coverage does not replace or substitute the mitigating effect of rewetting. Rather, we aim to encourage further research about mineral soil coverage as a peatland management measure in regions, where peatland rewetting is not supported, be it for reasons of national food and feed provision, economic incomes or political strategies.

Our field ¹⁵N trace experiment and laboratory incubation together provide the first insight into how mineral soil coverage influences the N balance of the plant–soil system in agriculturally managed drained peatland. Over the experimental period, mineral soil coverage of drained peatland significantly reduced the system fertilizer N loss. For the deeper peat layer, the effect of mineral soil coverage on peat decomposition and mineralization still needs to be further explored. In sum, the study suggests that mineral soil coverage, a measure used by farmers to counterbalance subsidence, provides an opportunity for reducing the environmental pollution induced by the agricultural use of drained peatland.

Funding

The work was supported by funding received from the Swiss Federal Office for the Environment (contract number 06.0091.PZ/R261-2425), and the China Scholarship Council (NSCIS 201806350221).

Declarations

Conflict of interest: The authors declare no competing interests.

Acknowledgments

We appreciate the help from Markus Jocher, Robin Giger, Steven Nagel, Martin Zuber and Shiva Ghiassi at Agroscope during field sampling and lab analysis. We are thankful for many useful discussions with Christof Ammann and Chloé Wüst, Agroscope. We are grateful to Bernhard Schneider for the opportunity to collaborate on the farm.

References

- Augustin, J., Merbach, W., Käding, H., Schmidt, W., Schalitz, G., Russow, R., Ende, H.P., 1997. N Balance experiments on fen grassland with ¹⁵N labelled fertilizer. *Isotopes in Environmental and Health Studies*. 33, 31-37. <https://doi.org/10.1080/10256019808036356>.
- Baldock, J.A., Skjemstad, J.O., 2000. Role of the soil matrix and minerals in protecting natural organic materials against biological attack. *Organic Geochemistry*. 31, 697-710. [https://doi.org/10.1016/S0146-6380\(00\)00049-8](https://doi.org/10.1016/S0146-6380(00)00049-8).
- Barrett, J.E., Burke, I.C., 2000. Potential nitrogen immobilization in grassland soils across a soil organic matter gradient. *Soil Biology and Biochemistry*. 30, 1707-1716. [https://doi.org/10.1016/S0038-0717\(00\)00089-4](https://doi.org/10.1016/S0038-0717(00)00089-4).
- Barrett, J.E., Burke, I.C., 2002. Nitrogen retention in semiarid ecosystems across a soil organic - matter gradient. *Ecological Applications*. 12, 878-890. [https://doi.org/10.1890/1051-0761\(2002\)012\[0878:NRISEA\]2.0.CO;2](https://doi.org/10.1890/1051-0761(2002)012[0878:NRISEA]2.0.CO;2).
- Bessler, H., Oelmann, Y., Roscher, C., Buchmann, N., Scherer-Lorenzen, M., Schulze, E.-D., Temperton, V.M., Wilcke, W., Engels, C., 2012. Nitrogen uptake by grassland communities:

- contribution of N₂ fixation, facilitation, complementarity, and species dominance. *Plant and Soil*. 358, 301-322. <https://doi.org/10.1007/s11104-012-1181-z>.
- Blodau, C., 2002. Carbon cycling in peatlands - A review of processes and controls. *Environmental Reviews*. 10, 111-134. <https://doi.org/10.1139/a02-004>.
- Booth, M.S., Stark, J.M., Rastetter, E., 2005. Controls on nitrogen cycling in terrestrial ecosystems: a synthetic analysis of literature data. *Ecological Monographs*. 75, 139-157. <https://doi.org/10.1890/04-0988>.
- Bowles, T.M., Atallah, S.S., Campbell, E.E., Gaudin, A.C.M., Wieder, W.R., Grandy, A.S., 2018. Addressing agricultural nitrogen losses in a changing climate. *Nature Sustainability*. 1, 399-408. <https://doi.org/10.1038/s41893-018-0106-0>.
- De Vries, F.T., van Groenigen, J.W., Hoffland, E., Bloem, J., 2011. Nitrogen losses from two grassland soils with different fungal biomass. *Soil Biology and Biochemistry*. 43, 997-1005. <https://doi.org/10.1016/j.soilbio.2011.01.016>.
- Dungait, J.A.J., Hopkins, D.W., Gregory, A.S., Whitmore, A.P., 2012. Soil organic matter turnover is governed by accessibility not recalcitrance. *Global Change Biology*. 18, 1781-1796. <https://doi.org/10.1111/j.1365-2486.2012.02665.x>.
- Elrys, A.S., Chen, Z., Wang, J., Uwiragiye, Y., Helmy, A.M., Desoky, E.M., Cheng, Y., Zhang, J.B., Cai, Z.C., Muller, C., 2022. Global patterns of soil gross immobilization of ammonium and nitrate in terrestrial ecosystems. *Global Change Biology*. <https://doi.org/10.1111/gcb.16202>.
- Evans, C.D., Peacock, M., Baird, A.J., Artz, R.R.E., Burden, A., Callaghan, N., Chapman, P.J., Cooper, H.M., Coyle, M., Craig, E., Cumming, A., Dixon, S., Gauci, V., Grayson, R.P., Helfter, C., Heppell, C.M., Holden, J., Jones, D.L., Kaduk, J., Levy, P., Matthews, R., McNamara, N.P., Misselbrook, T., Oakley, S., Page, S.E., Rayment, M., Ridley, L.M., Stanley, K.M., Williamson, J.L., Worrall, F., Morrison, R., 2021. Overriding water table control on managed peatland greenhouse gas emissions. *Nature*. 593, 548-552. <https://doi.org/10.1038/s41586-021-03523-1>.
- Ferré, M., Muller, A., Leifeld, J., Bader, C., Müller, M., Engel, S., Wichmann, S., 2019. Sustainable management of cultivated peatlands in Switzerland: Insights, challenges, and opportunities. *Land Use Policy*. 87, 104019. <https://doi.org/10.1016/j.landusepol.2019.05.038>.
- Fontaine, S., Barot, S., Barre, P., Bdioui, N., Mary, B., Rumpel, C., 2007. Stability of organic carbon in deep soil layers controlled by fresh carbon supply. *Nature*. 450, 277-280. <https://doi.org/10.1038/nature06275>.
- Franzluebbers, A.J., 2020. Holding water with capacity to target porosity. *Agricultural & Environmental Letters*. 5, e20029. <https://doi.org/10.1002/acl2.20029>.
- Fry, B., 2006. *Stable isotope ecology*. Springer.
- Jenkinson, D.S., Poulton, P.R., Johnston, A.E., Powlson, D.S., 2004. Turnover of nitrogen - 15 - labeled fertilizer in old grassland. *Soil Science Society of America Journal*. 68, 865-875. <https://doi.org/10.2136/sssaj2004.8650>.

- Jørgensen, C.J., Struwe, S., Elberling, B., 2012. Temporal trends in N₂O flux dynamics in a Danish wetland – effects of plant - mediated gas transport of N₂O and O₂ following changes in water level and soil mineral - N availability. *Global Change Biology*. 18, 210-222. <https://doi.org/doi:10.1111/j.1365-2486.2011.02485.x>.
- Kalu, S., Oyekoya, G.N., Ambus, P., Tammeorg, P., Simojoki, A., Pihlatie, M., Karhu, K., 2021. Effects of two wood-based biochars on the fate of added fertilizer nitrogen—a ¹⁵N tracing study. *Biology and Fertility of Soils*. 57, 457-470. <https://doi.org/10.1007/s00374-020-01534-0>.
- Kasimir, A., He, H., Coria, J., Norden, A., 2018. Land use of drained peatlands: Greenhouse gas fluxes, plant production, and economics. *Global Change Biology*. 24, 3302-3316. <https://doi.org/10.1111/gcb.13931>.
- Klein, K., Schellekens, J., Groß-Schmölders, M., von Sengbusch, P., Alewell, C., Leifeld, J., 2022. Characterizing ecosystem-driven chemical composition differences in natural and drained Finnish bogs using pyrolysis-GC/MS. *Organic Geochemistry*. 165, 104351. <https://doi.org/10.1016/j.orggeochem.2021.104351>.
- Klemetsson, L., Von Arnold, K., Weslien, P., Gundersen, P., 2005. Soil CN ratio as a scalar parameter to predict nitrous oxide emissions. *Global Change Biology*. 11, 1142-1147. <https://doi.org/10.1111/j.1365-2486.2005.00973.x>.
- Kuzyakov, Y., Friedel, J.K., K Stahr, 2000. Review of mechanisms and quantification of priming effects. *Soil Biology and Biochemistry*. 32, 1485-1498. [https://doi.org/10.1016/S0038-0717\(00\)00084-5](https://doi.org/10.1016/S0038-0717(00)00084-5).
- Leifeld, J., 2018. Distribution of nitrous oxide emissions from managed organic soils under different land uses estimated by the peat C/N ratio to improve national GHG inventories. *Science of the Total Environment* 631-632, 23-26. <https://doi.org/10.1016/j.scitotenv.2018.02.328>.
- Leifeld, J., Klein, K., Wust-Galley, C., 2020. Soil organic matter stoichiometry as indicator for peatland degradation. *Scientific Reports*. 10, 7634. <https://doi.org/10.1038/s41598-020-64275-y>.
- Leifeld, J., Menichetti, L., 2018. The underappreciated potential of peatlands in global climate change mitigation strategies. *Nature Communications*. 9, 1071. <https://doi.org/10.1038/s41467-018-03406-6>.
- Liu, Y., Wang, C., He, N., Wen, X., Gao, Y., Li, S., Niu, S., Butterbach-Bahl, K., Luo, Y., Yu, G., 2017. A global synthesis of the rate and temperature sensitivity of soil nitrogen mineralization: latitudinal patterns and mechanisms. *Global Change Biology*. 23, 455-464. <https://doi.org/10.1111/gcb.13372>.
- Loisel, J., Yu, Z., Beilman, D.W., Camill, P., Alm, J., Amesbury, M.J., Anderson, D., Andersson, S., Bochicchio, C., Barber, K., Belyea, L.R., Bunbury, J., Chambers, F.M., Charman, D.J., De Vleeschouwer, F., Fiałkiewicz-Koziele, B., Finkelstein, S.A., Gałka, M., Garneau, M., Hammarlund, D., Hinchcliffe, W., Holmquist, J., Hughes, P., Jones, M.C., Klein, E.S., Kokfelt, U., Korhola, A., Kuhry, P., Lamarre, A., Lamentowicz, M., Large, D., Lavoie, M., MacDonald,

- G., Magnan, G., Mäkilä, M., Mallon, G., Mathijssen, P., Mauquoy, D., McCarroll, J., Moore, T.R., Nichols, J., O'Reilly, B., Oksanen, P., Packalen, M., Peteet, D., Richard, P.J.H., Robinson, S., Ronkainen, T., Rundgren, M., Sannel, A.B.K., Tarnocai, C., Thom, T., Tuittila, E.S., Turetsky, M., Väiranta, M., van der Linden, M., van Geel, B., van Bellen, S., Vitt, D., Zhao, Y., Zhou, W., 2014. A database and synthesis of northern peatland soil properties and Holocene carbon and nitrogen accumulation. *Holocene*. 24, 1028-1042.
<https://doi.org/10.1177/0959683614538073>.
- Mariotti, A., 1983. Atmospheric nitrogen is a reliable standard for natural ¹⁵N abundance measurements. *Nature*. 5919, 685-687. <https://doi.org/10.1038/303685a0>.
- Mooshammer, M., Wanek, W., Zechmeister-Boltenstern, S., Richter, A., 2014. Stoichiometric imbalances between terrestrial decomposer communities and their resources: mechanisms and implications of microbial adaptations to their resources. *Frontiers in Microbiology*. 5, 22.
<https://doi.org/10.3389/fmicb.2014.00022>.
- Müller, C., Laughlin, R.J., Christie, P., Watson, C.J., 2011. Effects of repeated fertilizer and cattle slurry applications over 38 years on N dynamics in a temperate grassland soil. *Soil Biology and Biochemistry*. 43, 1362-1371. <https://doi.org/10.1016/j.soilbio.2011.03.014>.
- Mulvaney, R.L., Khan, S.A., Ellsworth, T.R., 2009. Synthetic nitrogen fertilizers deplete soil nitrogen: a global dilemma for sustainable cereal production. *Journal of Environmental Quality*. 38, 2295-2314. <https://doi.org/10.2134/jeq2008.0527>.
- Pijlman, J., Holshof, G., van den Berg, W., Ros, G.H., Erisman, J.W., van Eekeren, N., 2020. Soil nitrogen supply of peat grasslands estimated by degree days and soil organic matter content. *Nutrient Cycling in Agroecosystems*. 117, 351-365. <https://doi.org/10.1007/s10705-020-10071-z>.
- Rahman, M.K., Parsons, J.W., 1999. Uptake of ¹⁵N by wetland rice in response to application of ¹⁵N-labelled *Sesbania rostrata* and urea. *Biology and Fertility of Soils*. 29, 69-73.
<https://doi.org/10.1007/s003740050526>.
- Rihm, B., Künzle, T., 2019. Mapping nitrogen deposition 2015 for Switzerland. Technical Report on the Update of Critical Loads and Exceedance, including the years 1990, 2000, 2005 and 2010, Bern, Switzerland. <https://www.bafu.admin.ch>.
- Robertson, G.P., Vitousek, P.M., 2009. Nitrogen in agriculture: balancing the cost of an essential resource. *Annual Review of Environment and Resources*. 34, 97-125.
<https://doi.org/10.1146/annurev.environ.032108.105046>.
- Rowlings, D.W., Scheer, C., Liu, S., Grace, P.R., 2016. Annual nitrogen dynamics and urea fertilizer recoveries from a dairy pasture using ¹⁵N; effect of nitrification inhibitor DMPP and reduced application rates. *Agriculture, Ecosystems & Environment*. 216, 216-225.
<https://doi.org/10.1016/j.agee.2015.09.025>.

- Schindler, U., Müller, L., 1999. Rehabilitation of the soil quality of a degraded peat site. In: D.E., S., R.H., M., G.C., S. (Eds.), 10th International Soil Conservation Organization Meeting Purdue University, pp. 648-654.
- Schothorst, C.J., 1977. Subsidence of low moor peat soils in the western Netherlands. *Geoderma*. 17, 265-291. [https://doi.org/10.1016/0016-7061\(77\)90089-1](https://doi.org/10.1016/0016-7061(77)90089-1).
- Sebilo, M., Mayer, B., Nicolardot, B., Pinay, G., Mariotti, A., 2013. Long-term fate of nitrate fertilizer in agricultural soils. *Proceedings of the National Academy of Sciences*. 110, 18185-18189. <https://doi.org/10.1073/pnas.1305372110>.
- Shevtsova, L., Romanenkov, V., Sirotenko, O., Smith, P., Smith, J.U., Leech, P., Kanzyvaa, S., Rodionova, V., 2003. Effect of natural and agricultural factors on long-term soil organic matter dynamics in arable soddy-podzolic soils—modeling and observation. *Geoderma*. 116, 165-189. [https://doi.org/10.1016/s0016-7061\(03\)00100-9](https://doi.org/10.1016/s0016-7061(03)00100-9).
- Sinsabaugh, R.L., Lauber, C.L., Weintraub, M.N., Ahmed, B., Allison, S.D., Crenshaw, C., Contosta, A.R., Cusack, D., Frey, S., Gallo, M.E., Gartner, T.B., Hobbie, S.E., Holland, K., Keeler, B.L., Powers, J.S., Stursova, M., Takacs-Vesbach, C., Waldrop, M.P., Wallenstein, M.D., Zak, D.R., Zeglin, L.H., 2008. Stoichiometry of soil enzyme activity at global scale. *Ecology Letters*. 11, 1252-1264. <https://doi.org/10.1111/j.1461-0248.2008.01245.x>.
- Song, Y., Song, C., Hou, A., Ren, J., Wang, X., Cui, Q., Wang, M., 2018. Effects of temperature and root additions on soil carbon and nitrogen mineralization in a predominantly permafrost peatland. *Catena*. 165, 381-389. <https://doi.org/10.1016/j.catena.2018.02.026>.
- Sonneveld, M.P.W., Lantinga, E.A., 2011. The contribution of mineralization to grassland N uptake on peatland soils with anthropogenic A horizons. *Plant and Soil*. 340, 357-368. <https://doi.org/10.1007/s11104-010-0608-7>.
- Steffens, D., Pfanschilling, R., Feigenbaum, S., 1996. Extractability of ¹⁵N-labeled corn-shoot tissue in a sandy and a clay soil by 0.01 M CaCl₂ method in laboratory incubation experiments. *Biology and Fertility of Soils*. 22, 109-115. <https://doi.org/10.1007/BF00384441>.
- Stevens, W.B., Hoefft, R.G., Mulvaney, R.L., 2005. Fate of nitrogen - 15 in a long - term nitrogen rate study: II. Nitrogen uptake efficiency. *Agronomy Journal*. 97, 1046-1053. <https://doi.org/10.2134/agronj2003.0313>.
- Tateno, R., Takeda, H., 2010. Nitrogen uptake and nitrogen use efficiency above and below ground along a topographic gradient of soil nitrogen availability. *Oecologia*. 163, 793-804. <https://doi.org/10.1007/s00442-009-1561-0>.
- Templer, P., Mack, M., III, F.C., Christenson, L., Compton, J., Crook, H., Currie, W., Curtis, C., Dail, D., D'Antonio, C., 2012. Sinks for nitrogen inputs in terrestrial ecosystems: a meta - analysis of ¹⁵N tracer field studies. *Ecology*. 93, 1816-1829. <https://doi.org/10.1890/11-1146.1>.
- Tiemeyer, B., Albiac Borraz, E., Augustin, J., Bechtold, M., Beetz, S., Beyer, C., Drosler, M., Ebli, M., Eickenscheidt, T., Fiedler, S., Forster, C., Freibauer, A., Giebels, M., Glatzel, S., Heinichen,

- J., Hoffmann, M., Hoper, H., Jurasinski, G., Leiber-Sauheitl, K., Peichl-Brak, M., Rosskopf, N., Sommer, M., Zeitz, J., 2016. High emissions of greenhouse gases from grasslands on peat and other organic soils. *Global Change Biology*. 22, 4134-4149. <https://doi.org/10.1111/gcb.13303>.
- Wang, Y., Paul, S.M., Jocher, M., Alewell, C., Leifeld, J., 2022. Reduced nitrous oxide emissions from drained temperate agricultural peatland after coverage with mineral soil. *Frontiers in Environmental Science*. 10, 856599. <https://doi.org/10.3389/fenvs.2022.856599>.
- Wang, Y., Paul, S.M., Jocher, M., Espic, C., Alewell, C., Szidat, S., Leifeld, J., 2021. Soil carbon loss from drained agricultural peatland after coverage with mineral soil. *Science of the Total Environment*. 800, 149498. <https://doi.org/10.1016/j.scitotenv.2021.149498>.
- Wardle, D.A., 1998. Controls of temporal variability of the soil microbial biomass: a global-scale synthesis. *Soil Biology and Biochemistry*. 30, 1627-1637. [https://doi.org/10.1016/S0038-0717\(97\)00201-0](https://doi.org/10.1016/S0038-0717(97)00201-0).
- Wesselsperelo, L., Jimenez, M., Munch, J., 2006. Microbial immobilisation and turnover of ^{15}N labelled substrates in two arable soils under field and laboratory conditions. *Soil Biology and Biochemistry*. 38, 912-922. <https://doi.org/10.1016/j.soilbio.2005.07.013>.
- Yang, S., Liu, W., Guo, L., Wang, C., Deng, M., Peng, Z., Liu, L., 2022. The changes in plant and soil C pools and their C:N stoichiometry control grassland N retention under elevated N inputs. *Ecological Applications*. 32, e2517. <https://doi.org/10.1002/eap.2517>.
- Yu, Z., Loisel, J., Brosseau, D.P., Beilman, D.W., Hunt, S.J., 2010. Global peatland dynamics since the Last Glacial Maximum. *Geophysical Research Letters*. 37, L13402. <https://doi.org/10.1029/2010gl043584>.
- Zhang, M., Alves, R.J.E., Zhang, D., Han, L., He, J., Zhang, L., 2017. Time-dependent shifts in populations and activity of bacterial and archaeal ammonia oxidizers in response to liming in acidic soils. *Soil Biology and Biochemistry*. 112, 77-89. <https://doi.org/10.1016/j.soilbio.2017.05.001>.
- Zhang, X., Zhu, B., Yu, F., Cheng, W., 2021. Plant inputs mediate the linkage between soil carbon and net nitrogen mineralization. *Science of the Total Environment* 790, 148208. <https://doi.org/10.1016/j.scitotenv.2021.148208>.
- Zistl-Schlingmann, M., Kwatcho Kengdo, S., Kiese, R., Dannenmann, M., 2020. Management intensity controls Nitrogen-Use-Efficiency and flows in grasslands—A ^{15}N tracing experiment. *Agronomy*. 10, 606. <https://doi.org/10.3390/agronomy10040606>.

Supplementary Material

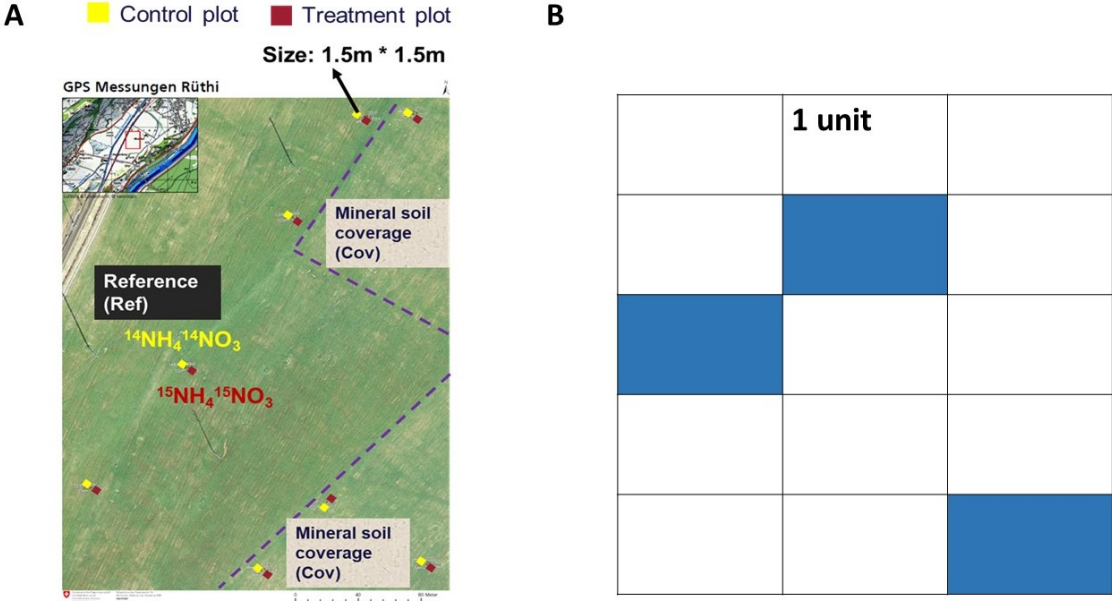


Figure S1. Location of experimental site (A) and the brief overview of the experimental set up (B)

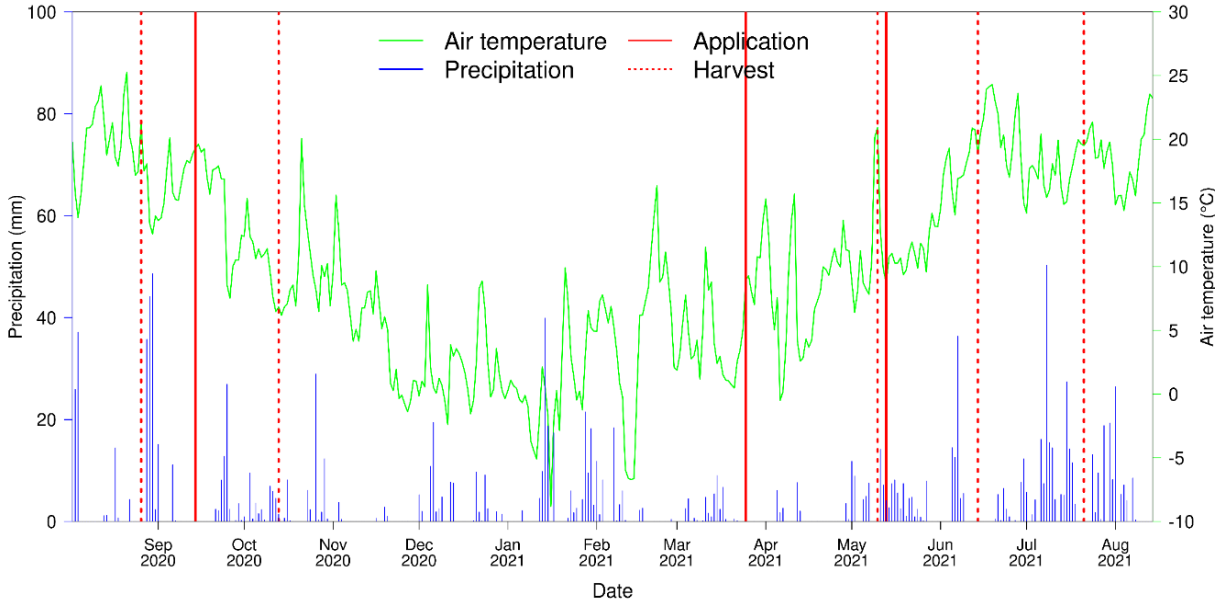


Figure S2. Overview of environmental conditions and field management during the experimental period.

Table S1. Soil properties of drained organic soil with (Cov) and without (Ref) mineral soil coverage, data were reported as mean \pm 1 standard error (se).

Site	Depth (cm)	Sampling time	N content (%)	C content (%)	C to N ratios
Cov	0 – 5	10.05.2021	0.34 \pm 0.04	5.79 \pm 0.27	18.65 \pm 2.01
Cov	5 – 15	10.05.2021	0.20 \pm 0.02	4.75 \pm 0.07	25.6 \pm 2.32
Cov	15 – 30	10.05.2021	0.13 \pm 0.02	3.94 \pm 0.08	47.24 \pm 14.12
Cov	30 – 60 (Mineral soil)	10.05.2021	0.09 \pm 0.02	3.76 \pm 0.15	51.69 \pm 8.55
Cov	30 – 60 (Peat)	10.05.2021	0.82 \pm 0.09	12.81 \pm 1.33	15.90 \pm 0.56
Ref	0 – 5	10.05.2021	1.44 \pm 0.05	18.99 \pm 0.49	13.17 \pm 0.18
Ref	5 – 15	10.05.2021	1.22 \pm 0.06	17.39 \pm 0.61	14.32 \pm 0.37
Ref	15 – 30	10.05.2021	1.11 \pm 0.04	17.46 \pm 0.79	15.75 \pm 0.29
Ref	30 – 60	10.05.2021	1.45 \pm 0.08	27.46 \pm 2.11	18.88 \pm 0.74
Cov	0 – 5	14.06.2021	0.35 \pm 0.03	6.17 \pm 0.28	18.46 \pm 1.44
Cov	5 – 15	14.06.2021	0.19 \pm 0.02	4.7 \pm 0.10	27.14 \pm 2.88
Cov	15 – 30	14.06.2021	0.10 \pm 0.02	3.61 \pm 0.27	58.25 \pm 19.95
Cov	30 – 60 (Mineral soil)	14.06.2021	0.10 \pm 0.02	4.18 \pm 0.25	49.61 \pm 5.96
Cov	30 – 60 (Peat)	14.06.2021	0.73 \pm 0.05	11.75 \pm 0.89	16.14 \pm 0.42
Ref	0 – 5	14.06.2021	1.34 \pm 0.17	19.27 \pm 0.55	23.11 \pm 10.11
Ref	5 – 15	14.06.2021	1.25 \pm 0.05	17.35 \pm 0.52	13.92 \pm 0.24
Ref	15 – 30	14.06.2021	1.11 \pm 0.04	17.14 \pm 1.16	15.37 \pm 0.66
Ref	30 – 60	14.06.2021	1.32 \pm 0.17	27.06 \pm 1.24	28.53 \pm 9.61
Cov	0 – 5	19.07.2021	0.36 \pm 0.03	6.50 \pm 0.21	18.57 \pm 1.05
Cov	5 – 15	19.07.2021	0.22 \pm 0.01	5.04 \pm 0.09	24.08 \pm 1.51
Cov	15 – 30	19.07.2021	0.12 \pm 0.02	3.97 \pm 0.08	49.64 \pm 15.02
Cov	30 – 60 (Mineral soil)	19.07.2021	0.14 \pm 0.04	4.33 \pm 0.44	44.68 \pm 8.28
Cov	30 – 60 (Peat)	19.07.2021	0.74 \pm 0.07	12.10 \pm 1.00	16.57 \pm 0.63
Ref	0 – 5	19.07.2021	1.47 \pm 0.05	19.35 \pm 0.50	13.21 \pm 0.19
Ref	5 – 15	19.07.2021	1.23 \pm 0.04	17.08 \pm 0.46	13.88 \pm 0.25
Ref	15 – 30	19.07.2021	1.12 \pm 0.03	17.92 \pm 0.69	15.96 \pm 0.29
Ref	30 – 60	19.07.2021	1.58 \pm 0.09	31.48 \pm 2.68	19.85 \pm 0.98
Cov	0 – 5	26.08.2020	0.38 \pm 0.03	6.08 \pm 0.19	16.56 \pm 0.92
Cov	5 – 15	26.08.2020	0.25 \pm 0.03	4.78 \pm 0.21	22.05 \pm 3.48
Cov	15 – 30	26.08.2020	0.17 \pm 0.03	3.98 \pm 0.18	28.21 \pm 4.53
Cov	30 – 60 (Mineral soil)	26.08.2020	0.18 \pm 0.02	4.23 \pm 0.20	26.25 \pm 4.41
Cov	30 – 60 (Peat)	26.08.2020	0.93 \pm 0.06	11.14 \pm 0.88	11.94 \pm 0.55

Ref	0 – 5	26.08.2020	1.74 ± 0.05	17.36 ± 1.31	10.02 ± 0.74
Ref	5 – 15	26.08.2020	1.56 ± 0.05	15.78 ± 1.05	10.23 ± 0.76
Ref	15 – 30	26.08.2020	1.46 ± 0.06	17.34 ± 1.42	11.97 ± 1.02
Ref	30 – 60	26.08.2020	1.78 ± 0.11	18.91 ± 1.61	10.99 ± 1.18
Cov	0 – 5	13.10.2020	0.40 ± 0.04	6.29 ± 0.25	16.46 ± 1.12
Cov	5 – 15	13.10.2020	0.27 ± 0.03	4.93 ± 0.17	19.82 ± 1.84
Cov	15 – 30	13.10.2020	0.18 ± 0.03	4.16 ± 0.11	27.84 ± 4.59
Cov	30 – 60 (Mineral soil)	13.10.2020	0.18 ± 0.03	4.17 ± 0.23	26.89 ± 4.15
Cov	30 – 60 (Peat)	13.10.2020	1.16 ± 0.07	10.69 ± 0.97	9.25 ± 0.72
Ref	0 – 5	13.10.2020	1.83 ± 0.08	17.12 ± 1.2	9.43 ± 0.67
Ref	5 – 15	13.10.2020	1.63 ± 0.06	15.35 ± 1.11	9.43 ± 0.56
Ref	15 – 30	13.10.2020	1.43 ± 0.08	15.35 ± 1.32	10.94 ± 0.94
Ref	30 – 60	13.10.2020	1.83 ± 0.1	20.78 ± 2.30	11.77 ± 1.58

Acknowledgments

Many appreciate to those kind people who support this thesis. Without them, this research would not be possible.

Firstly, I would like to thank my first supervisor, Jens Leifeld, for his great support during my Ph.D. studies. I appreciate so many discussions with him, from which I benefited greatly. He taught me so much about all the requisite details in scientific research, i.e., how to frame good stories of the field's experimental results and deal with uncertainties from data analysis. Moreover, he always supports and encourages me to not only focus on current topics but also learn new research topics. Thank you so much for setting me on the path to scientific research.

Many thanks to Christine Alewell for accepting me as an external Ph.D. student in her group. I have learned a lot from her comments and suggestions about my research and manuscripts. I sincerely appreciate those encouraging conversations when our manuscript is not going well with the Journal.

Markus Jocher, the problem solver, thank you a lot for not only setting up all of the instruments in the field but also lending a big helping hand whenever needed. Without you, the field experiment would not be possible.

I want to thank all the people from the KLIM group in Agroscope. Thank you for creating an enjoyable working environment. Sonja P, a big thank you for all the discussion about the field experiments and data analysis. Many appreciate Christof and Pierluigi for the small discussions about data analysis, N₂O emission results, and other small talks. Robin, Steven, and Marcio, I greatly appreciate your helping hand during field sampling and lab analysis. Sonja K, Chloé, Annelie, Kristy, Anne-Lena, Nina, Leonor, Miriam, Shauna, Eliza, Karl, Daniel, and Matthias, thank you for all the small discussions and help. Lena and Kate, thank you a lot for all the companies, you two make my Ph.D. life more colorful. Many appreciate all the civil service guys, especially Stefan, for helping during field samplings and lab analysis.

Many thanks to Chloé, Shauna, and Sonja P for improving my thesis with corrections and valuable comments.

Many appreciate to Sönke and Christophe at LARA lab at the University of Bern for supporting the radiocarbon analysis, and thanks to Martin and Shiva in Agroscope for helping with the isotope analysis. Thanks a lot.

I would like to also thank Bernhard not only for the farm collaboration but also for some helping hands and helpful discussions in the field.

I am very grateful to my parents and little brother, who always support me no matter what happens and where I am. Thank you.

非常感谢我的父母和弟弟，他们无条件的爱与鼓励是我在异乡求学之路上最大的动力。

Moreover, I want to thank my best friend, my husband, Shengli, for your patience with everything.

Curriculum vitae

First Name: Yuqiao

Surname: Wang

Date of birth: 01 July of 1994

Citizen of: China

Education

10. 2018 – present PhD

Agroscope, Climate and Agriculture Group and
University of Basel, Faculty of Science, Switzerland

09. 2016 – 06. 2018 Master of Agriculture.

Major in Crop Science. China Agricultural University, China

Diploma thesis: Comprehensive analysis of Agro-resource utilization efficiency in wheat-maize cropping system under different farming practice.

09. 2012 – 06. 2016 Bachelor of Agronomy.

Major in Agronomy. China Agricultural University, China

Diploma thesis: Dynamics of carbon footprint of wheat production in China

Journal Publications

1. **Wang, Y.**, Paul, S. M., Jocher, M., Alewell, C., Leifeld, J. (2022). Reduced nitrous oxide emissions from drained temperate agricultural peatland after coverage with mineral soil. *Frontiers in Environmental Science*, 157, 856599. <https://doi.org/10.3389/fenvs.2022.856599>.
2. **Wang, Y.**, Paul, S. M., Jocher, M., Espic, C., Alewell, C., Szidat, S., Leifeld, J. (2021). Soil carbon loss from drained agricultural peatland after coverage with mineral soil. *Science of the Total Environment*, 800, 149498. <https://doi.org/10.1016/j.scitotenv.2021.149498>.
3. He C., **Wang Y.**, Yu W., Kou Y., N'dri Yves B., Zhao X., Zhang H. (2022). Comprehensive analysis of resource utilization efficiency under different tillage systems in North China Plain. *Journal of Cleaner Production*, 347, 131289. <https://doi.org/10.1016/j.jclepro.2022.131289>.
4. Zhao X, Pu C, Ma S, Liu S, Xue J, Wang X, **Wang Y**, Li S, Lal R, Chen F, Zhang H., (2019). Management-induced greenhouse gases emission mitigation in global rice production. *Science of the Total Environment*, 649: 1299-1306. <https://doi.org/10.1016/j.scitotenv.2018.08.392>.

5. Zhao X, Liu S, Pu C, Zhang X, Xue J, Zhang R, **Wang Y**, Lal R, Zhang H, Chen F. (2016). Methane and nitrous oxide emissions under no-till farming in China: a meta-analysis. *Global Change Biology*, 22:1372-1384. <https://doi.org/10.1111/gcb.13185>.

Conference Talks

1. Wang, Y., Paul, S. M., Jocher, M., Alewell, C., Leifeld, J: The impact of cover fill on N₂O emissions from drained organic soil. Swiss Geoscience Meeting, Fribourg, Switzerland 2019.
2. Wang, Y., Paul, S. M., Jocher, M., Alewell, C., Leifeld, J: The impact of mineral soil coverage on N₂O emissions from organic soil drained for agriculture. Swiss Geoscience Meeting, 2020. Online.
3. Wang, Y., Paul, S. M., Jocher, M., Alewell, C., Leifeld: Effect of mineral soil cover on ¹⁴CO₂ respired from agricultural drained peatland. Eurosoil, 2021, Online.